AN X-RAY STUDY
OF THE STRUCTURE OF
RUBIDIUM DITHIONATE

AN X-RAY STUDY OF THE STRUCTURE OF RUBIDIUM DITHIONATE*

A Thesis

by

ANDRE VICTOR WENDLING,

Ing.E.S.E. (Paris), Lic.ès Sc.Math. (Sorbonne).

Submitted to the Faculty of Graduate Studies and Research of McGill University in partial fulfilment of the requirements for the degree of Doctor of Philosophy.

McGill University September 1937

- oOo -

---

* Bibliographic references: 541.27→541.63 and 548.2→548.73, Brussels extension of the Dewey decimal classification.

AN X-RAY STUDY OF
THE STRUCTURE OF RUBIDIUM DITHIONATE

ACKNOWLEDGMENTS

The writer desires to express his appreciation of the facilities for oral discussion and for use of apparatus provided by members of the departments of physics, chemistry and geological sciences at McGill University.

He is indebted particularly to Dr. R.P.D. Graham, professor of mineralogy, for his interest in the work of this thesis, for the loan of certain crystals and for much helpful discussion regarding certain of the crystallographic features of the present work.

Gratitude is expressed to Dr. F.F. Osborne, assistant professor of geology, for his supervision of the grinding and polishing of a slip of tourmaline, for the measurement of the optical activity of a crystal of rubidium dithionate and for much helpful discussion.

Special thanks are due to Dr. A.S. Eve and to Dr. A.N. Shaw, former and present heads of the department of physics for permission to spread the work of this thesis over several years. Without this consideration the experimental work of the thesis could not have been completed.

Grateful acknowledgment is made to Dr. R.W.G. Wyckoff of the Rockefeller Institute for Medical Research, New York, for helpful assistance during development of the experimental methods described in Section I.

Finally, the writer wishes to express his indebtedness to Dr. W.H. Barnes, assistant professor of chemistry, under whose supervision the work described in this thesis was carried out.

GENERAL TABLE OF CONTENTS

GENERAL INTRODUCTION

Some years ago at this University a start was made on a systematic X-ray study of the structure of the reportedly isomorphous dithionates of potassium, calcium, strontium and lead (1). From the beginning, however, difficulty was experienced due to the prevalence of twinning in crystals of these salts. In fact, only of potassium dithionate were crystals of trigonal symmetry obtained. Laue photographs of all specimens of the other dithionates mentioned showed pseudo-hexagonal symmetry.

The space group of potassium dithionate ($K_2S_2O_6$) was established as D_3^1 or D_3^2, a choice between the two depending on the relative positions of a dyad axis and a plane of symmetry (2). Since well-formed crystals were not obtained, it was not possible to establish the relative positions of these symmetry elements by optical methods. A new X-ray method is described in Section I of the present thesis which now permits such a distinction to be made even on a crystal fragment with no recognizable faces.

Helwig (3) and Huggins and Frank (4) independently completed structure investigations of $K_2S_2O_6$. The two proposed structures, however, are not identical. They will be discussed in detail later in this thesis.

Hägg (5) examined crystals of $K_2S_2O_6$ and of $Rb_2S_2O_6$ but, as will be shown later, it appears that the latter probably were twinned.

In view of the discrepancies between the results for the structure of $K_2S_2O_6$ it seemed of interest to make a study of the closely related isomorphous rubidium salt. During the course of this investigation trigonal and pseudohexagonal crystals of $K_2S_2O_6$ and of $Rb_2S_2O_6$ were obtained so that an X-ray examination of the nature of the twinning in these substances was undertaken.

The subject matter of this thesis has been divided into three sections. In the first, attention is drawn to the symmetry exhibited by Laue diagrams of orthogonal crystals obtained with the X-ray beam along lateral axes and a new X-ray method is described by means of which the members of certain pairs of space groups in the hexagonal system may readily be distinguished one from the other. The second section of this thesis deals with the X-ray study of the structure of rubidium dithionate during the course of which the theoretical arguments and experimental procedures developed in Section I were of material assistance. In the third section of this thesis is described the X-ray investigation of the nature of the twinning in crystals of $K_2S_2O_6$ and of $Rb_2S_2O_6$ which developed from the work described in Section II.

Each section of the thesis contains its own table of contents, introduction and discussion of results. An Appendix to Section I describes a study of the space group of tourmaline which was undertaken as an interesting application of the experimental methods described in that section. The calculation and use of logarithms of intensities instead of direct values when, as in the present work, visual estimations of observed intensities of diffraction spots are employed is justified in an Appendix to Section II. References to the literature, and figures, are numbered consecutively throughout the thesis and are listed at the end in a General Bibliography and a General List of Illustrations, respectively. The thesis closes with a General Summary and a Statement of the Claim of Original Work as required by the Faculty of Graduate Studies and Research.

SECTION I

LAUE DIAGRAMS OF ORTHOGONAL CRYSTALS

SECTION I

TABLE OF CONTENTS

INTRODUCTION TO SECTION I

During the course of the work on the structure of rubidium dithionate described in Section II of this thesis attention was directed to the types of Laue symmetry observed in photographs obtained with the X-ray beam along the lateral a and b (orthohexagonal) axes of trigonal crystals.

Since application of the Laue method of crystal structure analysis usually involves diagrams obtained with the beam along the direction of the principal axis, or inclined thereto by a few degrees only, the interesting features of photographs obtained with the beam along the directions of lateral axes have received little attention. The purpose of this section of the thesis, therefore, is to analyse the Laue symmetry to be expected under such conditions and to describe a new X-ray method, based thereon, for distinguishing between the members of certain pairs of space groups in the rhombohedral division of the hexagonal system. For convenience, the subject matter of this section is divided into two parts. An interesting application of the method developed in Part II to the space group of tourmaline is described in an Appendix.

It may be mentioned that the subject matter of this section already has appeared in print (6,7,8).

PART I

THE LAUE SYMMETRY EXHIBITED BY ORTHOGONAL CRYSTALS

It is of interest to examine the symmetry exhibited by Laue diagrams of crystals which possess a two-, three-, four- or six-fold symmetry axis and planes of symmetry containing this axis but with no plane of simple symmetry normal thereto. Two-fold axes perpendicular to the principal axis and not contained in the symmetry planes may be present but other elements of symmetry do not concern the present argument.

There are seven crystal classes, therefore, which must be considered, namely,

C_2^v - rhombic pyramidal,
C_4^v - ditetragonal pyramidal,
D_2^d - tetragonal scalenohedral,
T^d - hexacistetrahedral,
C_3^v - ditrigonal pyramidal,
D_3^d - ditrigonal scalenohedral,
C_6^v - dihexagonal pyramidal.

In the Laue method, however, a centre of symmetry is introduced automatically according to Friedel's Law due to the inability of the method to distinguish between the parallel planes (hkl) and $(\bar{h}\bar{k}\bar{l})$. Hence other classes exhibit the same Laue symmetry as those enumerated above. They may be grouped together as follows.

1. D_2 (rhombic bisphenoidal), C_2^v (rhombic pyramidal), D_2^h (rhombic bipyramidal).

2. C_4^v (ditetragonal pyramidal), D_2^d (tetragonal scalenohedral), D_4 (tetragonal trapezohedral), D_4^h (ditetragonal bipyramidal).

3. C_3^v (ditrigonal pyramidal), D_3 (trigonal trapezohedral), D_3^d (ditrigonal scalenohedral).

4. C_6^v (dihexagonal pyramidal), D_3^h (ditrigonal bipyramidal), D_6 (hexagonal trapezohedral), D_6^h (dihexagonal bipyramidal).

5. T^d (hexacistetrahedral), O (pentagonalicositetrahedral), O^h (hexacisoctahedral).

Of these five groups of crystal classes, 1,2,4 and 5 show the Laue symmetry of holohedral classes, i.e., D_2^h, D_4^h, D_6^h and O^h, respectively. In the Laue method all classes in these four groups appear to possess a plane of symmetry normal to the principal axes and planes of symmetry containing this axis whether or not such planes actually are present in the crystal.

Laue diagrams of the fifth group of classes, having the Laue symmetry of D_3^d, however, show only planes of symmetry containing the principal axis and no symmetry plane normal to this axis.

Unless this is recognized, some confusion may arise in practice when Laue photographs are obtained of crystals belonging to the classes under discussion. For example, in

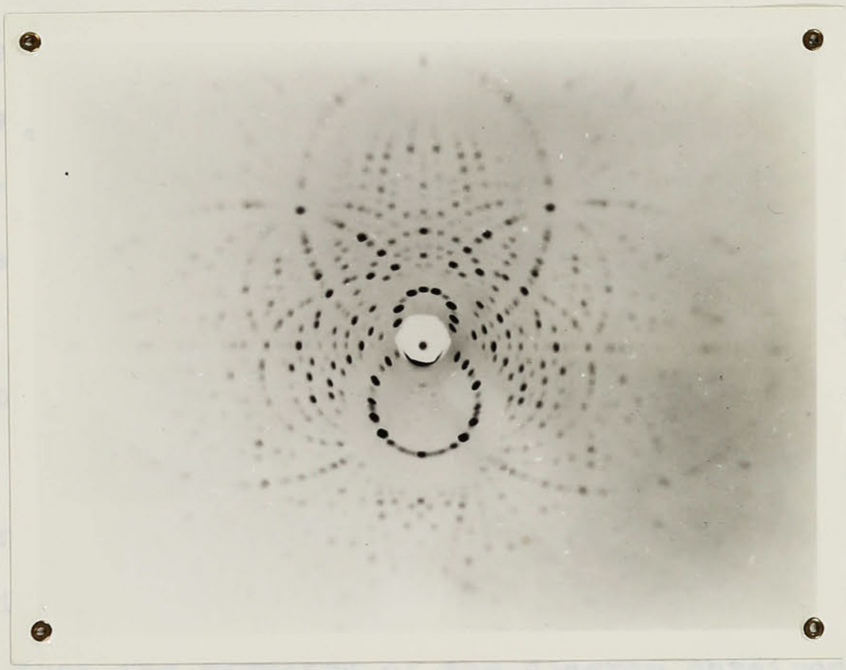

<u>FIGURE 1</u>

<u>Tourmaline</u>

(Polished Slip)

Beam along b axis

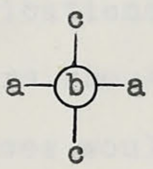

Figure 1, the diagram for tourmaline (C_3^v) with the beam along the b (orthohexagonal) axis is not symmetrical about the trace of the plane normal to the c axis. It appears to be set incorrectly about an axis perpendicular to the c axis and parallel to the diagram. Actually the photograph for Figure 1 was obtained as follows. A slip of tourmaline was polished with plane parallel sides of area much larger than the cross-sectional area of the X-ray beam. The plane of the polished surfaces coincided with the $(10\bar{1}0)$ plane to within 10 and 15 minutes of arc, respectively, in the prism zone and in the zone normal to the prism. The crystal slip was set optically so that the $(10\bar{1}0)$ plane was normal to the direction of the X-ray beam. The beam, therefore, coincided almost exactly with the b (orthohexagonal) axis.

That the symmetry of the diagram obtained, namely, only about the trace of the symmetry plane $(11\bar{2}0)$, is that which should be expected is clear from the following argument.

In Figure 2A, $\bar{a}0a$, $\bar{b}0b$, $\bar{c}0c$ are three straight lines intersecting at 0 and making angles of 90° with one another.

The figure MNPQRS is drawn as a regular bipyramid to avoid unnecessary complications. In the general case each of the points at the corners should consist of four points so that the indices of the faces would be (hkl), $(\bar{h}kl)$, $(h\bar{k}l)$, $(\bar{h}\bar{k}l)$, $(hk\bar{l})$, $(\bar{h}k\bar{l})$, $(h\bar{k}\bar{l})$, $(\bar{h}\bar{k}\bar{l})$, where h, k, and l have different values in each set of indices.

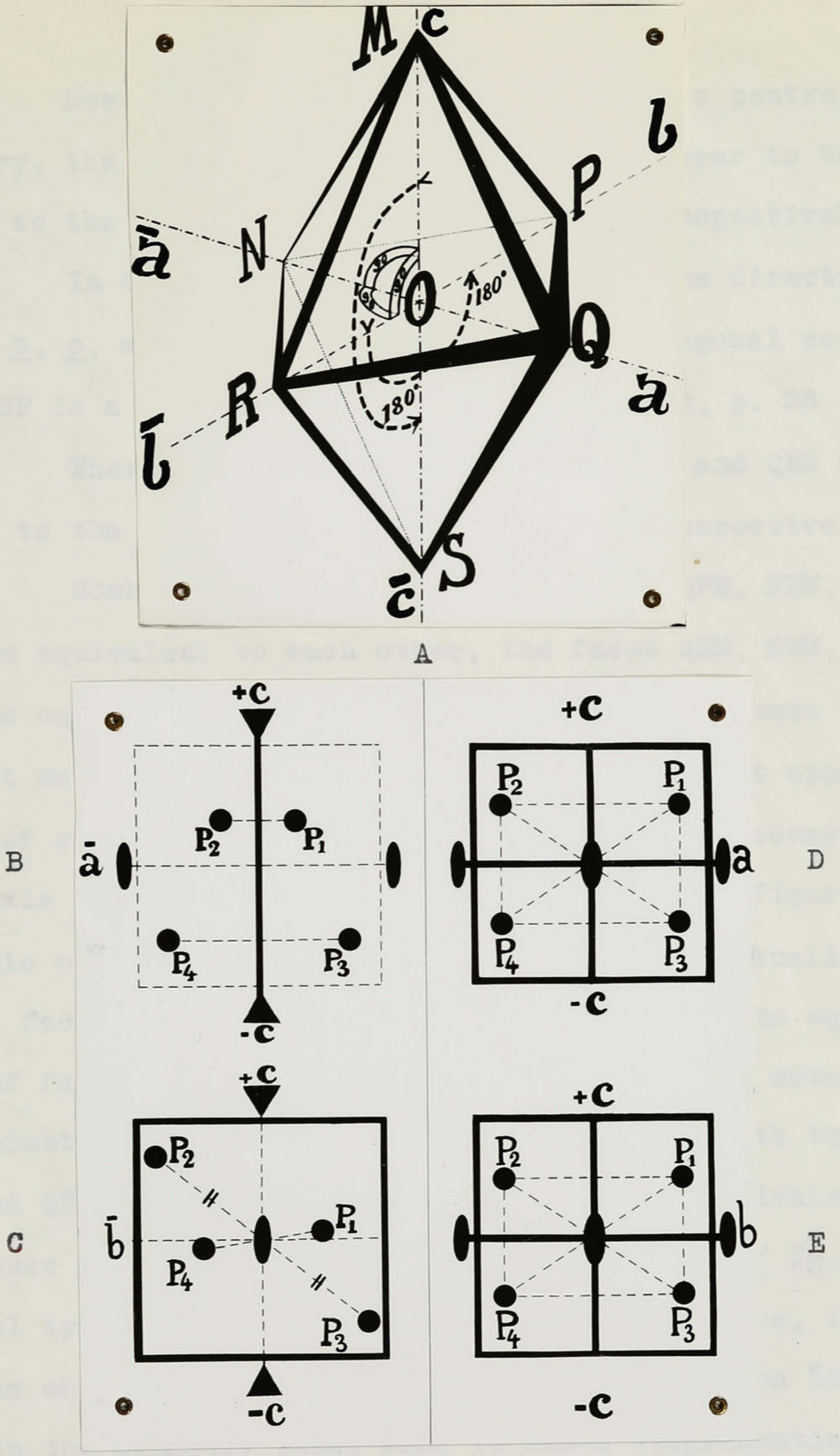

FIGURE 2

Schematic Diagrams illustrating

Laue Symmetry of Orthogonal Crystals

Beam along lateral axes.

Now, since the Laue method makes 0 a centre of symmetry, the faces NRS, QRS, QPS and NPS appear to be equivalent to the faces QPM, NPM, NRM and QRM, respectively ..... 1.

In tourmaline, $\bar{a}0a$, $\bar{b}0b$, $\bar{c}0c$ are the directions of the <u>a</u>, <u>b</u>, <u>c</u>, axes, respectively, in orthohexagonal coordinates, and MRSP is a plane of symmetry (see Appendix, p. 23).

Therefore, the faces QPM, QRM, QPS and QRS are equivalent to the faces NPM, NRM, NPS and NRS, respectively ..... 2.

Combining data 1 and 2, the faces QPM, NPM, QRS and NRS are equivalent to each other, the faces QRM, NRM, NPS and QPS are equivalent to each other, but these two sets of faces are not mutually equivalent. Hence QPNR does not appear as a plane of symmetry. It will be noted that $\bar{a}0a$ becomes a two-fold axis of symmetry because a rotation of the figure through an angle of 180° about $\bar{a}0a$ as axis brings the mutually equivalent faces NPM and QPM into coincidence with the equivalent pair of faces NRS and QRS, respectively, and the mutually equivalent faces NRM and QRM into coincidence with the faces NPS and QPS, respectively, to which they are equivalent. Thus the space group C_3^v possesses the Laue symmetry of D_3^d. The general type of symmetry to be expected, therefore, in a Laue diagram obtained with the beam along the direction $\bar{b}0b$ which lies in the symmetry plane MRSP is shown diagrammatically in Figure 2B. The points P_1, P_2, P_3, P_4 arise from the general pairs of planes $(h\bar{k}l)$, $(\bar{h}k\bar{l})$; $(\bar{h}\bar{k}l)$, $(hk\bar{l})$; $(h_1\bar{k}_1\bar{l}_1)$, $(\bar{h}_1k_1l_1)$;

$(h_1k_1l_1)$, $(\bar{h}_1\bar{k}_1\bar{l}_1)$ respectively, where h, k and l have not the same values as h_1, k_1 and l_1, respectively. The diagram is symmetrical only about the trace of the plane MRSP, shown as a full line in Figure 2B.

Similarly, since $\bar{a}0a$ appears to be a two-fold axis of symmetry, the type of Laue diagram obtained with the beam along this axis may be represented diagrammatically as in Figure 2C where the points P_1, P_2, P_3, P_4 arise from the general pairs of planes $(\bar{h}\bar{k}l)$, $(hk\bar{l})$; $(\bar{h}_1k_1l\ )$, $(h_1\bar{k}_1\bar{l}_1)$; $(\bar{h}_1\bar{k}_1\bar{l}_1)$, $(h_1k_1l_1)$; $(\bar{h}k\bar{l})$, $(h\bar{k}l)$, respectively, where h, k and l have not the same values as h_1, k_1 and l_1, respectively. The diagram exhibits only the trace of the two-fold axis normal to the diagram (shown as an ellipse at the centre) and consequently possesses only a centre of symmetry.

The same types of diagrams are obtained from crystals belonging to the classes D_3 and D_3^d since these classes also have the Laue symmetry of D_3^d.

As mentioned above, the other four groups of classes under examination exhibit Laue symmetry elements which make the plane QPNR appear as a plane of symmetry in addition to the plane MRSP. It will be seen that this makes the two sets of faces 1 and 2 mutually equivalent, so that QMNS also is a plane of symmetry, and the Laue diagrams with the beam along $\bar{b}0b$ and along $\bar{a}0a$, respectively, will have the general appearance shown in Figures 2D and 2E. They are symmetrical about the traces of the planes QPNR and MRSP (shown by full lines) which intersect in the traces of the two-fold axes $\bar{b}Ob$ and $\bar{a}Oa$, respectively, which are indicated by ellipses. They are symmetrical, therefore, about two lines at right angles intersecting in a centre of symmetry. The points P_1, P_2, P_3, P_4 arise from the four pairs of the eight sets of planes constituting the general form $\{hkl\}$, where h, k, and l have the same values, respectively, in each set of planes of the form. In the special case of the classes having the Laue symmetry of the class O^h (hexacisoctahedral), in which $\bar{a}Oa$ (or $\bar{b}Ob$) appears as a four-fold axis, the distances P_1P_3, P_1P_2, P_2P_4 and P_3P_4 in Figures 2D and 2E are all equal when the beam is along one of these two axes.

Figure 3 shows a Laue photograph of calamine (hemimorphite), class C_2^v, taken with the X-ray beam along a _b_ axis. It has the symmetry characteristics of Figure 2D.

In addition to tourmaline (C_3^v) and calamine (C_2^v), single crystal specimens of chalcopyrite (D_2^d), calcite (D_3^d), greenockite (C_6^v) and tetrahedrite (T^d) were examined and each showed the Laue symmetry to be expected from its class on the basis of the foregoing argument.

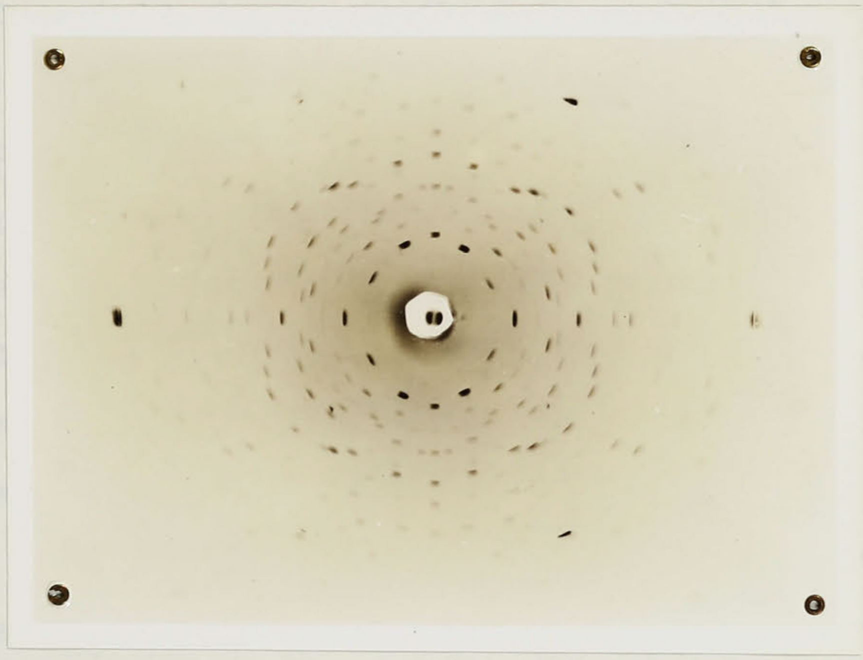

FIGURE 3

Calamine (Hemimorphite)

Beam along b axis

PART II

AN X-RAY METHOD FOR DISTINGUISHING BETWEEN CERTAIN SPACE GROUPS IN THE HEXAGONAL SYSTEM

(a) Introduction.

One of the difficulties which may be encountered in determining the space group of a given crystal belonging to one of certain classes in the hexagonal system arises from the fact that the conventional crystallographic axes do not always correspond to the true structural axes. This applies to the space groups of the ditrigonal bipyramidal (D_3^h) class of the hexagonal division, and to those of the ditrigonal pyramidal (C_3^v), trigonal trapezohedral (D_3), and ditrigonal scalenohedral (D_3^d) classes of the rhombohedral division whose structures are based on a hexagonal lattice (Γ_h).

This point has been emphasized particularly by Astbury and Yardley (9). In referring to their tabulated data on the hexagonal space groups they point out, that "it will be found that only in a very limited number of cases is it possible without complete examination to distinguish between groups in which the true structural hexagonal axes lie in the symmetry planes (C_{3v}^2, C_{3v}^4, D_{3h}^3, D_{3h}^4) and the corresponding groups in which they are perpendicular to the symmetry planes (C_{3v}^1, C_{3v}^3, D_{3h}^1, D_{3h}^2). For example, we can distinguish between C_{3v}^1 and C_{3v}^2 if there are two molecules only per cell, for then the molecule itself must possess a triad axis, and this is only possible in C_{3v}^2; but the tables alone do not distinguish between them if there are one, three or six molecules per cell. Similar considerations hold with regard to the pairs of groups in which the true hexagonal axes are parallel and perpendicular respectively to the dyad axes of the structure (D_3^2 and D_3^1; D_3^4 and D_3^3; D_3^6 and D_3^5; D_{3d}^3 and D_{3d}^1; D_{3d}^4 and D_{3d}^2)".

As will be established later, the crystal with which this thesis primarily is concerned belongs to the trigonal trapezohedral (D_3) class. It is of interest, therefore, to consider the symmetry elements of the nine pairs of space groups mentioned in the foregoing excerpt because it can be shown that, except in two cases, the Laue method of X-ray analysis is capable of allowing the correct choice to be made between the members of each pair.

The final choice of space group for rubidium dithionate, to be described in Section II of this thesis, was made possible by the application of the general experimental methods now to be described.

(b) Theoretical Argument.

The problem is simplified by an examination of the stereographic projections for the four crystal classes which contain the nine pairs of space groups under discussion. They are shown in Figure 4. The crystallographic ($\underline{a}$) axes are drawn as broken lines except where they lie in planes of symmetry when they are represented by full lines. They are marked $\underline{a}_1$, $\underline{a}_2$ and $\underline{a}_3$. It is convenient to introduce another set of axes in the

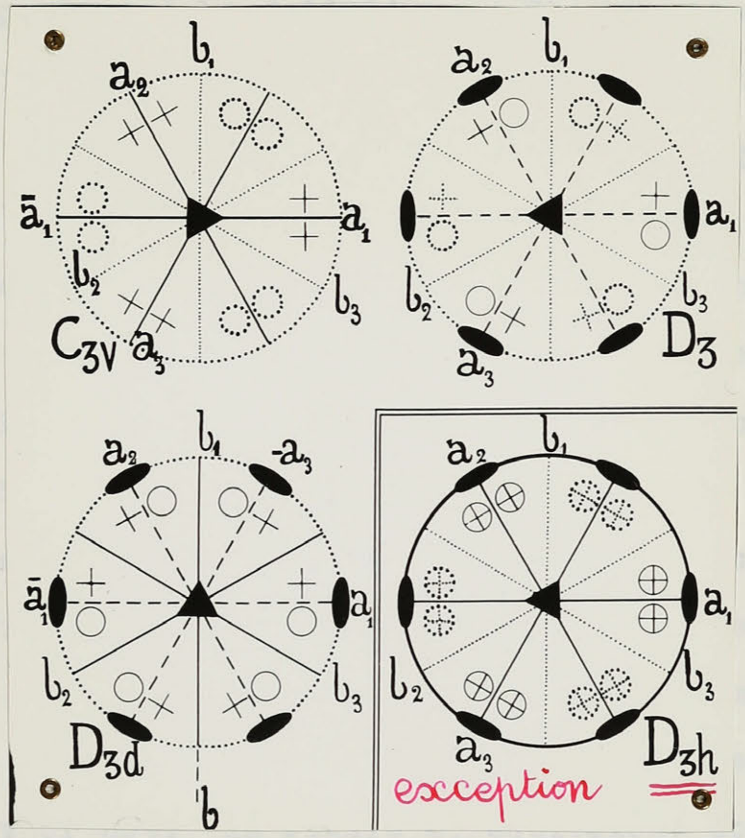

exception

FIGURE 4

Stereographic Projections

C_3^v, D_3, D_3^d, D_3^h

same plane as the *a* axes but at 30° to them. These are shown as dotted lines except when they lie in planes of symmetry when they are represented by full lines. They are marked $\underline{b}_1$, $\underline{b}_2$ and $\underline{b}_3$ and it will be seen that any given *b* axis makes angles of 30° and 90° with *a* axes (*e.g.*, $\underline{b}_2$ is at 30° to $\underline{a}_1$ and at 90° to $\underline{a}_2$). Following the usual convention, planes of symmetry perpendicular to the plane of projection are represented by full lines, two-fold rotation axes in the projection plane by ellipses, the triad (*c*) axes perpendicular to the plane of projection by equilateral triangles, equivalent points above the plane as crosses and below the plane as circles.

Since the Laue method is unable to distinguish a plane (hkl) from the parallel plane $(\bar{h}\bar{k}\bar{l})$ this method introduces an apparent centre of symmetry whether such a centre is present structurally or not. In Figure 4, equivalent points arising from this limitation of the X-ray method are shown as dotted crosses (above projection plane) and dotted circles (below projection plane). As a result it will be seen from the diagrams that the *b* axes become dyad axes in C_3^v, lie in planes of symmetry in D_3, and become dyad axes in planes of symmetry in D_3^h. This results in the well-known fact cited in Part I that C_3^v and D_3 appear as D_3^d and D_3^h appears as D_6^h, in Laue photographs taken with the beam along the principal (*c*) axis.

With the exception of the four space groups of the class D_3^h, the pairs under consideration can be grouped in two divisions as follows according to the symmetry to be expected from Laue photographs.

1. C_{3v}^1, C_{3v}^3, D_3^2, D_3^4, D_3^6, D_{3d}^3, D_{3d}^4, in which a axes coincide with dyad axes of rotation and b axes lie in symmetry planes perpendicular to the basal plane ($\perp$ to $\{0001\}$).

2. C_{3v}^2, C_{3v}^4, D_3^1, D_3^3, D_3^5, D_{3d}^1, D_{3d}^2, in which b axes coincide with dyad axes of rotation and a axes lie in symmetry planes perpendicular to the basal plane ($\perp$ to $\{0001\}$).

The Laue diagram obtained with the X-ray beam along an a axis, therefore, should show only a dyad axis through the undiffracted beam perpendicular to the photographic plate (Figure 2C, p.10A) if the space group is one of those in division 1 while the Laue photograph with the beam along a b axis should show one plane of symmetry perpendicular to the photographic plate (Figure 2B, p.10A).

Conversely, if the space group is one of those in division 2, the Laue diagram along the a axis should possess the plane of symmetry while that along the b axis should show only the dyad axis.

No such distinction however can be made between D_{3h}^3 and D_{3h}^1, or between D_{3h}^4 and D_{3h}^2, because it is clear from Figure 4 that in the Laue method both the a and b axes will appear to coincide with dyad axes in planes of symmetry. Hence Laue diagrams obtained with the beam along either an a or b axis will possess two planes of symmetry intersecting at right angles as in Figures 2D and 2E, p.10A.

(c) Procedure.

The following experimental procedure, therefore, can be adopted with success in the space group examination of crystals belonging to the five classes (except D_3^h) under review.

Following the usual methods (e.g., 9, p.221) possible space groups are reduced to one of the pairs given in divisions 1 and 2 above, recognizing the fact that D_3^3 and D_3^4 are identical with D_3^5 and D_3^6, respectively, except that they are in opposite rotatory sense.

The crystal is then mounted on a spectrograph equipped with goniometric arcs and a Laue photograph is taken with the beam along the c axis. The time consumed in obtaining a good symmetrical Laue diagram along the c axis is very much reduced if a crystal is available which has at least one recognizable face. Otherwise a number of successive photographs may have to be taken with intermediate calculations and settings on the arcs before the c axis is made to coincide with the direction of the X-ray beam.

Since the a and b axes are important zone axes their positions are readily identified on the c axis Laue diagram by simple visual examination. The crystal is then turned on the arcs so as to bring one of these axes into coincidence with the axis of rotation of the spectrograph, leaving the c axis along the direction of the X-ray beam. If there is any doubt as to whether an a or a b axis is now in the axis of rotation, an oscillation photograph is taken and the primitive translation along the axis of rotation is obtained. Suppose that the axis of rotation coincides with the a axis. Then in this position the crystal is set with the c axis along the direction of the beam, the a axis in the axis of rotation and hence a b axis lies parallel to the photographic plate (at 90° to a plane containing the a and c axes). The crystal is rotated through 90° thus placing a b axis in coincidence with the direction of the X-ray beam and a second Laue picture is taken along the b axis. The crystal in this position has an a axis in the axis of rotation, a b axis along the beam and the c axis parallel to the plate (at 90° to a plane containing the a and b axes). Finally the crystal is rotated on the arcs through 30° about the c axis thus placing a b axis in the axis of rotation of the spectrograph and an a axis along the direction of the beam and a third Laue picture is taken with the beam along the a axis. This may be followed by a second oscillation picture from which the primitive translation along the new axis of rotation can be calculated.

If the primitive translation along the a axis is a_0, then that along the b axis is equal to $a_0\sqrt{3}$ so that, from the two oscillation photographs mentioned above, the positions of the a and b axes can be determined and the second and third

Laue photographs can be identified as along the b and a (or a and b) axes, respectively.

The symmetry of the Laue diagrams along the a and b axes immediately shows whether the space group is one of those in division 1 or division 2.

(d) Experimental Test.

One of the best established structures based on a space group falling within the scope of this method is that of α-quartz (10, pp. 239,242). This crystal has been assigned to the space group D_3^4 (and D_3^6) with a_0 equal to 4.9Å. and c_0 equal to 5.39Å.

A Laue photograph with the X-ray beam along the c axis of a crystal of quartz is shown in Figure 5. Radiation from a molybdenum target was employed. An oscillation picture of the crystal without change of setting gave a value of about 4.9Å. for the primitive translation along the axis of rotation. Hence in the Laue diagram (Figure 5) an a axis is vertical and a b axis is horizontal. The crystal was turned through 90° about the vertical a axis and a Laue picture was taken along the b axis. This photograph is reproduced in Figure 6 and shows a horizontal plane of symmetry. The crystal was then rotated through 30° about a horizontal axis perpendicular to the direction of the beam, thus making an a axis coincide with the direction of the X-ray beam. A Laue photograph of the crystal in this position is given in Figure 7, which possesses

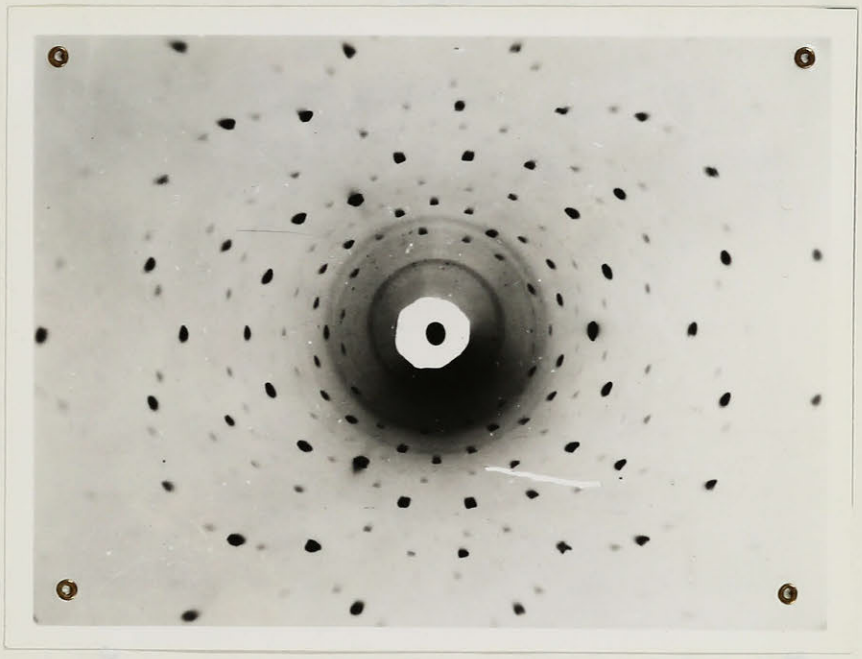

FIGURE 5

α-Quartz

Beam along c axis

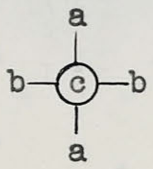

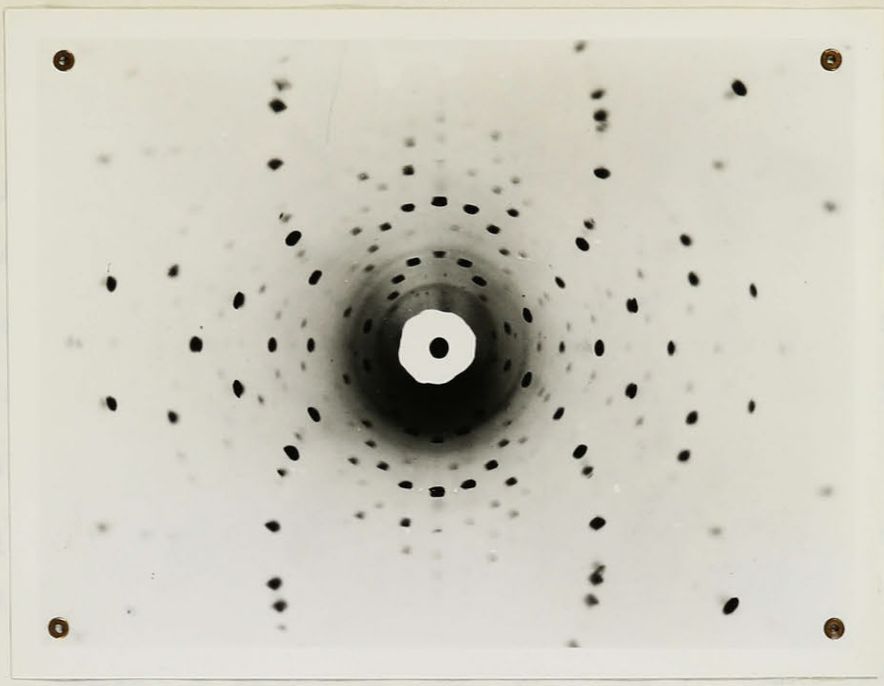

FIGURE 6

α-Quartz

Beam along b axis

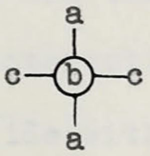

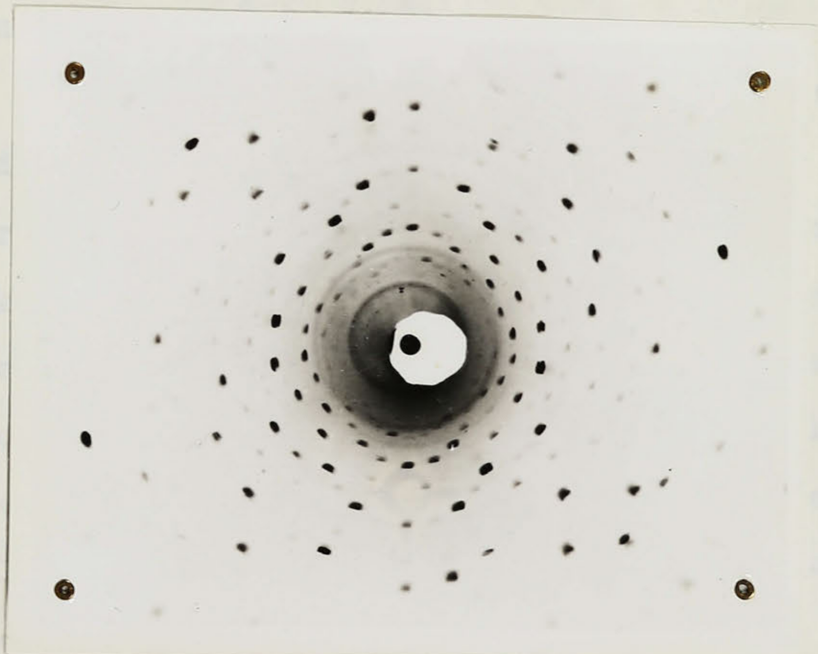

FIGURE 7

α-Quartz

Beam along a axis

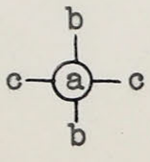

only a dyad axis of symmetry through the central beam perpendicular to the plane of the picture. An oscillation picture of the crystal without change of setting showed a primitive translation of about 8.5Å. along the axis of rotation. Hence a b axis is vertical ($b_o = a_o\sqrt{3} = 8.49$Å) and an a axis coincides with the direction of the beam in Figure 7.

Figure 5 exhibits the symmetry of D_3^d. The c axis is thirded as can be shown by a search for reflections from the planes $\{0001\}$. The space group therefore is D_3^3 (and D_3^5) or D_3^4 (and D_3^6) since these are the only space groups in C_3^v, D_3 or D_3^d having this characteristic. Finally, from the data above, the dyad axes coincide with the a axes so that the space group must be D_3^4 (and D_3^6).

In many cases the experimental procedure may be simplified. For example, if the size of the unit cell has been determined previously, a single oscillation picture will show which is the a or b axis and, if the space group has been unequivocally reduced to one of the pairs specified, then a Laue photograph either along an a or a b axis will give the position of the dyad axes. Thus two Laues and one oscillation would yield sufficient data for the final choice of space group to be made between the members of any pair.

(e) Discussion.

The advantages of the method described above can be brought out by an examination of the literature pertaining to the determination of the space group of potassium dithionate. Barnes and Helwig (2) reduced the possible space groups to D_3^1 or D_3^2 but made no attempt to choose between these two. Huggins and Frank (4) arrived at D_3^2 by an extensive comparison of intensities. This involved working out two structures for the crystal simultaneously, based on D_3^1 and D_3^2, respectively, and eliminating that based on D_3^1 as not satisfying observed intensity requirements. Such a procedure involves a great deal of extra labour which is saved if the choice of space group can be made before placing the diffracting centres in the unit cell. Helwig (3) showed that the space group must be D_3^2 by identifying the position of a dyad axis in the structure from a crystallographic examination of a crystal of the salt, measuring the primitive translation along this axis with the X-ray spectrometer and thus proving that the dyad axes coincide with the a axes. This method, however, involves the use of a crystal having a sufficient number of well-developed faces to allow the direction of the dyad axes (D_3, D_3^d) or symmetry planes (C_3^v, D_3^d) to be fixed. It is not applicable to a crystal or crystal fragment having no, or very few, identifiable faces. Finally Hägg (5) reported the space group of potassium dithionate as D_3^2 on the basis of the fact that the dyad axes are parallel to the shortest identity period of the basal plane, that is, coincide with the structural a axes, without giving the experimental procedure by which he located the dyad axes in the crystal and thus reached this conclusion.

As a further test of the simple method described in the present section, it was applied to a fragment of a crystal of potassium dithionate. The Laue diagrams obtained with the beam along *a* and *b* axes possessed a dyad axis and a plane of symmetry, respectively, and thus further confirmed the space froup as D_3^2.

The advantages of this method, therefore, are due to its simplicity, its applicability to crystal fragments having no identifiable faces and to the saving of labour arising from the fact that it allows the final choice of space group to be made without reference to the relative positions of the diffracting centres in the unit cell.

APPENDIX TO SECTION I

THE SPACE GROUP OF TOURMALINE

(a) Introduction.

The crystal structure of tourmaline has been investigated by Kulaszewski (11) and by Machatschki (12). The crystal belongs to the ditrigonal pyramidal (C_3^v) class of the hexagonal system (13, v.1, p. 348; 14, v.2, p. 742 although misprinted as ditrigonal bipyramidal on p. 744).

Kulaszewski made a study of a clear rose-red crystal from the Wolkenburg and Penig region in Saxony. She indexed the Laue diagrams obtained with the X-ray beam (tungsten radiation) perpendicular respectively to (0001), $(01\bar{1}1)$, $(11\bar{2}0)$, $(10\bar{1}1)$, $(50\bar{5}2)$, and $(10\bar{1}0)$, and the spectrograms obtained with the beam (molybdenum K_α radiation) parallel to (0001), $(01\bar{1}1)$, $(11\bar{2}0)$, $(10\bar{1}1)$, $(01\bar{1}0)$, and $(10\bar{1}0)$, respectively. From the Laue photographs she concludes that the underlying lattice is hexagonal (Γ_h) since the Bravais-Miller indices of the majority of planes from which reflections were recorded do not satisfy the rhombohedral criterion that $h-i-l = 3p$ (15,16), where the indices are taken as $(hikl)$ instead of the more customary $(hkil)$, and p is an integer. The size of the unit cell is given in Table II below. The oscillation photographs showed a thirding of the c axis and of that perpendicular to $(10\bar{1}0)$, i.e., the b axis in orthohexagonal coordinates. Data for the hexagonal lattice eliminate the space groups C_{3v}^5 and C_{3v}^6 which are based on Γ_{rh}. The thirding of $\{0001\}$ eliminates C_{3v}^3 and C_{3v}^4 since for these space groups the (0001) spacing should be equal to $1/6\ c_o$ if the c axis is thirded. Kulaszewski concludes that the space group must be either C_{3v}^1 or C_{3v}^2 but that "eine Entscheidung, ob C_{3v}^1 vorleigt oder C_{3v}^2, kann vorläufig nicht getroffen werden". The number of formula weights per cell was not determined because of the scarcity of accurate chemical analyses of tourmaline claimed for the time.

Machatschki, in a paper largely devoted to an attempt at the establishment of a chemical formula to represent the composition of tourmaline, reports the results of a c axis rotation photograph of a black crystal from Grundesund, Norway, and a spectrometric examination of a pale red specimen from San Diego, California, and of a pale rose-red tourmaline from Pala, California. His results for the size of the unit cell are given in Table II below. From the data obtained, chiefly with the crystal from San Diego, he identifies reflections from other planes which confirm the underlying lattice as hexagonal and not rhombohedral. He finds that $\{0001\}$ is thirded, thus eliminating C_{3v}^3 and C_{3v}^4, and concludes that the space group must be either C_{3v}^1 or C_{3v}^2 with three formula units of the type $XY_9Si_6B_3H_xO_{31}$ per cell.

In connection with the development of the method for distinguishing between certain pairs of space groups in the hexagonal system described in Part II of this section of the thesis, tourmaline offered an interesting case for application of the method since in neither of the previous investigations was any attempt made to choose between C_{3v}^1 and C_{3v}^2. Furthermore the writer had at his disposal a crystal of a clear bottle-green colour in contrast to the black and red specimens previously examined so that the present investigation extends the study of tourmalines to that variety. Unfortunately no record of the origin of the green crystal could be found.

(b) X-ray Examination and Results.

Before proceeding with the assignment of tourmaline to either C_{3v}^1 or C_{3v}^2 an investigation of certain important sets of planes was made by the use of the single crystal oscillation method on a Bernal Photogoniometer (17) with cylindrical camera. The K_α radiation from a copper target in a Shearer X-ray tube equipped with a nickel filter was employed. Due to the number of data presented by Kulaszewski and by Machatschki it was not deemed necessary to make a complete examination of the crystal but simply to check their data as a precautionary measure in eliminating all space groups except C_{3v}^1 and C_{3v}^2.

Reflections from planes having the indices given in Table I below were sought for with the results indicated. The indices of planes from which reflections were observed are marked p while those from which no reflections were recorded are labelled a. The determination of reflection positions and the indexing of the oscillation photographs were carried out by the reciprocal lattice method (18).

TABLE I

1.	2.	3.	4.	5.	6.	7.
(0001) a	$(10\bar{1}0)$ a	$(10\bar{1}1)$ p	$(10\bar{1}1)$ p	$(20\bar{2}1)$ p	$(11\bar{2}0)$ p	$(11\bar{2}1)$ a
(0002) a	$(20\bar{2}0)$ a	$(20\bar{2}2)$ a	$(10\bar{1}2)$ p	$(20\bar{2}2)$ a	$(22\bar{4}0)$ p	$(11\bar{2}2)$ a
(0003) p	$(30\bar{3}0)$ p	$(30\bar{3}3)$ p	$(10\bar{1}3)$ a	$(20\bar{2}3)$ a	$(33\bar{6}0)$ a	$(11\bar{2}3)$ p
(0004) a	$(40\bar{4}0)$ a	$(40\bar{4}4)$ a	$(10\bar{1}4)$ p	$(20\bar{2}4)$ p	$(44\bar{8}0)$ p	$(11\bar{2}4)$ a
(0005) a	$(50\bar{5}0)$ a	$(50\bar{5}5)$ p	$(10\bar{1}5)$ p	$(20\bar{2}5)$ p	$(55\overline{10}.0)$p	$(11\bar{2}5)$ a
(0006) p	$(60\bar{6}0)$ p	$(60\bar{6}6)$ p	$(10\bar{1}6)$ p	$(20\bar{2}6)$ p	$(66.\overline{12}.0)$p	$(11\bar{2}6)$ p

The size of the unit cell is given in Table II. The values of a_0 and c_0 were determined with a probable error of less than 1%.

TABLE II

Unit Cell Dimensions of Tourmaline

Origin	Colour	a_o	c_o	c/a	Reference
Saxony	rose-red	16.23Å.	7.26Å.	0.44805	Kulaszewski (11)
Norway	black	16.02Å.	7.22Å.	0.4507	Machatschki (12)
Pala, Calif	pale red	15.87Å.	7.13Å.	0.4491	"
San Diego, Calif..	rose-red	15.81Å.	7.10Å.	0.4490	"
(Unknown)	green	15.85Å.	7.07$_5$Å.	0.4464	This thesis

The differences among the unit cell dimensions shown in this table are not surprising in view of the variations in composition possessed by tourmalines from different localities. They are in agreement with the range of values for the axial ratio (c/a) based on the results of crystallographic studies, for example, 0.4474 (14,v.1, p.744), 0.44805 (19), 0.45130 (19), and 0.54149 (19).

Since the observed ratio c/a agrees with the crystallographic value it is probable that the lattice is Γ_h. From the data in columns 1, 2, 3, and 6 of Table I it will be seen that those reflections which are obtained for the first six orders of (0001), (10$\bar{1}$0), (10$\bar{1}$1), and (11$\bar{2}$0) occur at the positions on the films calculated on the assumption that the lattice is hexagonal. Spots were not obtained at positions corresponding to the spacings of the corresponding planes (111), (1$\bar{2}$1), (100), and (1$\bar{1}$0), respectively, of a rhombohedral lattice based on the same c/a ratio. It should be noted that all oscillations were taken over angular ranges such as to exclude reflections from sets of planes having spacings approaching those of the particular set of planes under examination.

These data, therefore, show by another method of investigation that the underlying lattice is Γ_h (9, p.246). This eliminates C_{3v}^5 and C_{3v}^6 from further consideration since both of these space groups are based on Γ_{rh} (9, p.248).

The data in columns 1, 3, 4, and 5 of Table I show that $\{m0\bar{m}l\}$ is not halved when l is odd. Hence the space group cannot be C_{3v}^3 (9, p.248).

Finally, C_{3v}^4 is not possible since the data in columns 1 and 7 of Table I show that $\{mm\overline{2m}l\}$ is not halved when l is odd (9, p.248).

This leaves only C_{3v}^1 and C_{3v}^2 as possible space groups for tourmaline and is in agreement with the results of the earlier investigations.

In addition to the thirding of $\{000l\}$ and $\{10\bar{1}0\}$ observed by Kulaszewski it may be noted that the present data indicate that reflections from planes of the form $\{11\bar{2}l\}$ appear only when l is an integral multiple of 3 (see column 7, Table I), and from planes of the form $\{m0\bar{m}3\}$ only when m is an integral multiple of 3 (see, for example, $(10\bar{1}3)$, $(20\bar{2}3)$, and $(30\bar{3}3)$, and some evidence was obtained for the absence of reflections from $(40\bar{4}3)$ and $(50\bar{5}3)$ and the presence of one from $(60\bar{6}3)$).

Having confirmed the space group as either C_{3v}^1 or C_{3v}^2 a series of Laue photographs was taken, using the radiation from a molybdenum target in the X-ray tube.

The crystal was mounted with the *c* axis along the beam. The Laue diagram (Figure 8) showed the symmetry D_3^d which is in agreement with the crystallographic assignment of tourmaline to the class C_3^v. From the positions of the spots on this photograph the directions of the *a* and *b* (orthohexagonal) axes were identified. The position of the crystal was altered on the arcs so as to make one of these directions coincide exactly with the axis of rotation of the spectrograph. The position of the layer lines on an oscillation picture with the crystal in this setting showed that an *a* axis was in the axis of rotation. The crystal was turned through an angle of 90° about this axis from the position occupied for the Laue picture with the beam along the *c* axis, thus making a *b* axis coincide with the direction of the beam. The Laue diagram obtained with the crystal in this position showed a horizontal plane of symmetry (Figure 9). The *b* axis, therefore, lies in a plane of symmetry which passes through the *c* axis.

Finally the crystal was rotated through an angle of 30° about the *c* axis thus placing a *b* axis in the axis of rotation and an *a* axis along the direction of the beam. The Laue diagram obtained with the crystal in this setting exhibited only a centre of symmetry (Figure 10). The *a* axis, therefore, appears to lie in a dyad axis of symmetry.

From these observations the space group of tourmaline

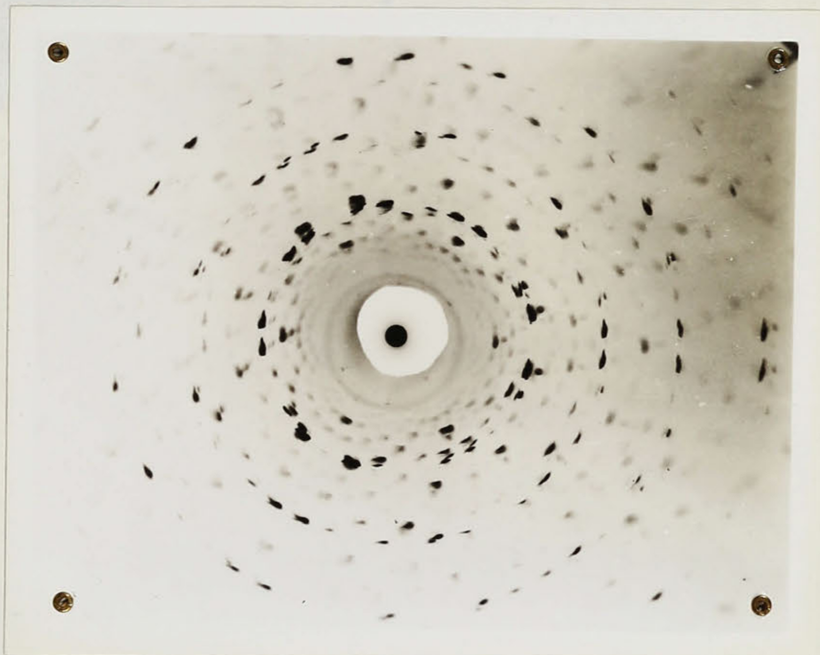

FIGURE 8

Tourmaline

Beam along c axis

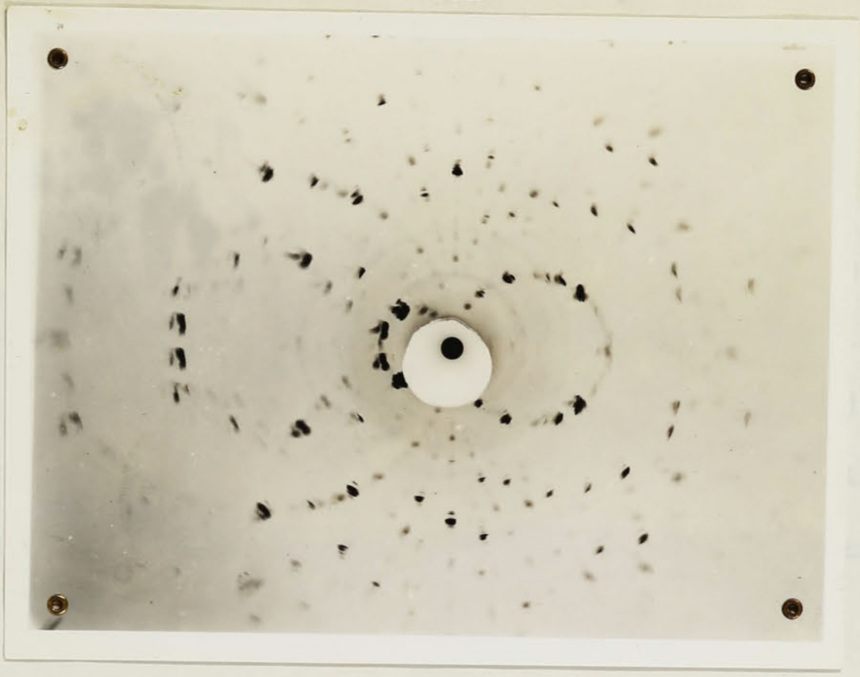

FIGURE 9

Tourmaline

Beam along b axis

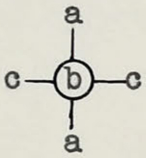

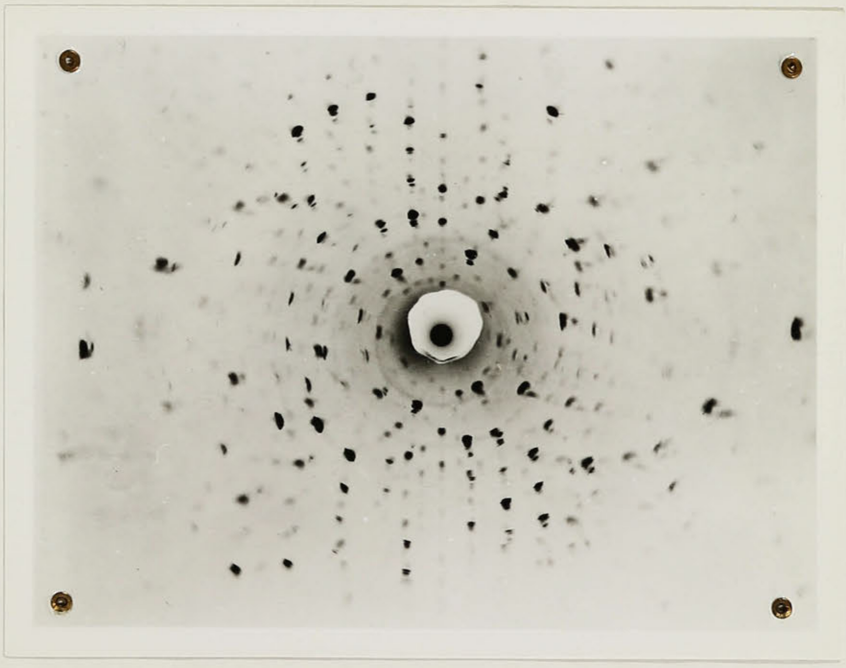

FIGURE 10

Tourmaline

Beam along a axis

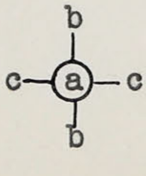

must be C_{3v}^1 and cannot be C_{3v}^2 (see p.17).

In conclusion it is of interest to note that Figures 8, 9, and 10 exhibit the same symmetry elements as the corresponding figures on pages 88, 99, and 104, respectively, of the paper by Kulaszewski (11) so that the distinction between C_{3v}^1 and C_{3v}^2 might have been made at that time.

SECTION II

THE STRUCTURE OF RUBIDIUM DITHIONATE

SECTION II

TABLE OF CONTENTS

INTRODUCTION TO SECTION II

The space group of potassium dithionate was established by Barnes and Helwig (2) in 1931 as D_3^1 or D_3^2.

Later in the same year Huggins and Frank (4) and Helwig (3) reported the results of complete structure investigations of this salt. Both structures are in agreement on the following points: space group, D_3^2; number of formula units ($K_2S_2O_6$) per cell, 3; special positions (20, p. 154),

2S in (c) : $00u;\ 00\bar{u}$

4S in 2(d) : $1/3,\ 2/3,\ u;\ 2/3,\ 1/3,\ \bar{u}$

3K in (e) : $uu0;\ 0\bar{u}0;\ \bar{u}00$

3K in (f) : $uu,\ 1/2;\ 0\bar{u},\ 1/2;\ \bar{u}0,\ 1/2$

18O in 3(g) : $xyz;\ y-x,\ \bar{x}z;\ \bar{y},\ x-y,\ z;$

$yx\bar{z};\ \bar{x},\ y-x,\ \bar{z};\ x-y,\ \bar{y}\bar{z}$

There is, however, marked disagreement between the two sets of numerical values proposed for the fourteen undetermined parameters involved, particularly between those for oxygen. This is evident from a comparison between columns 3 and 4 of Table I. Better agreement is obtained by interchanging Helwig's x and y coordinates as in column 5 of Table I. This has been pointed out by Wyckoff (22, p. 60).

TABLE I

Reported Parameters for $K_2S_2O_6$

Atom	Special Positions	Helwig (3)	Huggins and Frank(4,21)	Helwig (revised)
S	(c)	0, 0, .16	0, 0, .16	0, 0, .16
S	(d)	2/3, 1/3, .27	1/3, 2/3, .27	1/3, 2/3, .27
S	(d)	2/3, 1/3, .59	1/3, 2/3, .59	1/3, 2/3, .59
K	(e)	.39, .39, 0	.375, .375, 0	.39, .39, 0
K	(f)	.31, 0, .50	.690, .690, 1/2	.69, .69, 1/2
O	(g)	.18, .09, .22	.165, .11, .23	.09, .18, .22
O	(g)	.48, .24, .65	.615, .17, .34	.48, .24, .35
O	(g)	.58, .42, .21	.505, .21, .80	.58, .42, .79

Helwig (3) has criticized the structure proposed by Huggins and Frank (4) on the grounds that their diagram for the projection of the unit cell on the basal plane possesses a lower symmetry than that of D_3^2 and that certain planes which should scatter with equal intensities are reported to have very different *F* values (e.g., ($11\bar{2}0$), 54; ($\bar{1}2\bar{1}0$), 85: ($33\bar{6}0$), 37; ($6\bar{3}\bar{3}0$), 68). Helwig admits that in his own suggested structure there is an appreciable discrepancy between calculated and observed intensities for ($33\bar{6}0$) and for ($44\bar{8}0$) and concludes that "a small adjustment to the structure is perhaps still necessary" (3, p. 490).

In reply to Helwig, Huggins (21) has admitted the presence of two errors in his original paper (4), namely, the values for *u* in the potassium parameters (corrected figures: 0.375, 0.690) and inclusion of the wrong diagram for the projection of the unit cell on the basal plane. Regarding the different *F* values for planes of the same form, Huggins explains that "these F values were calculated ... without making any correction for the differences in absorption and in the number of cooperating planes through the crystal for different reflections" (21, p. 456). It may be noted that Huggins apparently means the total number of planes (of a given set of indices) through the whole crystal in a given direction when he refers to the "number of cooperating planes". In its generally accepted and recognized meaning the expression signifies the number of planes of a given form which are mutually equivalent insofar as X-radiation is concerned. In its usual sense, therefore, the "number of cooperating planes" is a constant of a given form of a given crystal class; it is not a function of the length of path through the crystal as a whole.

Huggins (21) states that he has recalculated F values for the more numerous reflections listed by Helwig (3) using (a) the method of Helwig, (b) the method of Huggins and Frank but with Helwig's parameters, (c) the method of Huggins and Frank with their parameters. He reports the same measure of agreement with observed intensities in the three cases but claims that the third gave the best results. Huggins' most serious criticism of Helwig's structure, however, is based on the fact that Helwig's parameters lead to suspiciously short potassium-to-oxygen distances in two cases (2.2Å. and 2.31Å.) whereas the values of Huggins and Frank (4, 21) give reasonable interionic distances throughout the structure. This fact also has been emphasized by Wyckoff (22, p. 60).

The structure of rubidium dithionate has been considered briefly by Huggins and Frank (4) and by Hägg (5).

In connection with their work on potassium dithionate Huggins and Frank (4) refer to the structure of the rubidium salt as follows.

"Sufficient data were also obtained from $Rb_2S_2O_6$ crystals to show that it has the same type of structure as the potassium salt, as would be expected from the crystallographic data. From the distances between layer lines the unit distances a_0 and c_0 were determined as about 10.0Å. and 6.3Å. respectively, in agreement with the density, which we roughly determined as 3.00 g./cc., and the axial ratio ($\underline{a}$:$\underline{c}$=1:0.6307) as given by Groth, if there are three 'molecules' per unit.

"Although we have made no attempt to determine accurately the parameters a comparison ... of the observed intensities with values of $\underline{F}^2$ calculated on the assumption that the parameters are the same as for $K_2S_2O_6$ ... shows quite good agreement. We therefore conclude that the true parameters are not very different in the two cases." (4, p. 590).

Hägg (5) has published the results of an X-ray examination of both $K_2S_2O_6$ and $Rb_2S_2O_6$. He agrees with Huggins and Frank that the two are isomorphous, belong to the space group D_3^2 and that there are three formula units per cell. The dimensions of the cells given by Hägg are in good agreement with those of Barnes, Helwig, Huggins and Frank for $K_2S_2O_6$ and with those of Huggins and Frank for $Rb_2S_2O_6$. In addition to the aforementioned set of special positions selected by Helwig and by Huggins and Frank for $K_2S_2O_6$, Hägg considers that the six K (or six Rb) may be either in (e)+(f) [as given by Helwig and by Huggins and Frank] or in (g). As he points out, the structure possesses 15 or 14 undetermined parameters depending on whether the metal ions are placed in (g) or in (e)+(f). He concludes, probably with justice, that an exact determination of all of these parameters can only be obtained with the help of absolute intensity measurements. He then proceeds to a criticism of the work of Huggins and Frank and claims that their suggested structure cannot be correct. Taking the prism reflections ($\{hk.0\}$) as an example, he recalculated the F values using the data of Huggins and Frank and obtained rather large differences in certain cases, thus implying errors in calculation on the part of Huggins and Frank. Minor differences are attributed to the fact that Hägg used slightly different atomic F curves. Hägg claims to have examined a number of possible structures but to have been unable to find one giving an acceptable intensity distribution. The principal interest attached to Hägg's paper, however, lies in the fact that he was using unwittingly a crystal of rubidium dithionate which appears to have been twinned. This aspect of Hägg's work will be considered in greater detail in Section III of the present thesis.

In view of the discrepancies among the reported data for potassium dithionate and due to the meagre information available for rubidium dithionate the present investigation of the structure of the latter salt was undertaken.

CRYSTALLOGRAPHY

(a) Brief Literature Survey.

Crystals of rubidium dithionate ($Rb_2S_2O_6$) contain no water of crystallization and are very stable under ordinary conditions.

Wyrouboff (23) reports that he has obtained orthorhombic crystals and concludes that hexagonal specimens arise from a ternary association of orthorhombic lamellae.

"Dans les hyposulfates anhydres de potassium et de rubidium, la forme primitive qui existe dans certaines conditions à l'état normal est orthorhombique, et les cristaux hexagonaux sont le résultat d'un croisement ternaire de lamelles appartenant à cette forme." (23, p. 366).

He claims never to have encountered trigonal forms and considers such forms, reported by Fock (24), to be exceptional.

Groth (14, v.2, p. 690), however, assigns rubidium dithionate to the trigonal trapezohedral (D_3, rhombohedral enantiomorphy) class of the hexagonal system.

Piccard (25) found the axial ratio (a/c) to be 1/0.6307.

Groth (14, v.2, p. 690) reports the angle between rhombohedral axes as $\alpha = 108° 56'$.

Refractive indices are given by Topsøe and Christiansen (26) as

ω_C, 1.4556 ω_D, 1.4574 ω_F, 1.4623

ε_C, 1.5041 ε_D, 1.5078 ε_F, 1.5167

for the ordinary index (ω) and the extraordinary index (ε) using the C, D and F Fraunhofer lines.

Pape (27) has determined the specific optical activity of potassium dithionate but not of the rubidium salt. For $K_2S_2O_6$ he reports rotations per mm. of the C, D. E and F lines of 6.182°, 8.385°, 10.51° and 12.33°, respectively. The specific rotation of $K_2S_2O_6$, therefore, is a little more than one-third that of quartz. Wyrouboff (23, p. 362) states that rubidium dithionate is optically active but that rotation of the plane of polarization is very slight and can only be detected in crystals of two to three mm. thickness.

(b) New Optical Measurements.

As will be apparent later, it was of importance in the space group determination of rubidium dithionate to confirm the presence of optical activity if possible.

A large flat hexagonal prism with its basal plane as a "contoured contact face" (13, v.1, p. 391) was examined in convergent light between crossed Nicols in a polarizing microscope. The single black cross and the circular concentric rings characteristic of uniaxial crystals (13, v.2, p. 831) were obtained. Furthermore, although the thickness of the prism was not very great, the rings were very close together indicating rather large double refraction. By means of a quarter-wave mica plate the sign of the double refraction was found to be positive (13, v.2, p. 1052). These observations are in agreement with the measurements of Topsøe and Christiansen (26), namely, that $\varepsilon_D-\omega_D$ = 1.5078-1.4574 = 0.0504. The magnitude of the double refraction may be compared with that of calcite ($\omega_D-\varepsilon_D$ = 0.1719) and contrasted with that of apatite ($\omega_D-\varepsilon_D$ = 0.0044), the former having a large and the latter a small birefringence (13, v.2, p. 920).

No optical activity was observed in this crystal, however, in spite of the fact that the thickness was of the same order of magnitude (2 to 3 mm.) stated by Wyrouboff (23, p. 362) as suitable for detection of this phenomenon. The absence of optical activity probably was due to twinning since, as Miers (28, pp. 54, 102) points out, optical activity is not observed when an enantiomorphous crystal forms a reflection twin of a right- and a left-handed individual. It is also possible that manifestation of optical activity in parallel polarized light may have been prevented by a slightly imperfect setting of the crystal since the birefringence is relatively large. The black cross and concentric circles in convergent polarized light does not prove that the optic axis of the crystal coincides exactly with the direction axis of the illuminating beam of light.

Later, after many recrystallizations, a small crystal, possessing the prism and two rhombohedral forms and with basal plane faces at both ends, was obtained. A Laue photograph taken with the X-ray beam along the c axis proved that this crystal was not twinned. It had a length of between 1.5 and 1.7 mm. along the c axis. Examination between crossed Nicols in parallel polarized light showed a rotation towards the left of between 3° and 3.5°. The specific rotation, therefore, was about 2° per mm., about one-quarter of that found for potassium dithionate by Pape (27) but much greater than that implied by Wyrouboff's observation on rubidium dithionate cited previously. It is probable, therefore, that Wyrouboff's crystals were twinned.

The crystal was too small in cross-section to show the black cross in convergent polarized light so that these data on specific rotation are complementary to the earlier observations on the large flat prism. It was not possible to identify the small faces of the left trigonal pyramid of the second order or those of the left positive trigonal trapezohedron characteristic of left-handed crystals. Although it was impossible to measure the refractive indices with precision, the ordinary index (ω) was estimated as about 1.46 by the immersion method (13, v.2, p. 1183). This agrees with the observations of Topsøe and Christiansen (26).

These data, therefore, although meagre and inexact due to the nature of the crystals available, at least satisfactorily confirm previously existing optical data on rubidium dithionate for the purpose of the structure investigation later to be described.

EXPERIMENTAL METHODS AND TECHNIQUE

(a) Preparation of Dithionates

There are several methods available for the preparation of dithionates. That developed by Rose (29, p. 89) is of more or less general applicability and was adopted for the preparation of the potassium and rubidium salts required for the work described in this thesis. The method has been outlined by Barnes and Helwig (2) and hence need not be given in detail here.

Essentially, however, the procedure is as follows. Sulphur dioxide is bubbled through a cold aqueous suspension of manganese dioxide. The resulting solution containing manganese dithionate is treated with barium hydroxide, thus precipitating manganese as hydroxide and leaving barium dithionate in solution. Excess barium hydroxide is removed by treatment with carbon dioxide. From the solution of barium dithionate, crystalline $BaS_2O_6.2H_2O$ is obtained by evaporation and is employed as the source material for the preparation of other dithionates.

If, as in the case of potassium and rubidium, the cation of the desired dithionate forms a soluble sulphate, warm solutions containing equivalent weights of barium dithionate and the sulphate of the desired cation are mixed, barium sulphate is precipitated and the dithionate of the desired cation remains in solution.

If the cation sulphate is insoluble, the carbonate is treated with an equivalent weight of dithionic acid prepared by the addition of an equivalent weight of H_2SO_4 to a solution of barium dithionate and the subsequent removal of $BaSO_4$ by filtration.

After preparation of potassium and rubidium dithionates by this method the crystals were purified by many recrystallizations from distilled water. Although no quantitative measurements were made, the proportion of single crystals as compared with pseudo-hexagonal (twinned) specimens of $Rb_2S_2O_6$ appeared to increase with the number of recrystallizations.

In spite of numerous precautions during growth of the crystals no really excellent untwinned specimens with many well-developed faces were obtained. Those of $K_2S_2O_6$ in general were better than those of $Rb_2S_2O_6$.

(b) Density of $Rb_2S_2O_6$

The density of rubidium dithionate was determined by the Retgers suspension method (13, v.1, p. 635). Small transparent crystals, free from any visible cavities, were selected. They were placed in a solution of methylene iodide and benzene to which benzene was added drop by drop until the crystals remained in suspension after vigorous shaking. The solution, having the same density as the crystals, was then transferred to a pycnometer and its density was determined in the usual way. The value obtained was 2.85_5 g./cc. at 20°C. No attempt was made to estimate the density with greater accuracy since the value was required only for the determination of the number of formula units of $Rb_2S_2O_6$ per cell and the highest possible accuracy is not necessary for this purpose. The present result is in reasonably good agreement with the determinations of Huggins and Frank (4) [3.00 g./cc.] and of Hägg (5) [2.81 g./cc.] and probably is more accurate.

The crystals employed in the present density determination presumably were twins. Since density, however, is a scalar property it is not affected by twinning.

Finally, it was observed that the solution used in the density measurement has no chemical effect on crystals of rubidium dithionate even after some months of contact.

(c) X-ray Equipment.

The X-ray tube was of the Shearer gas-type described by Bragg and Bragg (30, pp. 34, 295) and supplied by Hilger (London). Targets of molybdenum and of tungsten were employed for Laue photographs. Copper radiation (K_α = 1.539Å.), filtered with nickel foil to remove the K_β line, was used for complete rotation and for oscillation pictures. Power was supplied to the tube from a 60 k.V.A. Watson transformer. The tube is self-rectifying and was operated usually at about 30 to 45 k.V. and 1 to 5 m.A. depending on the target and on the type of photograph desired.

Photographs were taken on a Bernal Universal X-ray Photogoniometer supplied by Pye (Cambridge) and fully described by Bernal elsewhere (17). This spectrograph is suitable only for the usual types of flat plate and cylindrical cameras.

No ionization spectrometer was available so that it was impossible to make absolute intensity measurements. The present work, therefore, is restricted by the qualitative nature of visually estimated relative intensities.

(d) Interpretation of Data.

1. Laue Diagrams.

Gnomonic projections of Laue diagrams (10, pp. 128-144) were used to determine the symmetry and to check the primitive translation ratios (c/a, b/c, b/a) of the unit cell and to index the diffraction spots. They were employed extensively in the investigation of the nature of twinning in crystals of $K_2S_2O_6$ and of $Rb_2S_2O_6$ to be described in Section III of this thesis.

2. Oscillation Diagrams.

Oscillation diagrams were indexed, and settings of the crystal on the spectrograph were calculated, by means of the reciprocal lattice method of Ewald and Bernal (18; 10, pp. 111-121).

It is convenient, particularly in the construction of the reciprocal lattice, and for the setting up of gnomonic projection nets for the interpretation of Laue diagrams when the beam is along a lateral axis, to convert Bravais-Miller indices $(HK\bar{I}L)$ into trirectangular ones (hkl). The conversion formulae are

$$\begin{array}{lll} h = H & \qquad & H = h \\ l = L & & L = l \\ k = H+2K & & K = (k-h)/2 \\ \;\; = K+I & & I = H+K \end{array}$$

3. Intensities.

For the construction of atomic F curves, the data of Pauling and Sherman (31) were found to be the most satisfactory. This point will be discussed in detail later.

After summation of the structure amplitude, F (HK.L), over every ion in the unit cell the intensity of the diffracted beam $(I \propto |F|^2)$ was multiplied by the polarization factor $(P = (1 + \cos^2 2\theta)/\sin 2\theta)$ to give the simple intensity formula

$$I \propto |F|^2 \, (1 + \cos^2 2\theta)/\sin 2\theta \qquad (10, \text{p.}121).$$

Since comparison of intensities was made only between different orders of interference of the same planes, the number of planes in the form $\{HK.L\}$ was not involved and, since Cu-K_α radiation was employed exclusively for the oscillation photographs, there was no necessity for taking the wave-length into account.

For comparison of relative intensities the logarithms of the calculated intensities $\left[\log P|F|^2\right]$ were plotted, instead of the direct values, in order to obtain more readily comparable curves. This is justified since, as previously mentioned, relative intensities were estimated visually and according to Fechner's law "sensation varies as the logarithm of the excitation." This point is discussed in greater detail in the Appendix to this section (see p.120).

UNIT CELL, BRAVAIS LATTICE AND SPACE GROUP

(a) Symmetry Elements. Crystal Class.

A Laue photograph of $Rb_2S_2O_6$, taken with the X-ray beam along the principal axis, is shown in Figure 11. The symmetry exhibited is that of D_3^d (compare Figure 4, p. 15A) so that the crystal can at once be referred to C_3^v, D_3 or D_3^d since, by the operation of Friedel's law, these three classes have the Laue symmetry of D_3^d. But the only classes in the hexagonal system that are optically active are C_3, C_6, D_3 and D_6. Observations already have been recorded to establish the fact that untwinned crystals of $Rb_2S_2O_6$ possess optical activity. Therefore, from the Laue symmetry and the fact of optical activity, crystals of rubidium dithionate must belong to the crystal class D_3(rhombohedral enantiomorphy; trigonal trapezohedral). This agrees with the classification of Groth (14, v.2, p. 690) based on crystallographic data.

(b) Dimensions of the Unit Cell.

Having satisfactorily confirmed the crystal class, the primitive translations of the unit cell were determined in

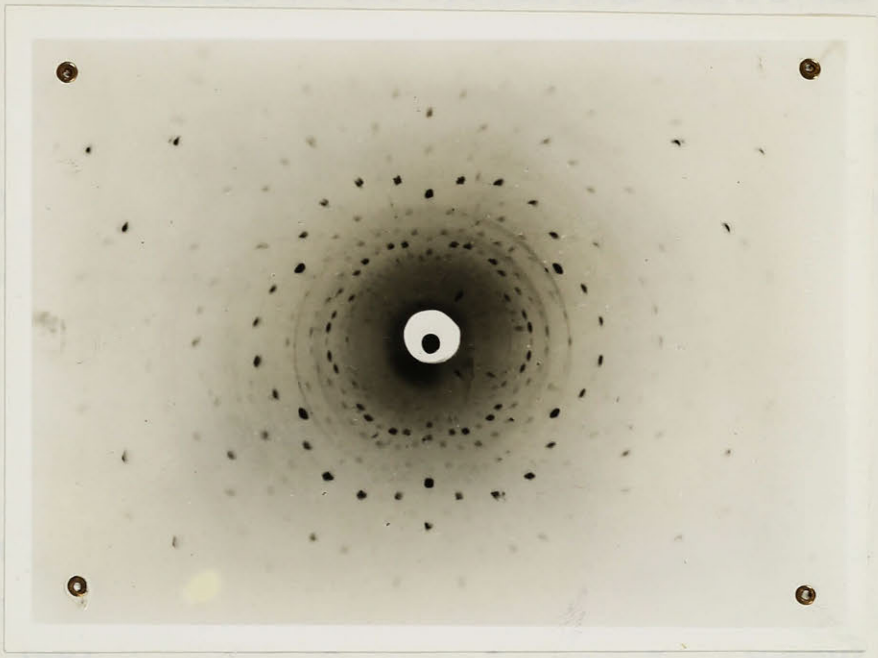

FIGURE 11

Rubidium Dithionate

(Single Crystal)

Beam along c axis

Tungsten Radiation

Crystal-to-plate = 3.15 cm.

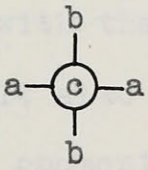

the usual way from the distances of the layer lines above and below the equator in complete rotation photographs about the three orthohexagonal axes (10, p.112, formulae 34a, 34b). The axial ratio (c/a) and the value of $(\sin\alpha)/2$ (where α is the angle between corresponding rhombohedral axes) were calculated.

The radius of the cylindrical camera was standardized as 2.97 cm. from a complete rotation photograph of rock salt.

In Table II the results for the constants of the unit cell of $Rb_2S_2O_6$ are compared with those of previous workers.

TABLE II

Constants of the Unit Cell of $Rb_2S_2O_6$

	a_0(Å.)	b_0(Å.)	c_0(Å.)	c/a	$(\sin\alpha)/2$
This Thesis	10.02	17.39	6.35	0.6337	0.813_3
Huggins & Frank (4)	10.0	-	6.3	0.63	-
Hägg (5)	10.144	-	6.409	0.6318	-
Piccard (25)	-	-	-	0.6307	0.812

The orthohexagonal (b) axis lies in the plane of the a axes (normal to the c axis) and at 90° and 30°, respectively, from adjacent a axes. Hence $b_0 = a_0\sqrt{3} = 10.02\sqrt{3} = 17.35$Å., in good agreement with the value (17.39Å.) determined directly from a b axis rotation photograph.

From Table II it will be seen that the axial ratio (c/a) agrees within 1/2% with that found by Piccard from a crystallographic study. It also agrees within 1/4% with the ratio determined from the gnomonic projection nets described in Section III of this thesis.

The values for the spacings of different planes observed in oscillation photographs showed the same order of agreement (1/4 to 1/5%) with corresponding spacings calculated directly from the data of this thesis recorded in Table II.

(c) Number of Formula Units of $Rb_2S_2O_6$ per Cell.

The volume of the hexagonal cell is given by

$$v = c_o(a_o)^2 \sqrt{3}/2$$
$$= (6.35(10.02)^2 \sqrt{3}/2)10^{-24}\text{cm.}^3$$

and the mass per cell by

$$m = v\rho = (6.35(10.02)^2 \sqrt{3}/2)10^{-24}2.855$$
$$= 1.57_6 \times 10^{-21}\text{g.}$$

The formula weight of $Rb_2S_2O_6$ is equal to

$$M = 2(85.44)+2(32.06)+6(16.00)$$
$$= 331.00\text{g.}$$

and hence the mass per formula unit is

$$331.00/(6.064 \times 10^{23}) = 5.45_8 \times 10^{-22}\text{g.}$$

The number of formula units of $Rb_2S_2O_6$ per cell, therefore, is equal to

$$(1.57_6 \times 10^{-21})/(5.45_8 \times 10^{-22}) = 2.89$$
$$= 3$$

since the number of formula units per cell must be a whole number.

This number agrees with that found by Huggins and Frank (4) and by Hägg (5).

(d) Bravais Lattice and Space Group.

Following the method described in Section I, Part II, of this thesis, Laue photographs obtained with the X-ray beam along a and b axes, respectively, of a trigonal crystal of $Rb_2S_2O_6$ showed immediately that the a axes are two-fold symmetry axes while the b axes appear to lie in planes of symmetry containing the c axis. The only space groups of the class D_3 in which this condition is fulfilled are D_3^2 and D_3^7 (9, plates 17 and 18). Of these, the former is based on the hexagonal Bravais lattice (Γ_h) while the latter is based on the rhombohedral lattice (Γ_{rh}).

Assuming a hexagonal lattice, the number of formula units of $Rb_2S_2O_6$ per cell has been shown to be 3. This is possible in D_3^2 (9, p. 249).

On the other hand, if the lattice really were rhombohedral, the number of formula units per cell should be 2.89(8/3) = 7.7 (i.e., 8) which is not possible in D_3^7 (9, p. 246).

Furthermore, an examination of the hexagonal indices, particularly those of complex character, of points on the gnomonic projections of Laue diagrams (see Section III) proved at once that, for the great majority of planes represented, the expressions

$$(2H+K+L)/3, \ (K-H+L)/3, \ (-2K-H+L)/3,$$

where H, K, L are Bravais-Miller indices, are not integral. This fact supplies further evidence in favour of a hexagonal rather than a rhombohedral lattice (10, p. 184).

Thus, the Bravais lattice must be Γ_h (hexagonal) and the space group must be D_3^2.

In order to confirm this conclusion without recourse to the number of formula units per cell, all possible space groups (D_3^1, D_3^2, D_3^3, D_3^4, D_3^5, D_3^6, D_3^7) may be examined. Of these D_3^3, D_3^4, D_3^5 and D_3^6 are characterized by a thirding of $\{0001\}$ whereas D_3^1, D_3^2 and D_3^7 have no "abnormal spacings." (9, p. 249).

Five-degree oscillation photographs resulted in the unequivocal identification of reflections from each of the first seven orders of (0001). This fact immediately eliminates D_3^3, D_3^4, D_3^5 and D_3^6 from further consideration. Furthermore, the observed spacings were those calculated on the basis of a hexagonal lattice and not 3/2 of these values as should be the case if the underlying lattice were rhombohedral.

Oscillation photographs also led to the identification of reflections from the first eight orders of $(10\bar{1}0)$ and from five of the six possible orders of $(11\bar{2}0)$. The observed spacings of $(10\bar{1}0)$ were $(a_0\sqrt{3})/2$, $(a_0\sqrt{3})/4$, $(a_0\sqrt{3})/6$, etc. corresponding to Γ_h and not 2/3 of these values corresponding to Γ_{rh}. Similarly, observed spacings of $(11\bar{2}0)$ were $a_0/2$, $a_0/4$, $a_0/6$, etc. corresponding to Γ_h and not twice these values corresponding to Γ_{rh}. There is no doubt, therefore, that the Bravais lattice is Γ_h. This eliminates D_3^7.

Of the two remaining space groups, D_3^1 and D_3^2, it has been shown above that the Laue diagrams obtained with the beam along lateral axes are compatible only with D_3^2. This space group is represented by C_{321} in the complete Hermann-Mauguin notation and alternatively by H_{312} (33, v.1, p.41).

In order to avoid any possible ambiguity in the use of three letters (hkl) for trirectangular coordinates it may be stated at this point that rhombohedral coordinates are not employed in any part of this thesis since the crystals under discussion are based on the hexagonal Bravais lattice Γ_h.

Finally, it may be noted that the space group of rubidium dithionate has been established unequivocally by methods which are entirely independent of any knowledge regarding the detailed internal structure of the crystal.

STRUCTURE

(a) Special Positions

The special positions for the space group D_3^2 (hexagonal axes) as listed by Wyckoff (20, p.154) are as follows:

One equivalent position:

(a) 000. (b) 00,1/2

Two equivalent positions:

(c) $00u$; $00\bar{u}$. (d) $1/3,2/3,u$; $2/3,1/3,\bar{u}$.

Three equivalent positions:

(e) $uu0$; $0\bar{u}0$; $\bar{u}00$. (f) $uu,1/2$; $0\bar{u},1/2$; $\bar{u}0,1/2$.

Six equivalent positions:

(g) xyz; $y-x,\bar{x}z$; $\bar{y},x-y,z$; $yx\bar{z}$; $\bar{x},y-x,\bar{z}$; $x-y,\bar{y}\bar{z}$.

Six rubidium atoms, six sulphur atoms and eighteen oxygen atoms must be placed in the unit cell because the cell contains three formula units of $Rb_2S_2O_6$.

Since dithionates ionize in aqueous solution to give $(S_2O_6)^=$ as the anion it is probable that this ion retains its identity in the crystal in the same manner as do other compound anions, such as $(SO_4)^=$, $(CO_3)^=$, $(NO_3)^-$, etc. Furthermore it is probable that the $(S_2O_6)^=$ ion has the general form O_3-S-S-O_3 in which case its most probable position would place the two sulphur atoms on a three-fold axis with three oxygens associated with each sulphur in much the same way as three of the four oxygens in the tetrahedral $(SO_4)^=$ ion. The assumption of this form for the dithionate ion is supported by the results of a study of the Raman Effect in aqueous solutions of sodium dithionate (34), from which Pringsheim and Yost conclude that in the dithionate ion the two sulphur atoms have a common bond, are equivalent and symmetrical to each other and to the two groups of oxygen atoms.

The most logical positions for the six sulphur atoms in the cell, therefore, would appear to be in pairs on the three-fold axes. Thus the two equivalent sulphur atoms of one dithionate radical may be placed in the special positions (c) with the other two pairs in two sets of (d) positions. The six sulphurs, therefore, have the following sets of special positions as shown in Figure 12.

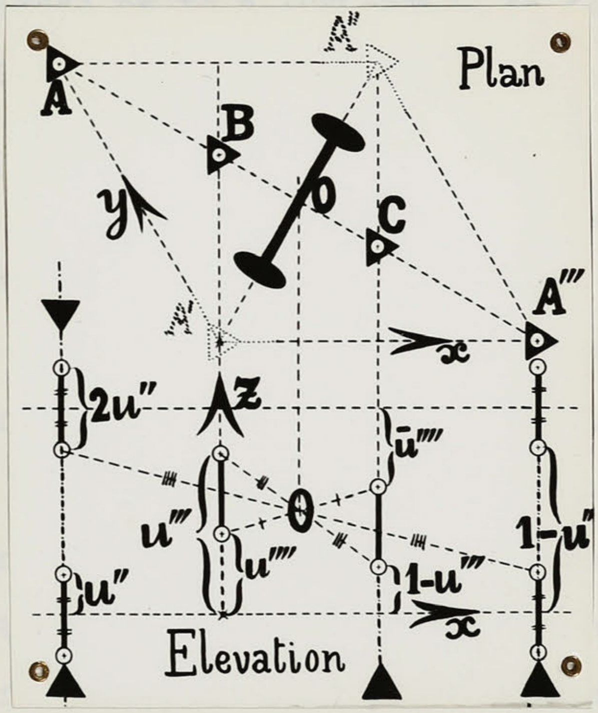

FIGURE 12

Vertical Parameters of the S Atoms

(c) $00u''$; $00\bar{u}''$

(d) $1/3,2/3,u'''$; $2/3,1/3,\bar{u}'''$

(d)' $1/3,2/3,u''''$; $2/3,1/3,\bar{u}''''$

The S-S distance in the dithionate ion, therefore, is equal to $c_o(2u'')$ or to $c_o(u'''-u'''')$, so that

$$2c_ou'' = c_o(u'''-u'''')$$

from which

$$2u'' = u'''-u'''' \quad \ldots\ldots\ldots\ldots\ldots\ldots\ldots\ldots\ldots \quad 1.$$

Due to the very restricted nature of the special positions (a), (b), (c), (d), (e), (f) it is obvious that no combinations of these positions will now place three oxygen atoms adjacent to each of two sulphur atoms and still retain an O_3-S-S-O_3 unit. This was confirmed by constructing diagrams of oxygen positions according to the different combinations possible. It follows, therefore, that the eighteen oxygen atoms must occupy three sets of (g) positions.

Largely from considerations of available space and in order to hold the structure together the most probable positions for the six rubidium ions are (e) + (f). Positions (a), (b), (c), (d) can be discarded since the dithionate ions already have been placed on these verticals (00; 1/3,2/3; 2/3,1/3). As will be shown later, reflections from odd orders of (0001) are relatively weak in intensity - apparently due to a halving of the contributions from the rubidium ions. This suggests that the rubidium ions probably are equally divided between vertical parameters of 0 and 1/2 as in (e) + (f) and are not situated all in one plane as in 2(e) or 2(f). The suggestion of Hägg (5) that they may be in (g) will be shown later to be incompatible with the observed intensity distribution of the basal plane reflections.

The most probable special positions, therefore, of the scattering centres in the cell of rubidium dithionate are as follows.

6 Rb in

(e) $uu0;\ 0\bar{u}0;\ \bar{u}00.$

(f) $u'u',1/2;\ 0\bar{u}',1/2;\ \bar{u}'0,1/2.$

6 S in

(c) $00u'';\ 00\bar{u}''.$

(d) $1/3,2/3,u''';\ 2/3,1/3,\bar{u}'''.$

(d)' $1/3,2/3,u'''';\ 2/3,1/3,\bar{u}''''.$

18 O in

(g) $xyz;\ y-x,\bar{x}z;\ \bar{y},x-y,z;\ yx\bar{z};\ \bar{x},y-x,\bar{z};\ x-y,\bar{y}\bar{z}.$

(g)' $x'y'z';\ y'-x',\bar{x}'z';\ \bar{y}',x'-y',z';$
$y'x'\bar{z}';\ \bar{x}',y'-x',\bar{z}';\ x'-y',\bar{y}'\bar{z}'.$

(g)" $x''y''z'';\ y''-x'',\bar{x}''z'';\ \bar{y}'',x''-y'',z'';$
$y''x''\bar{z}'';\ \bar{x}'',y''-x'',\bar{z}'';\ x''-y'',\bar{y}''\bar{z}''.$

(b) Nature of the Interatomic Bonds.

The most probable types of bond among the rubidium, sulphur and oxygen atoms are those which complete the outermost shell of eight electrons (35) either by complete transfer or by mutual sharing of electrons. Since rubidium certainly is present in the crystal as the ion Rb^+ (36 electrons outside the nucleus), the only uncertainty lies in the valence numbers to be assigned to S and to O in the dithionate ion $(S_2O_6)^=$.

Three possibilities are conceivable. They are represented diagramatically in Figure 13. The valence numbers and numbers of external electrons are as follows.

A. Rb^+, 36; S^{5+}, 11; O^{2-}, 10.

B. Rb^+, 36; S^{2+}, 14; O^{1-}, 9.

C. Rb^+, 36; S^o, 16; $(O^o, 8/O^{-1}, 9) \propto 2/1$

Of these, A and C are improbable since, in neither case, are rare gas configurations attained for all the atoms. Furthermore, in C the three oxygen atoms associated with each sulphur atom are not identical one with another. Since there are two O^o and one O^{1-}, however, the "average" valence number may be considered formally as (1/3)- and the atomic F value at $(\sin\theta)/\lambda$ equal to 0.0 may be taken as 8.33.

(c) Atomic F Curves.

The variation of atomic scattering power with $(\sin\theta)/\lambda$ for different valence numbers of the atoms involved is given in Table III and shown (with the exception of $O^{(1/3)-}$ and S^{5+}) in Figure 14. The values are based on data of Pauling and Sherman (31), those for S^{5+}, S^{2+}, $O^{(1/3)-}$, O^{1-} having been obtained by interpolation.

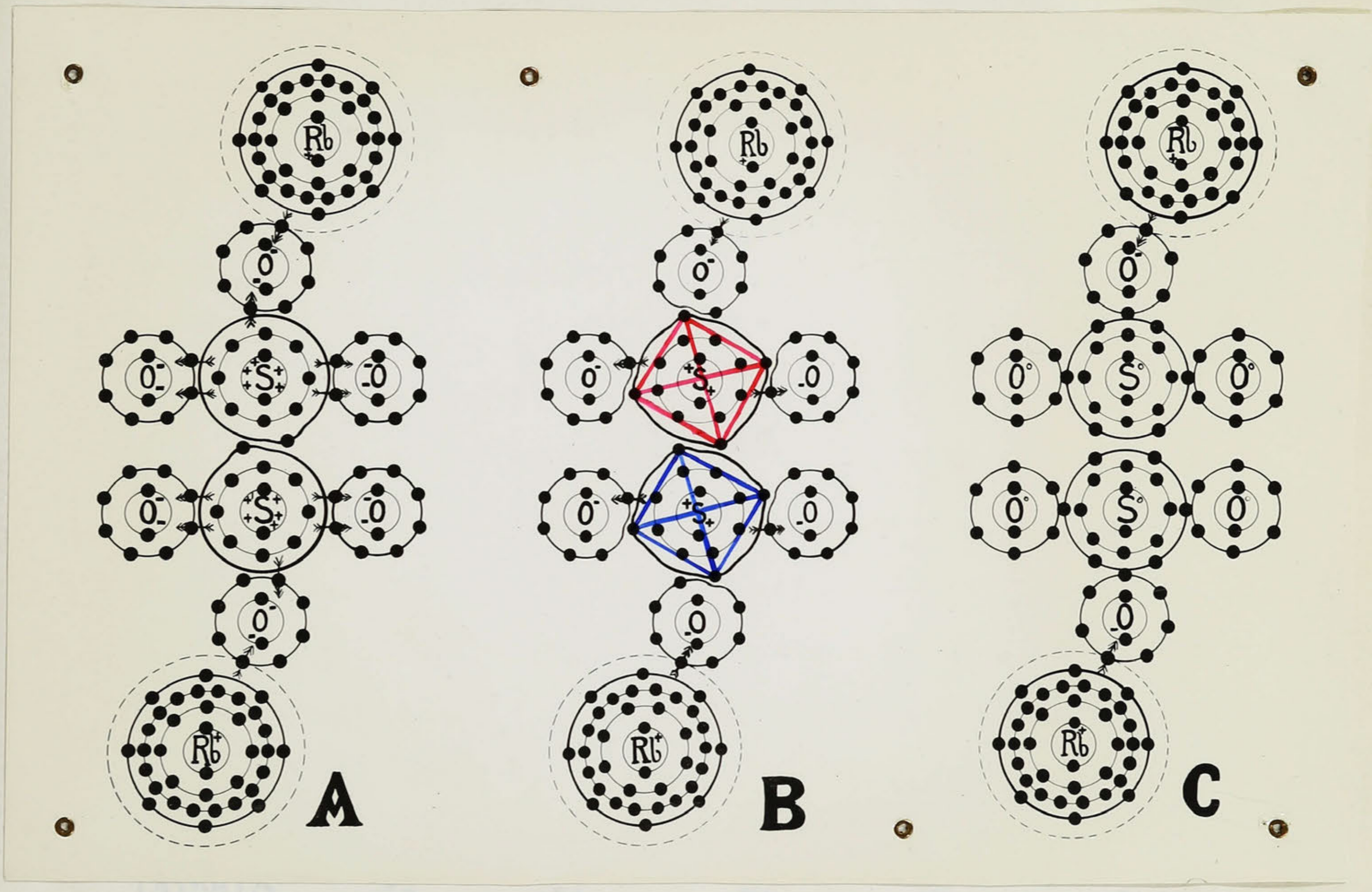

FIGURE 13

Possible Interatomic Bonds in $Rb_2S_2O_6$

TABLE III

Atomic F Values

$(\sin\theta)/\lambda \times 10^{-8}$	Rb^{1+}	O^{0}	$O^{(1/3)-}$	O^{1-}	O^{2-}
0.0	36.00	8.00	8.33	9.00	10.00
0.1	32.64	7.36	7.67	8.25	9.15
0.2	27.44	5.82	6.06	6.44	7.07
0.3	24.22	4.14	4.31	4.49	4.84
0.4	22.19	2.90	2.95	3.06	3.22
0.5	19.71	2.19	2.21	2.25	2.32
0.6	16.89	1.80	1.81	1.81	1.83
0.7	14.22	1.63	1.63	1.62	1.61
0.8	12.15	1.54	1.53	1.52	1.51
0.9	10.47	1.49	1.48	1.47	1.46
1.0	9.34	1.44	1.44	1.43	1.42
1.1	8.44	1.38	1.38	1.37	1.37
1.2	8.16	1.31	1.31	1.30	1.29
1.3	7.47	1.23	1.24	1.26	1.22
1.4	7.15	1.15	1.15	1.14	1.14

$(\sin\theta)/\lambda \times 10^{-8}$	S^{6+}	S^{5+}	S^{2+}	S^{0}	S^{2-}
0.0	10.00	11.00	14.00	16.00	18.00
0.1	9.88	10.58	12.7	14.1	15.5
0.2	9.47	9.69	10.4	10.8	11.2
0.3	8.86	8.88	8.95	8.96	8.97
0.4	8.09	8.09	8.11	8.16	8.21
0.5	7.22	7.26	7.4	7.52	7.64
0.6	6.31	6.37	6.55	6.67	6.79
0.7	5.44	5.49	5.65	5.73	5.81
0.8	4.64	4.67	4.76	4.80	4.84
0.9	3.92	3.93	3.98	4.00	4.02
1.0	3.34	3.34	3.35	3.36	3.37
1.1	2.89	2.89	2.89	2.88	2.87
1.2	2.51	2.51	2.49	2.49	2.49
1.3	2.22	2.22	2.21	2.20	2.19
1.4	1.98	1.97	1.96	1.96	1.96

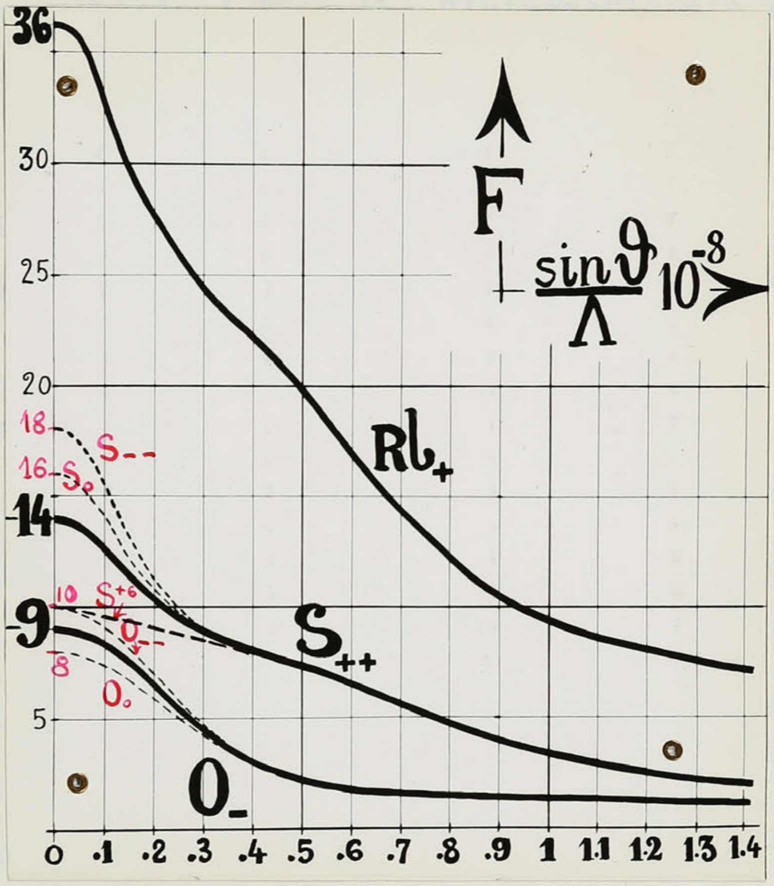

FIGURE 14

Atomic F Curves

Scattering powers also were calculated by the method of Fermi and Thomas (36) based on caesium as a typical atom (37; 10, p.98) and another set of values compiled by James and Brindley was obtained from the "Internationale Tabellen" (33, v.2, p.571).

In view of the statement of Huggins and Frank (4) that the parameters of $Rb_2S_2O_6$ probably are not very different from those of $K_2S_2O_6$, the following calculations were made.

Applying the $K_2S_2O_6$ parameters (a) of Helwig (3), revised as shown in Table I, and (b) of Huggins and Frank (4, 21), respectively, to $Rb_2S_2O_6$, values of $\log I = \log P|F|^2$ for the basal plane reflections were calculated for the three (A, B, C) possible combinations of valence numbers already discussed (Figure 13) using scattering powers based on (1) the data of the "Internationale Tabellen", (2) the Pauling-Sherman values given in Table III, and (3) the Fermi-Thomas system.

The results of these calculations (except those based on the Fermi-Thomas method) are shown in Table IV where the letters and figures have the significance indicated in the preceding paragraph.

TABLE IV

$\log I = \log P|F|^2$

(0001) l	I (obs.)	A1a	A1b	A2a	A2b	B1a	B1b	B2a	B2b	C1a	C1b	C2a	C2b
4	v.s.	4.52	4.53	4.53	4.54	4.52	4.53	4.52	4.53	4.52	4.52	4.52	4.53
6	s.	4.10	4.12	4.13	4.16	4.10	4.12	4.13	4.15	4.10	4.12	4.13	4.15
5	m.	3.37	3.18	3.49	3.29	3.38	3.18	3.44	3.24	3.39	3.19	3.47	3.27
2	w.	4.42	4.38	4.10	4.03	4.43	4.41	4.17	4.11	4.43	4.40	4.25	3.41
3	w.	2.84	2.70	2.95	2.78	2.83	2.70	2.92	2.77	2.85	2.72	2.90	2.76
1	v.w.	3.36	3.19	3.40	3.22	3.44	3.33	3.48	3.32	3.47	3.33	3.50	3.36
7	a.	1.65	0.12	1.76	$\bar{1}.97$	$\bar{1}.68$	0.08	1.51	0.85	1.73	0.12	1.29	1.16

A, B, C } valence numbers as on page 57, this thesis.

1	scattering factors according to the "Internationale Tabellen".
2	scattering factors according to Pauling and Sherman.
a	parameters of $K_2S_2O_6$ according to Helwig.
b	parameters of $K_2S_2O_6$ according to Huggins and Frank.

In no case was perfect agreement obtained between the relative order of log I (calculated) and of I (observed); for example, see l = 1 and l = 2 in Table IV. This indicated that $Rb_2S_2O_6$ probably has parameters that are not exactly the same as either of those sets (3,4,21) proposed for $K_2S_2O_6$.

An examination of Table IV shows that whereas the "Internationale Tabellen" as contrasted with the Pauling-Sherman scattering factors make no appreciable difference to the log I values for (0001), they give definitely higher figures for (0002). Since log I for (0002) is much larger than the observed relative intensities in all cases, the Pauling-Sherman factors, therefore, appear to be less objectionable than the others. Furthermore, although the differences between log I for (0005), medium, and (0003), weak, are not very different between the 2a and 2b sets of values, the latter (involving the parameters of Huggins and Frank) give lower figures for log I (0002) than the former. The best agreement, therefore, between observed and calculated intensities is found for the combinations A2b, B2b, C2b. Objections to the A and C sets of atomic numbers already have been pointed out (see p.57). Insofar, therefore, as parameters of $K_2S_2O_6$ can be applied directly to $Rb_2S_2O_6$ the evidence indicates that the best and most probable combination of variables is B2b, <u>i.e.</u>, the valence number combination of Rb^{1+}, 36; S^{2+}, 14; O^{1-}, 9; the scattering factors of Pauling and Sherman and the parameters of Huggins and Frank.

As was expected, none of the sets of values based on the Fermi-Thomas scattering factors were as satisfactory as those involving the Pauling-Sherman data, since a general treatment such as the former usually is not as reliable as a special consideration of each individual case as in the latter. For this reason the results of the application of the Fermi-Thomas method are not included in Table IV and the Fermi-Thomas system will receive no further mention in this thesis.

(d) Vertical Parameters.

Since the heights (1/2 and 0) of the rubidium ions are fixed, the first part of the geometry of the structure is concerned with the vertical parameters of the atoms S^{2+} and O^{1-} constituting the dithionate ions.

As a basis for calculation it may be assumed that each sulphur and its three adjacent oxygen atoms are in the same relative positions as in the sulphate ion (regular tetrahedron) and that the S-O distance is 1.495Å. (33,19,3,2). The validity of these assumptions will be examined later.

The sulphate tetrahedron is shown in perspective in Figure 15A and its projection on the plane DAMH (Figure 15A) in Figure 15B.

Since the radius R of the circumscribed sphere is 3/4 of the height of the tetrahedron and 3 times the radius of the inscribed sphere, it follows that SH = (AH)/4 and that

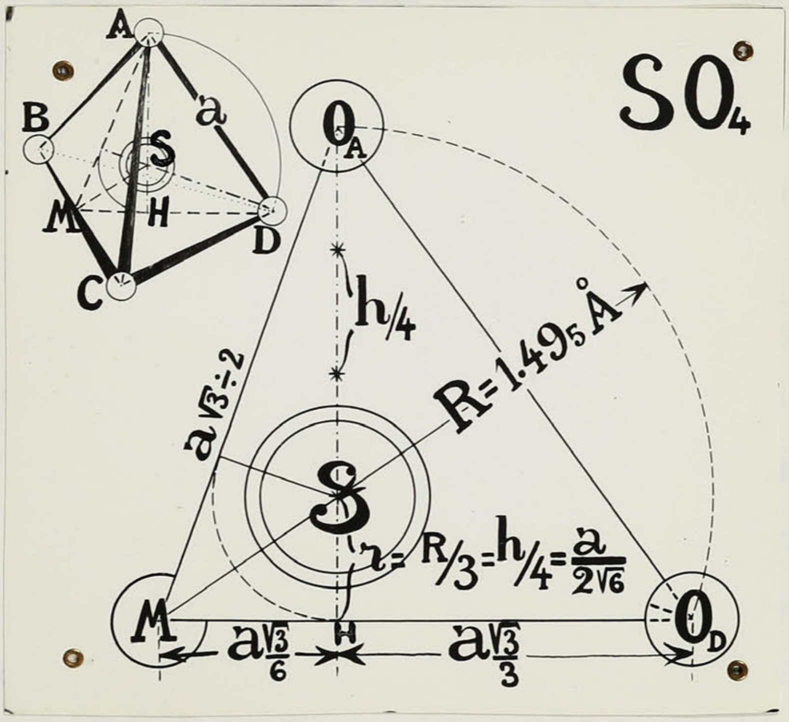

FIGURE 15

The Sulphate Tetrahedron

$MH = (MD)/3 = (AM)/3 = (a\sqrt{3})/6$, so that $HD = 2MH = a\sqrt{3}/3$ and $AH = \sqrt{(AD)^2-(HD)^2} = \sqrt{a^2-(a^2/3)} = a\sqrt{2/3}$ and $SA = R = 3(AH)/4 = (3a\sqrt{2/3})/4 = (a\sqrt{3/2})/2$.

Thus the distance between adjacent oxygen atoms is $AD = a = R2\sqrt{2/3} = 2.441$Å. and the height of the sulphur atom S above the plane (BCD) of the three oxygen atoms is $r = h/4 = R/3 = 0.498$Å., where R is the S-O distance (1.495Å.).

In terms of parameters (*i.e.*, c_0), $r = 0.498/c_0 = 0.498/6.35 = 0.0785$.

Now, according to equation 1 (p. 55), $2u'' = u''' - u''''$, so that, if the S-S distance ($2u''$) in the dithionate ion is known, u''' can be expressed in terms of u''''. Assuming, therefore, that this distance is the same as that in the pyrite structure (34), $2u''$ may be taken as 2.09Å., or, in parameters, $2u'' = 2.09/6.35 = 0.33$, so that $u'' = 0.165$. This assumption will be justified later from intensity considerations.

The distance, in terms of vertical parameters, between a sulphur atom and the nearest plane of oxygen atoms is

$r = z-u'' = (1-z') - u''' = u'''' - (1-z'') = 0.0785$ 2

and thus $z = u'' + 0.0785 = 0.165 + 0.0785 = 0.243_5$.

The following expressions now give the relationships between u''', z' and z'', respectively, and the undetermined u''''.

(a) $u''' = 2u'' + u''''$ (equation 1, p. 55)

$= 0.33 + u''''$.

(b) $(1-z')-u''' = 0.0785$ (equation 2, p. 63)

$$\begin{aligned} z' &= 1-0.0785-u''' \\ &= 1-0.0785-0.33-u'''' \\ &= 0.5915-u''''. \end{aligned}$$

(c) $u''''-(1-z'') = 0.0785$ (equation 2, p. 63)

$$\begin{aligned} z'' &= 1+0.0785-u'''' \\ &= 1.0785-u''''. \end{aligned}$$

In order to fix u'''' and as a test of the foregoing values for u'' (0.165) and for z (0.2435), reflections from the basal planes were examined.

The general structure factor for $\{0001\}$ is

$$\begin{aligned} F = {} & 3Rb^{1+}\{1+\cos \pi l\} + 2S^{2+}\{\cos 2\pi u''l + \\ & + \cos 2\pi u'''l + \cos 2\pi u''''l\} + \\ & + 6O^{1-}\{\cos 2\pi zl + \cos 2\pi z'l + \\ & + \cos 2\pi z''l\}. \end{aligned}$$

Obviously only vertical parameters are involved in this expression and it will be observed that reflections from the even orders in general should be stronger in intensity than those from the odd orders since the comparatively heavy rubidium ions make no contribution to the scattering in the latter case.

The following Table VI lists the values for the reflection angle θ (in radians), $(\sin \theta)/\lambda$, the polarization factor ($P = (1+\cos^2 2\theta)/\sin 2\theta$), log P and the scattering powers of Rb^{1+}, S^{2+}, O^{1-} (from Figure 14, p. 58A), respectively, for the seven orders of (0001) observed.

TABLE VI

(0001) l	θ (radians)	(sinθ)/λ x 10^{-8}	P	log P		F values	
					Rb^{1+}	S^{2+}	O^{1-}
1	0.1215	0.0787	8.075	0.907	33.86	13.25	8.60
2	0.2448	0.1575	3.785	0.578	29.52	11.25	7.32
3	0.3722	0.2363	2.275	0.357	26.18	9.65	5.80
4	0.5063	0.3149	1.510	0.179	23.88	8.90	4.25
5	0.6509	0.3937	1.418	0.152	22.32	8.16	3.15
6	0.7273	0.4726	1.004	0.0017	20.34	7.59	2.48
7	1.0072	0.5512	1.327	0.123	18.20	6.96	2.03

Inserting the appropriate data of Table VI in the general structure factor equation for $\{0001\}$, $\log I = \log P|F|^2$ was calculated for l = 1,2,3,4,5,6,7, respectively, and for different values of u''''. The results were plotted in terms of log I against u'''' for the different values of l, as shown in Figure 16.

It was not necessary to cover the complete range $0 \leqslant u'''' \leqslant 1$ because changing u'''' into $\bar{u}''''$ merely interchanges the x and y coordinates (see (d)', p. 55) which are not involved in the general structure factor for $\{0001\}$, so that the range $0 \leqslant u'''' \leqslant 1/2$ is equivalent in this case to the range $1/2 \leqslant u'''' \leqslant 1$. Furthermore, it will be observed in Figure 16 that the log I curves are symmetrical about the abscissa $u'''' = 0.335$. Thus u'''' must have some value u_A'''' between 0 and 0.335 or the symmetrical value (see Figure 16), $u_B'''' = u_A'''' + 2(0.335 - u_A'''')$.

For no value of u'''' either with the scattering factors of Pauling and Sherman (Table VI) or with those of the "Internationale Tabellen" was it possible to obtain values of

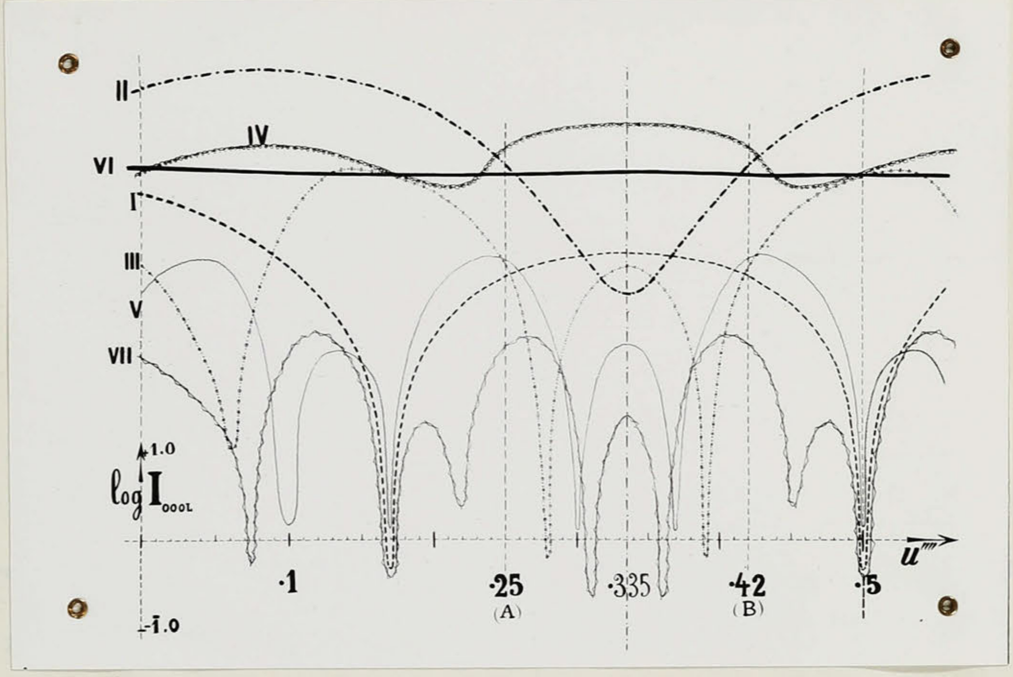

FIGURE 16

Log I$_{\{0001\}}$

$(h/4)c_o = 0.0785$

log I for the different orders of reflection from $\{0001\}$ in perfect agreement with the observed relative order of intensities. The best value was $u_A'''' = 0.25$ ($u_B'''' = 0.42$) using the atomic F curves of Pauling and Sherman.

The visually estimated relative order of intensities is given herewith,

(0004)	v.s.
(0006)	s.
(0005)	m.
(0002)	w.
(0003)	w.
(0001)	v.w.
(0007)	a.

where the letters have their usual significance (s., strong; m., medium; w., weak; v., very; a., absent).

In Figure 16 it will be observed that in the range $0 < u'''' < 0.243$ the second order is the strongest and the fifth order falls below the third from 0.075 to 0.245. Furthermore, in the range $0.26 < u'''' < 0.335$ the fifth and the third orders are below the first and the third also appears below the seventh from 0.265 to 0.29. Finally for $u'''' > 0.29$ the fifth order again drops below the third. It will be seen that the second order alone prevents perfect agreement with the relative order of observed intensities being reached for any value of u''''. In Figure 16 the second order is comparable with the third only in the neighbourhood of $u''' = 0.32$ but here the second and third orders are below the first and the fifth is below these three. For values of $u''' < 0.32$, the second order rapidly becomes too high. If the second order is neglected, however, it will be found that the range of possible values for u''' is limited to $0.246 < u''' < 0.253$.

Therefore, taking u_A''' as 0.25 and retaining the Pauling-Sherman scattering factors for Rb^{1+}, S^{2+} and O^{1-}, the effects of modifying the S-S distance in the dithionate ion and of flattening the SO_3 pyramid were examined.

It was found that any significant change in the S-S distance (2.09Å.) led to even more discordant results than those shown in Figure 16. It may be concluded, therefore, that the S-S distance in the dithionate ion cannot be far from 2.09Å. and hence that the value of the parameter u'' must be close to 0.165.

On the other hand, decreasing the vertical distance of the sulphur atom from the plane of the three nearest oxygen atoms $\left[SH = r = (h/4)c_0 \text{ in Figure 15, p.62A} \right]$ gave more acceptable results as shown in Table VII.

TABLE VII

($u''' = 0.25$ or 0.42)

(0001)	I	log I (calculated)			
l	(obs.)	$(h/4)/c_0 =$ 0.0785	0.065	0.06	0.05
4	v.s.	4.48	4.49	4.49	4.49
6	s.	4.17	4.14	4.13	4.09
5	m.	3.22	3.58	3.68	3.81
2	w.	4.26	4.30	4.31	4.36
3	w.	3.15	3.42	3.50	3.63
1	v.w.	3.00	3.22	3.29	3.41
7	a.	2.26	1.36	1.93	2.25

It has been pointed out that for $r = (h/4)/c_0 = 0.0785$ the calculated value of log I for the second order is too high. It is clear from Table VII that decreasing $(h/4)c_0$, although causing a slight increase in log I for the second order, results in an appreciable rise for the third order, thus diminishing the difference between the second and third orders. Below $(h/4)/c_0 = 0.05$, however, the value for the second order rises rapidly to meet that for the fourth at $(h/4)/c_0 = 0.03$. Also, with decreasing values of $(h/4)/c_0$, the magnitude of log I falls for the sixth order and rises for the fifth. Values for the second order, however, should be below those for the sixth and fifth but in all cases are higher. Hence the effect of diminishing $(h/4)c_0$ is to increase the magnitude of the discrepancy between the sixth and second orders and to decrease it between the fifth and second. Finally, values of log I calculated for the seventh order first fall and then rise with decreasing values of $(h/4)/c_0$ and thus, in conjunction with the increase

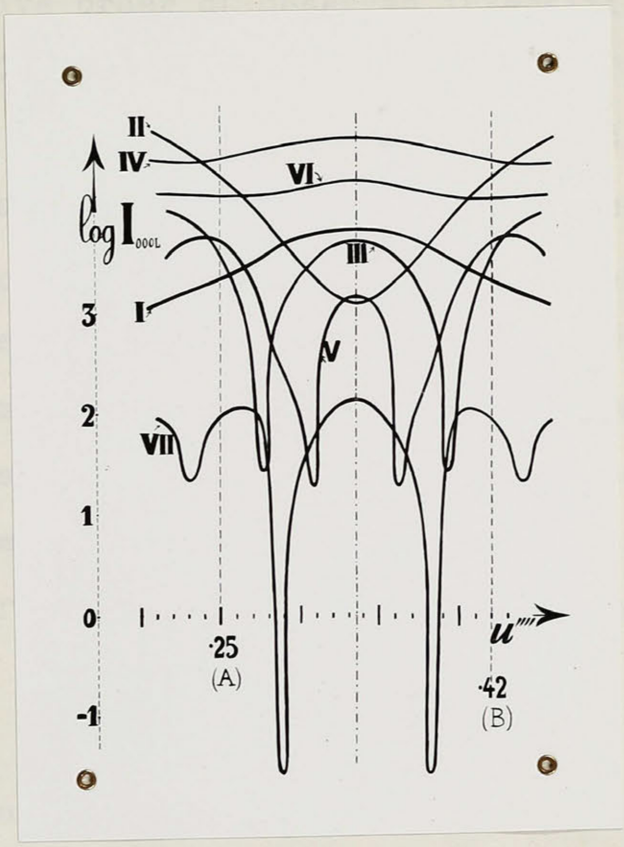

FIGURE 17

Log I$_{\{0001\}}$

$(h/4)c_0 = 0.06$

in those for the second order, limit the extent to which decreasing the distance $(h/4)/c_0$ profitably may be considered. The best compromise between relative values of log I (calculated) and the relative order of observed intensities is obtained when $(h/4)/c_0 = 0.06$. With this value, curves of log I calculated for different values of u''' between 0.21 and 0.335 are shown in Figure 17 and it will be observed that decreasing the distance $(h/4)/c_0$ from 0.0785 (Figure 16) to 0.06 (Figure 17) makes no other value of u''' more acceptable than 0.25.

It may be mentioned that increasing the distance $(h/4)/c_0$ above 0.0785 does not improve the position of the second order which again rises and, in addition, it results in bringing the fifth and sixth orders closer together until they meet at 0.10.

The foregoing discussion of the vertical parameters of the dithionate ions may be summarized by stating that, with assumptions of $u'' = 0.165$ and $(h/4)/c_0 = 0.0785$, the result of the eight sets of possible variations involving constant, increasing and decreasing values of u'' and $(h/4)/c_0$, respectively, showed that the best agreement between observed and calculated intensities for the first seven orders of (0001) was obtained with $u'' = 0.165$, $(h/4)/c_0 = 0.06$, $u'''_A = 0.25$ ($u'''_B = 0.42$). The S-O distances in the SO_3 pyramids and the relative positions of the SO_3 groups in each dithionate ion about the vertical axes will be discussed in connection with the lateral parameters of the structure and in the Discussion.

Before leaving the vertical parameters, however, it is of interest to examine the positions of the rubidium ions. As previously mentioned, although the special positions (e)+(f) are the most probable, available interionic distances in the cell do not prohibit the placing of the six rubidium ions in 2(e), 2(f) or (g), respectively.

In 2(e) or in 2(f) the six rubidium ions would all be at the same level (0 or 1/2), whereas in (e)+(f) three are at 0 and three at 1/2, thus halving the c axis insofar as rubidium contributions to the structure factor are concerned. Thus the odd orders of (0001) should be abnormally weak in intensity if the rubidium ions are in (e)+(f), whereas this should not be the case if the rubidium ions are in 2(e) or in 2(f). The values of log I calculated for 2(e), 2(f) and (e)+(f), respectively, are compared with the observed intensities of the first seven orders of (0001) in Table VIII. It is obvious that the rubidium ions cannot be either in 2(e) or in 2(f).

TABLE VIII

(0001)	I	log I (calculated)		
1	(obs.)	(e)+(f)	2(e)	2(f)
1	v.w.	3.29	5.45	5.59
2	w.	4.31	4.31	4.31
3	w.	3.50	4.51	4.94
4	v.s.	4.49	4.49	4.49
5	m.	3.68	4.72	3.915
6	s.	4.13	4.13	4.13
7	a.	1.93	4.13	4.26

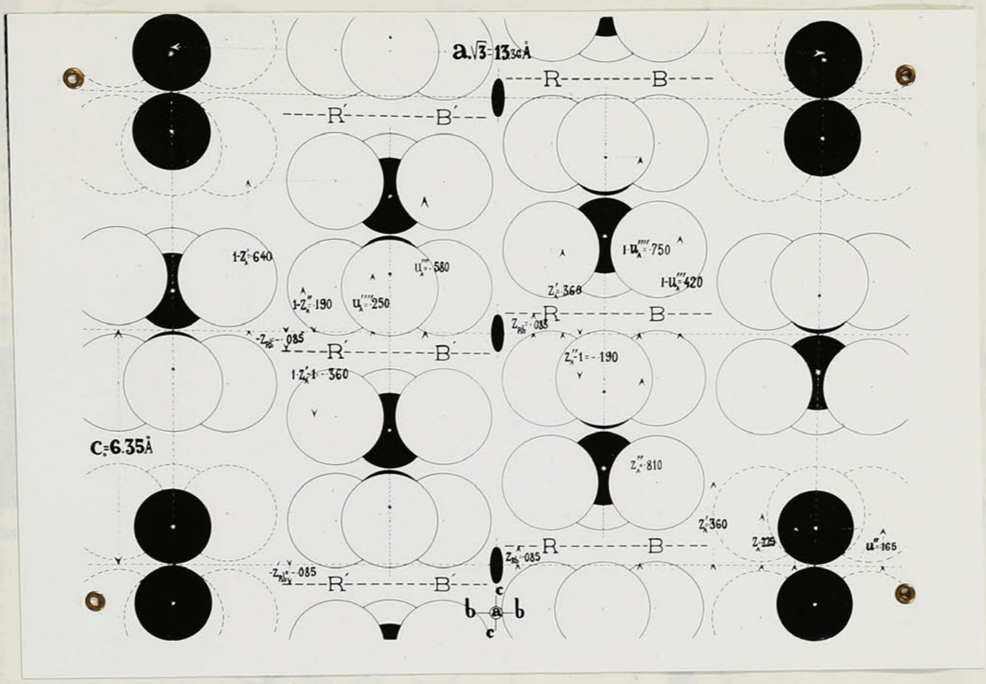

FIGURE 18A

Diagram showing Vertical Parameters of

Possible Planes of Rb^+ in (g) Positions

($u'''_A = 0.58$, $u''''_A = 0.25$, $z'_A = 0.36$, $z''_A = 0.81$)

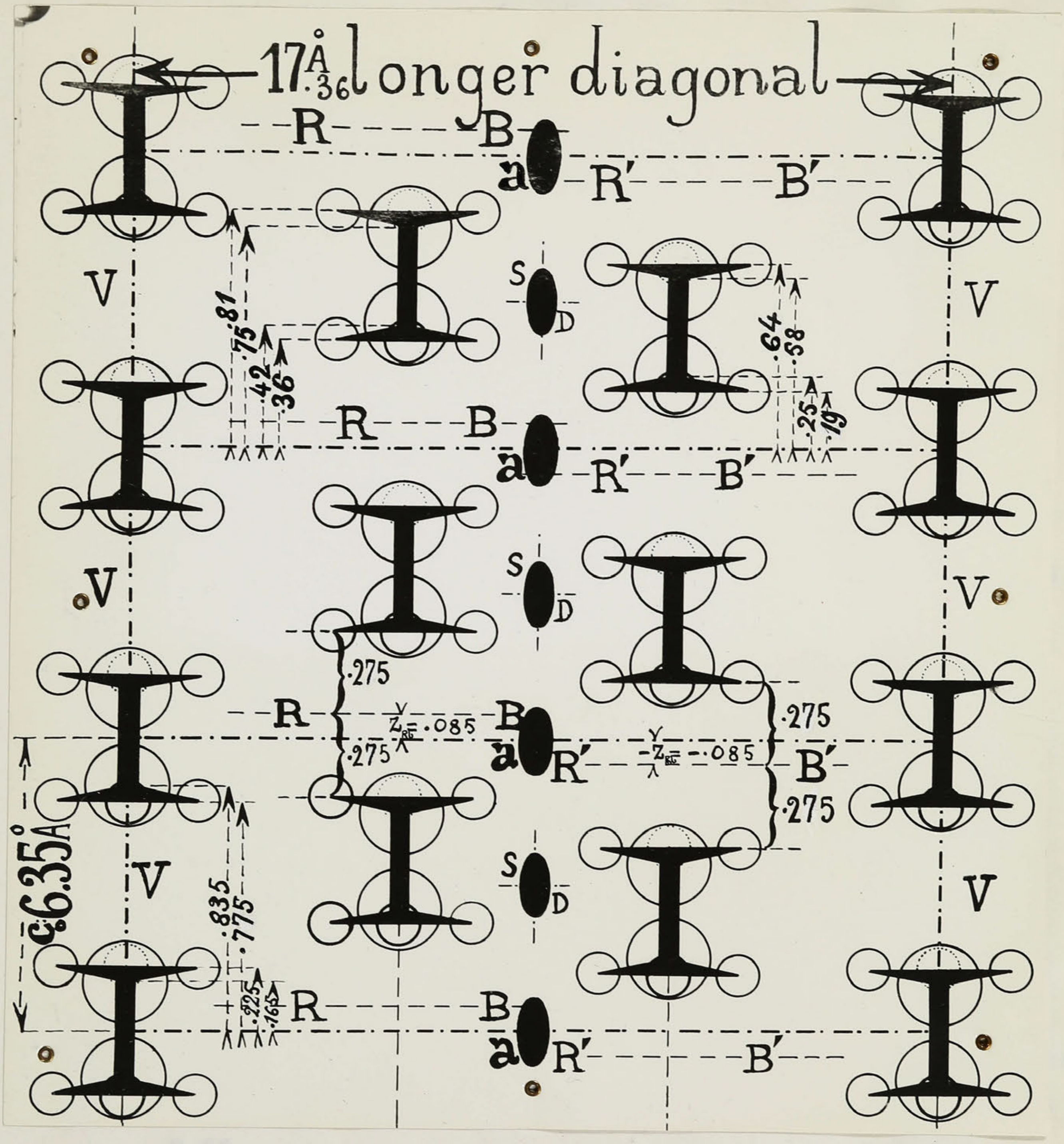

FIGURE 18B

Diagram showing Vertical Parameters of Possible Planes of Rb$^+$ in (g) Positions

(u'''_B = 0.75, u''''_B = 0.42, z'_B = 0.19, z''_B = 0.64)

If the six rubidium ions are placed in (g) another unknown vertical parameter (z_{Rb}) is introduced. The rubidium ions thereby occur in layers corresponding to RB and R'B' in Figure 18 at heights z_{Rb} and $\bar{z}_{Rb}$, respectively.

The most logical position for the layer RB is equidistant from the planes of oxygen atoms whose vertical parameters are z' and z"-1, respectively. Making this assumption, the value of z_{Rb} can be calculated as follows.

$$z' = 1-\left[(h/4)/c_o\right] - u''' \quad \text{(see p. 64)}$$
$$= 1-0.06-(0.33+u'''')$$

Although either u_A''' (0.25) or u_B''' (0.42) may be assumed for this calculation, it will be shown later than $u'''' = u_A''' = 0.25$.

Hence

$$z' = 1-0.06-0.33-0.25$$
$$= 0.36,$$

and

$$z'' = 1+\left[(h/4)/c_o\right] -u''' \quad \text{(see p. 64)}$$
$$= 1+0.06-0.25$$
$$= 0.81,$$

so that,

$$z''-1 = -0.19$$

The vertical distance between the oxygen planes under discussion is equal to $z'-(z''-1) = 0.36+0.19 = 0.55$, so that $z_{Rb} = (\frac{0.55}{2} - 0.19) = 0.085$.

Replacing the vertical parameters 0 and 1/2 by 0.085 and -0.085 for z_{Rb} and $\bar{z}_{Rb}$ of the (g) positions, calculated values of log I are given in Table IX.

TABLE IX

(0001)	I	log I (calculated)	
l	(obs.)	(e)+(f)	(g)
1	v.w.	3.29	5.31
2	w.	4.31	3.04
3	w.	3.50	3.61
4	v.s.	4.49	3.96
5	m.	3.68	3.73
6	s.	4.13	4.22
7	a.	1.93	4.11

It is evident that, as in the cases of 2(e) and 2(f), the calculated values of log I for the odd orders are too high. Thus, although only one possible value of z_{Rb} has been tested, it is evident that the rubidium ions must be close to $z_{Rb} = 0$ and 1/2, thus favouring (e)+(f) as the most probable positions.

The vertical parameters of the cell, therefore, are as follows.

Rb^{1+} : 0 and 1/2

S^{2+} : $u'' = 0.165$

: $u'''' = u''''_A = 0.25$, or

$= u''''_B = 0.42$.

: $u''' = u'''_A = 2u''+u''''_A = 0.58$, or

$= u'''_B = 2u''+u''''_B = 0.75$

O^{1-} : $z = u''+\left[(h/4)/c_o\right] = 0.225$

: $z' = z'_A = 1-u'''_A-\left[(h/4)/c_o\right] = 0.36$, or

$= z'_B = 1-u'''_B-\left[(h/4)/c_o\right] = 0.19$.

: $z'' = z''_A = 1+\left[(h/4)/c_o\right]-u''''_A = 0.81$, or

$= z''_B = 1+\left[(h/4)/c_o\right]-u''''_B = 0.64$.

A choice between the A and B alternative values will be made later.

(e) Lateral Parameters.

The vertical distance between a sulphur atom and the plane of the three nearest oxygen atoms $\left[(h/4)/c_0\right]$ has been established as about 0.06 c_0 = 0.06 x 6.35 = 0.381Å. which now replaces the original assumption of 0.498Å. Assuming the same sulphur-to-oxygen distance (1.495Å.) as before, the radius of the circle passing through the centres of the three oxygen atoms, B, C, D, of Figure 15A (p.62A) thus becomes, as in Figure 19A, $R' = \sqrt{(1.495)^2-(0.381)^2} =$ 1.44_6Å. Hence the distance between two adjacent oxygen atoms of the same SO_3 group is now $1.44_6\sqrt{3} = 2.50_4$Å. (see Figure 19A) instead of 2.44_1Å. (as on p. 63). In terms of c_0, this is equal to $(2.50_4/c_0) = (2.50_4/10.02) = 0.25$.

The symmetry elements of the space group D_3^2 permit any orientation of the dithionate ion at B in Figure 12 (p.54A) about a vertical axis or any positions of its two constituent SO_3 groups relative to each other about this axis. The relative positions of the SO_3 groups making up the dithionate ion at C automatically follow any changes in those at B by virtue of the symmetry involved. Possible variations of the dithionate ions A at the corners of the cell (Figure 12) from what will be referred to hereafter as the "close-packed" arrangement (shown in Figure 19A), however, are limited to equal left- and right-handed turns of the upper and lower SO_3 groups, respectively, or vice versa, since the edges of the

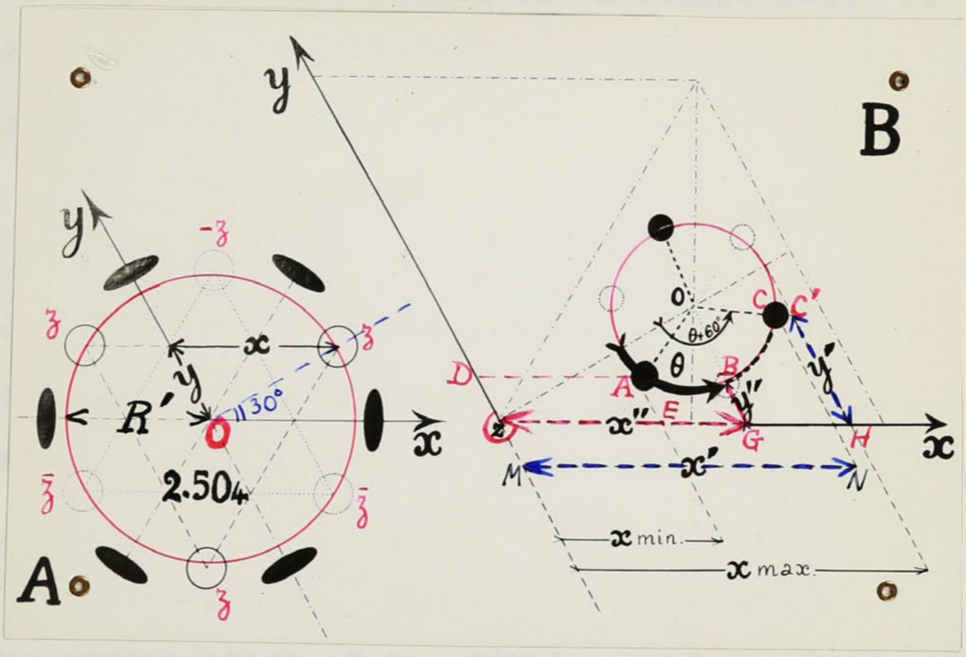

FIGURE 19

A. Plan of "Close-packed" Dithionate Ion

B. Diagram illustrating Dependence of y", x', y' on x" for "Close-packed" Dithionate Ion cell are along two-fold axes of symmetry. These conditions are illustrated in Figure 20.

In order to fix the lateral parameters it may be assumed temporarily that all the dithionate ions have the close-packed structure indicated in Figure 19A. It is then possible to determine the lateral (x and y) parameters of the oxygen atoms of the dithionate ions at the corners of the cell. It is clear from Figure 19A that, since the axes Ox, Oy and their bisector (the smaller diagonal of the cell) are two-fold axes of symmetry, the centre of the oxygen atom with coordinates x, y is at 30° from Ox and at 90° from Oy. Hence, $y = (x/2) = (R'\sqrt{3})/3 = (2.50_4)/3$, or, in terms of a_o, $y = (2.50_4)/3(10.02) = 0.083_3$, and $x = 2y = 0.166_6$.

Of the four lateral parameters (x', y', x'', y'') for the oxygen atoms of the dithionate ions within the cell, any three may be determined if the fourth is known. In Figure 19B, consider a point B on the circumference of a circle with centre at O (corresponding to C in Figure 12, p.54A) and with radius (R') equal to 1.44_6Å. The lateral coordinates of O are $x_o = 2/3$, $y_o = 1/3$. From a diagram such as Figure 19B drawn to a large scale (1cm. $\equiv$ 0.1002Å = $0.01a_o$) so that readings could be made directly in parameters (<u>i.e.</u>, in terms of a_o), $x''_B = ZG$ and $y''_B = BG$ for any point B could be determined. Since close-packing of the SO_3 groups of each dithionate ion has been assumed, the coordinates of the point C (corresponding

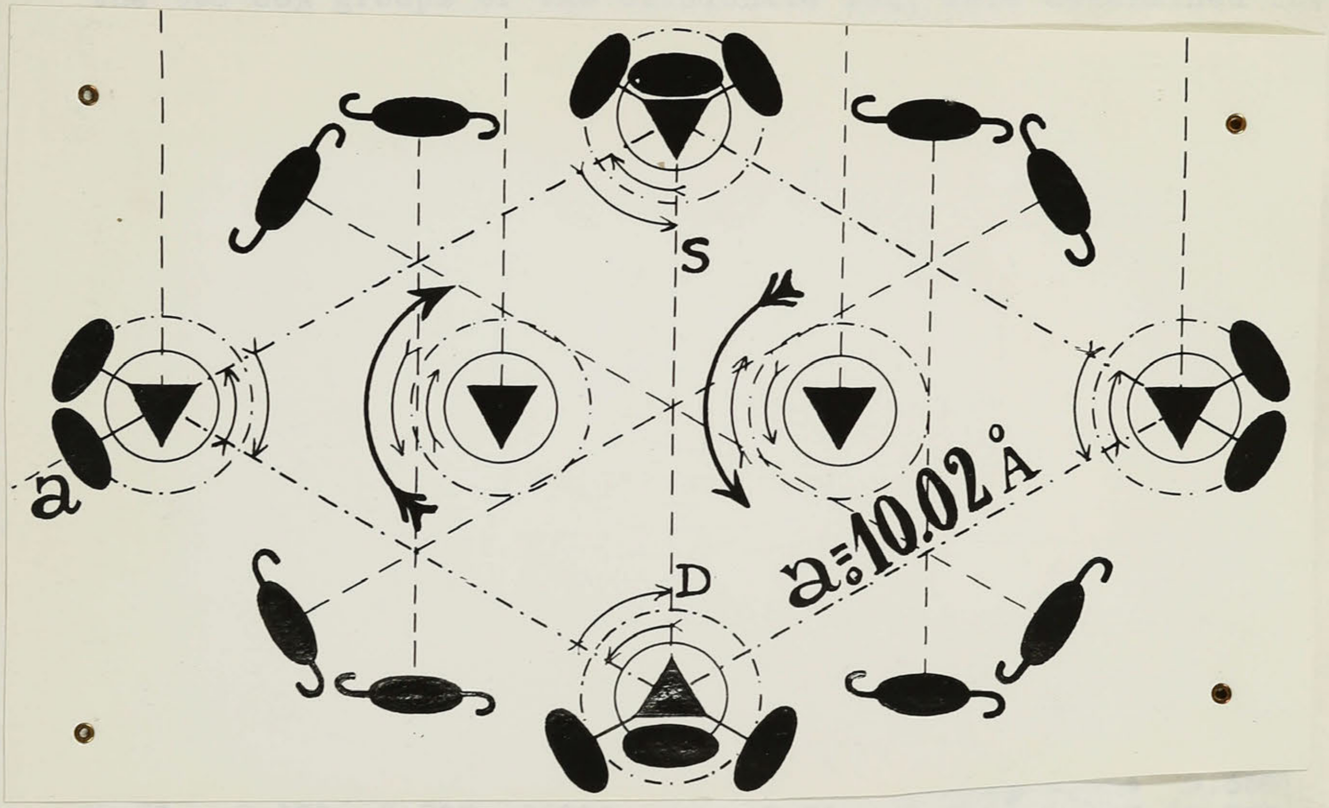

FIGURE 20

Symmetry Elements of D_3^2 showing Permissible Rotations of SO_3 Groups about Vertical Axes to B in the other SO_3 group) are $x_c' = MN$, $y_c' = C'H$. Thus x', y', x'', y'', fixing the positions of the oxygen atoms in the two SO_3 groups of the dithionate ion, were determined for all possible orientations about the vertical axis. Due to the three-fold nature of this axis it was necessary only to consider an angular range of 120°. The following Table X gives the values of y'', x', y' corresponding to x'' over the appropriate range $0.750 > x'' > 0.501_6$ for $R' = 1.44_6$ Å.

TABLE X

x"	y"	x'	y'
0.501_6	0.251	0.585	0.168
0.51	0.211_5	0.633	0.176
0.52	0.194	0.661	0.187
0.53	0.185	0.679	0.196_5
0.54	0.178_4	0.695	0.206_5
0.55	0.173_5	0.710	0.216_5
0.56	0.171	0.723_5	0.226
0.57	0.168_5	0.735	0.236_7
0.58	0.168	0.746_4	0.247
0.59	0.168	0.755_5	0.256_5
0.60	0.169	0.765	0.266_5
0.61	0.170_5	0.773_6	0.276_5
0.62	0.172_5	0.780	0.286
0.63	0.175_5	0.788_3	0.296
0.64	0.178_5	0.795	0.306_5
0.65	0.182	0.801_5	0.316_5
0.66	0.187	0.806_6	0.327
0.67	0.192	0.812_3	0.336_8
0.68	0.197	0.817	0.347_5
0.69	0.203	0.820	0.357
0.70	0.209_5	0.824	0.367
0.71	0.216_5	0.827	0.376_6
0.72	0.223_6	0.830	0.387_5
0.73	0.231_6	0.830_5	0.396_5
0.74	0.241	0.832	0.406_5
0.75	0.251	0.832	0.416_6
0.76	0.261_5	0.831_5	0.426_4
0.77	0.272_5	0.829_6	0.436_5
0.78	0.285_4	0.827_6	0.447_5

Graphical treatment not only was easier and less time-consuming than individual calculations would have been but it also enabled the effect of modifying the sulphur-to-oxygen distance (and thence R') to be determined immediately by simply drawing circles of appropriate radii.

The two lateral parameters (u, u') defining the positions of the rubidium ions [(e)+(f), p.56] may have any value from 0 to 1 insofar as the symmetry elements of the cell are concerned and, furthermore, they are entirely independent of each other. The relatively high atomic number of rubidium, however, makes the contribution of the rubidium ions to the general structure factor for $\{m0\bar{m}0\}$ of major importance so that reflections from this form were employed for the determination of u and u'.

When x = 2y (see p. 74) the general structure factor for $\{m0\bar{m}0\}$ is given by

$$\begin{aligned} F = {} & 2\,Rb^{1+}(\cos 2\pi um + \cos 2\pi u'm + 1) \\ & + 2\,S^{2+}\left[1 + 2\cos \pi m \cos (\pi m)/3\right] \\ & + 2\,O^{1-}\left[\cos 2\pi mx + 2\cos 2\pi my \right. \\ & + \cos 2\pi mx' + \cos 2\pi my' + \cos 2\pi m(x'-y') \\ & \left. + \cos 2\pi mx'' + \cos 2\pi my'' + \cos 2\pi m(x''-y'')\right] \end{aligned}$$

In the following Table XI are recorded the values for $(\sin\theta)/\lambda$, log P and the scattering factors for Rb^{1+}, S^{2+}, O^{1-}.

TABLE XI

$(m0\bar{m}0)$ m	$(\sin\theta)/\lambda \times 10^{-8}$	log P	Rb^{1+}	S^{2+}	O^{1-}
1	0.0576	1.048	34.6	13.65	8.80
2	0.1152	0.731	32.0	11.25	8.05
3	0.1728	0.530	28.8	11.00	7.00
4	0.2304	0.371	26.3	9.85	5.90
5	0.2880	0.236	24.5	9.10	4.80
6	0.3456	0.120	23.3	8.60	3.80
7	0.4032	0.034	22.2	8.20	3.05
8	0.4608	0.000	20.7	7.90	2.55

The contributions of the oxygen atoms to the structure factor for $\left\{m0\bar{m}0\right\}$ is relatively small and is a minimum, at least insofar as the second, fourth, fifth, seventh and eighth orders are concerned, when $x'' = 0.75$ ($y'' = 0.251$, $x' = 0.832$, $y' = 0.416_6$, see Table X, p. 75). For this value of x'', the structure factor contributions from the oxygen atoms for the orders named lie between -0.10 and 0.11 while the total structure factor (F) has values between 12.21 and 49.31. For the third and sixth orders the oxygen contributions are -41.83 and -22.8 respectively, in total values of 169.1 and 89.8, respectively. This is of no importance, however, since the contributions of the sulphur atoms, which are zero for all values of m not integral multiples of 3, raise the calculated values of log I for the third and sixth orders above the values for the other orders under almost all conditions. The first order cannot be discussed since its calculated position on the photographic films came within the area shielded with lead to prevent impingement of the undiffracted beam on the film during exposure.

Taking the values for u and u' proposed by Huggins and Frank (0.375, 0.69) and by Helwig (0.39, 0.69) for the potassium ions in potassium dithionate as a guide, the following Table XII shows the values of log I calculated for various combinations of u and u' over the ranges 0.36 to 0.39 for u and 0.69 to 0.715 for u', assuming $x'' = 0.75$ so as to remove the influence of the oxygen atoms as completely as possible.

TABLE XII

log I (calculated)

(m0m̄0)	I	u =	0.36	0.375	0.375	0.375	0.375	0.375	0.375
m	(obs.)	u' =	0.712	0.69	0.70	0.705	0.71	0.712	0.715
3	v.s.		5.18	4.10	4.99	4.97	4.95	4.94	4.93
6	s.		4.25	3.35	4.03	3.94	3.84	3.80	3.73
8	m.		3.52	3.24	3.39	3.50	3.63	3.68	3.77
4	w.		3.44	1.41	2.79	3.07	3.27	3.33	3.42
7	w.		3.33	3.11	3.41	3.49	3.54	3.55	3.55
5	v.w.		2.78	3.25	3.31	3.30	3.25	3.23	3.17
2	a.		0.09	3.20	2.90	2.73	2.52	2.43	2.27

log I (calculated)

(m0m̄0)	I	u =	0.375	0.38	0.38	0.38	0.39	0.39
m	(obs.)	u' =	0.72	0.69	0.695	0.70	0.69	0.712
3	v.s.		4.90	4.99	4.98	4.77	5.07	5.09
6	s.		3.61	4.09	4.02	3.94	4.38	3.77
8	m.		3.86	3.21	3.27	3.36	2.97	3.52
4	w.		3.54	1.51	2.39	2.81	2.06	3.45
7	w.		3.53	3.28	3.43	3.54	3.59	3.87
5	v.w.		3.04	3.48	3.45	3.43	3.62	3.68
2	a.		2.02	3.39	3.27	3.15	3.67	3.30

A careful examination of Table XII shows that, of the combinations listed, the only ones for which the relative order of values of log I (calculated) is in agreement with the relative order of observed intensities are 0.36, 0.712; 0.375, 0.712; 0.375, 0.71, of which the last may be discarded on the grounds that it leads to calculated values for the fourth and fifth orders that are too nearly identical. Neither the potassium parameters of Huggins and Frank (0.375, 0.69) nor of Helwig (0.39, 0.69) give satisfactory results.

It is of interest to see if any progress can be made on the basis of interionic distances. The radius of the ionic domain of Rb^+ is greater than that of K^+ by about 0.137Å. in the iodides, 0.149Å. in the bromides, and 0.147Å. in the chlorides (38, p. 419). From empirical values determined by Wasastjerna (38, p. 428), and based on a consideration of molar refractive indices of crystals, the difference is 0.20Å. On the assumption that the radius of Cs^+ is equal to the radius of I^-, the radius of the ionic domain of Rb^+ is greater than that of K^+ by 0.148Å. (38, p. 421). The difference between the radii of the ionic domains of Rb^+ and K^+, therefore, may be taken as approximately 0.15.

Potassium-to-oxygen distances have been determined as 2.79Å. to 2.81Å. in KH_2PO_4(39), 2.72Å. to 2.95Å. in $KAl(SO_4)_4$ (40), 2.73Å. to 3.12Å. in $KClO_3$ (41) and 2.71Å. to 3.50Å. in K_2SO_4 (42). The minimum potassium-to-oxygen distance, therefore, appears to be about 2.71Å. If to this be added the difference (0.15) between the radii of the atomic domains of Rb^+ and K^+, a value of 2.86Å. is obtained for a minimum estimate of the distance from rubidium to oxygen. In Rb_2SO_4 the minimum rubidium-to-oxygen distance calculated from data cited by Wyckoff (10, p. 294) is 2.99Å. although Ogg (43) gives 2.89 from his experimental data and 2.88 as the sum of atomic radii based on Pauling's figures.

Hence, assuming a rubidium-to-oxygen distance of 2.86Å. between the rubidium ions at $R(\bar{u}00)$ and $R'(0\bar{u}',1/2)$, respectively, and the nearest oxygen atoms of the dithionate ion, the vertical axis of which passes through the point S of Figure 21, possible values of u and u' may be calculated. In Figure 21 the circle, with centre at S, passing through the points O_1, O_2, O_3, O_4, O_5, O_6 represents the projection of the locus of the possible positions of the oxygen atoms of the dithionate ion at the corner (S) of the cell. It has been pointed out previously (see p. 73) that the two-fold nature of the a axes requires that a right-handed turn about a vertical axis of one of the SO_3 groups of the dithionate ion at S from the close-packed arrangement must be accompanied by a left-handed turn of the same magnitude on the part of the other SO_3 group and vice versa. Bearing this in mind, the points O_1, O_2, O_3, O_4, O_5, O_6 represent the projections of arbitrarily chosen possible positions of an oxygen atom having the lateral parameters $\bar{y}$, x-y. Since the vertical

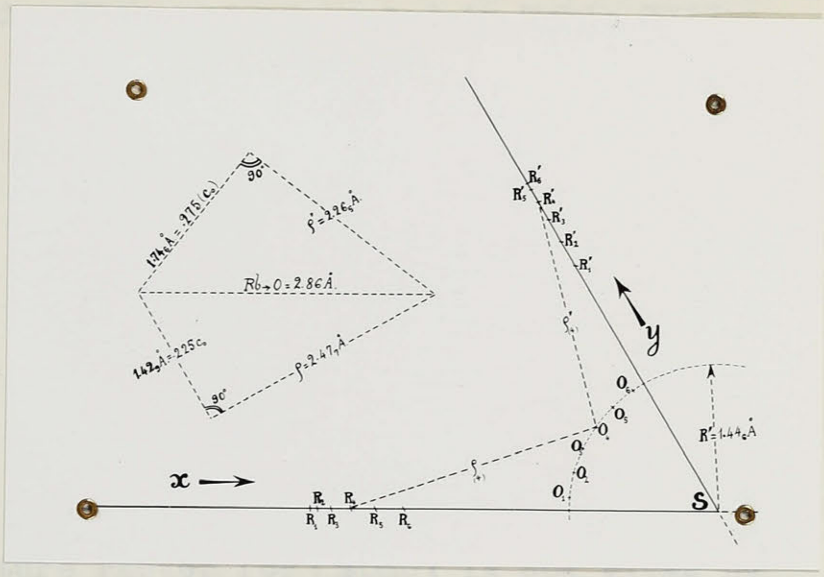

FIGURE 21

Relative Positions of Rb^+ (R,R') and O^- (O) of Dithionate Ion at Corner of Cell for Rb^+-to-O^- Distance of 2.86Å.

parameter z is known (0.225, see p.72) the values of u and u' defining the possible positions ($\bar{u}00$; $0\bar{u}'$, 1/2) of the rubidium ions at R_1, R_2, R_3, R_4, R_5, R_6 and R'_1, R'_2, R'_3, R'_4, R'_5, R'_6, respectively, on the assumption that in all cases the rubidium-to-oxygen distance shall be 2.86Å., may readily be calculated. They are presented in Table XIII.

TABLE XIII

	O_1	O_2	O_3	O_4	O_5	O_6
y	0.139	0.129	0.117	0.101	0.081	0.058
x-y	0.009	0.028	0.042	0.064	0.086	0.106
u	0.392	0.390	0.384	0.375	0.360	0.342
u'	0.730	0.712	0.697	0.676	0.658	0.653_5

Since x no longer is equal to 2y (compare p. 74) the structure factor for $\{m0\bar{m}0\}$ is now given by

$$\begin{aligned} F = {} & 2\,Rb^{1+}(\cos 2\pi um + \cos 2\pi u'm + 1) \\ & + 2\,S^{2+}\left[1 + 2\cos \pi m \cos(\pi m)/3\right] \\ & + 2\,O^{1-}\Big[\cos 2\pi mx + \cos 2\pi my \\ & + \cos 2\pi m(x-y) + \cos 2\pi mx' \\ & + \cos 2\pi my' + \cos 2\pi m(x'-y') \\ & + \cos 2\pi mx'' + \cos 2\pi my'' \\ & + \cos 2\pi m(x''-y'')\Big] \end{aligned}$$

Substituting values of x, y, u, u' from Table XIII and retaining the values of x", y", x', y' previously employed (see p. 77), log I was calculated for the various orders of $(m0\bar{m}0)$ and the results are shown in Table XIV.

TABLE XIV

			log I (calculated)					
$(m0\bar{m}0)$	I	u =	0.392	0.390	0.384	0.375	0.360	0.342
m	(obs.)	u' =	0.730	0.712	0.697	0.676	0.658	0.643_5
3	v.s.		4.77	4.88	4.92	5.04	5.09	5.00
6	s.		3.32	3.75	4.06	4.31	4.45	4.51
8	m.		4.06	3.67	3.37	3.36	3.63	3.61
4	w.		3.91	3.59	2.85	2.67	3.38_5	3.28_5
7	w.		4.03	4.04	3.74	2.01	3.15	3.01
5	v.w.		4.10	3.85	3.66	3.60	3.66	3.98
2	a.		3.10	3.26	3.38	3.53	3.54	3.45

It will be seen that in no case is satisfactory agreement obtained between the relative order of calculated (log I) and observed intensities. The least objectionable of the u, u' combinations is u = 0.360, u'=0.658, although the fifth and second orders yield values for log I that are too high and that for the fourth order should be somewhat lower.

The shape of the log I curves for different values of x" over the range 0.585 to 0.832, as shown in Figure 22, disposes of the possibility that more acceptable agreement might be obtained for some value of x" other than 0.75. It will be observed that, although log I for the fifth order is sensitive to changes in the value of x", the second order is essentially constant over the complete range of values, and is too high. Since the structure factor for $\{m0\bar{m}0\}$ does not involve vertical parameters the log I *vs*. x" curves have a period of 60° when the two SO_3 groups of the dithionate ions within the cell are assumed, as in the present case, to be close-packed.

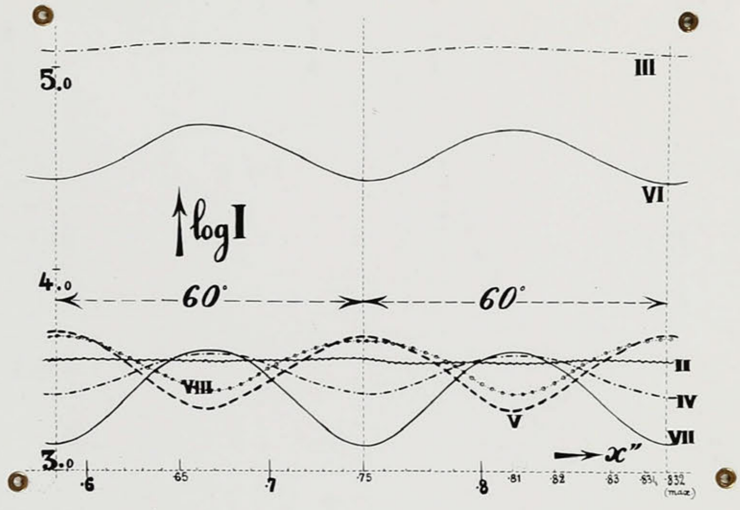

FIGURE 22

Log I$_{\{mOmO\}}$ vs. x"

Dithionate Ions "Close-packed"

(u = 0.360; u' = 0.658)

Furthermore, if the close-packed arrangement of the dithionate ions within the cell is to be preserved, it can be shown that it is not possible to maintain a minimum rubidium-to-oxygen distance of 2.86Å. between the rubidium ion R'_5(u' = 0.658) and any two of the oxygens of heights z' and z'', respectively, of the nearest dithionate ion within the cell for any orientation of this ion about a vertical axis. This is clear from Figure 23. In this figure, S_1 represents the projection of the centre of the sulphur atoms of lateral coordinates 2/3, 1/3 and the circle through the points A, B, C, P, etc. is the projection of the locus of the positions of the oxygen atoms. The line PR'_5,therefore, represents the projection of the shortest rubidium-to-oxygen distance. Since the axis through S_1 is a three-fold axis it is necessary only to consider oxygen positions over an angular range of 120°. The lines S_1A and S_1F, therefore, have been drawn at 60° to the left and right, respectively, of $S_1R'_5$. The arcs BME and CND represent the intersections of a sphere of radius 2.86Å. and centre at R'_5 with horizontal planes at heights z'_A (0.36, see p. 72) and z''_A (0.81, see p. 72). The arcs BCPDE and CPD, therefore, represent the projections of oxygen positions at heights z'_A and z''_A, respectively, which are prohibited by the restriction that the rubidium-to-oxygen distance be not less than 2.86Å. Consequently, permissible positions are limited to the ranges AB and EF for the oxygen atoms at height z'_A and

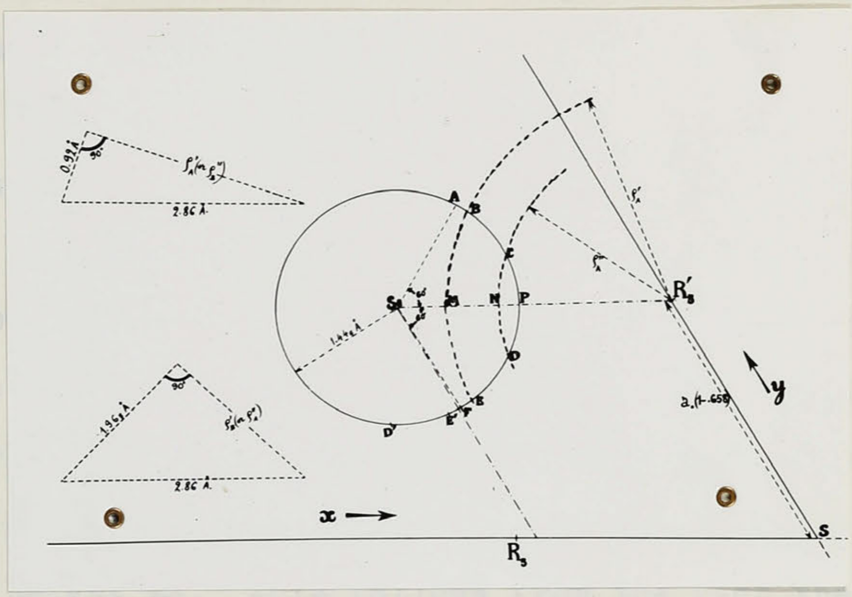

FIGURE 23

Permissible and Prohibited Ranges of x', y' and of x", y" for Rb^+-to-O^- Distance of 2.86Å.

to AC and DF for those at height z''_A. For the close-packed arrangement, oxygen atoms at z'_A are separated laterally from those at z''_A by an angle of 60°. Hence, it will be found that placing an oxygen atom at height z'_A within either range of possible positions AB or EF results in an oxygen atom at height z''_A falling within the prohibited range CPD or, similarly, placing an oxygen atom at height z''_A within either range of possible positions AC or DF automatically places an oxygen atom at height z'_A within the prohibited range BCPDE. The same argument is valid if z'_B and z''_B are employed instead of z'_A and z''_A, respectively, except that in the former case the arc BME in Figure 23 is at height z''_B (0.64) and hence BCPDE is a prohibited range for oxygen atoms at height z''_B and the arc CND is at height z'_B (0.19) and hence CPD is impossible for oxygen atoms at height z'_B. This follows from the fact that $z''_A - 0.50 = 0.31 = 0.50 - z'_B$ and $z''_B - 0.50 = 0.14 = 0.50 - z'_A$, and that the vertical parameter of the rubidium ion at R'_5 in Figure 23 is 0.50.

If, however, the assumption of a close-packed arrangement be abandoned, rubidium-to-oxygen distances are satisfactory when oxygen atoms are in positions within the ranges E'FE (where E'F is equivalent to BA) and D'FD (where D'F is equivalent to CA), at heights z'_A and z''_A, respectively.

Since the range E'FE is relatively small (13°), x' may be fixed for purposes of calculation at 0.67 (corresponding to the point F in Figure 23). For this value of x' the variation in log I for values of x" over the range $0.57 \leqslant x'' \leqslant 0.768$ (corresponding to D'F D in Figure 23) is shown in Figure 24. The best agreement with the relative order of observed intensities occurs when $x'' = 0.75$ although the fourth order in Figure 24 is too low. It may be mentioned that for no other value of x' in the range $0.652 \leqslant x' \leqslant 0.689$ (corresponding to E'F E in Figure 23) is satisfactory agreement obtained. For the same reasons as those presented in the preceding paragraph, the foregoing argument may be applied when z'_B, z''_B are involved instead of z'_A, z''_A except that E'FE and D'FD then represent permissible ranges for oxygen atoms at heights z''_B and z'_B, respectively, instead of z'_A and z''_A, respectively.

It appears to be impossible, therefore, to maintain a minimum rubidium-to-oxygen distance as high as 2.86Å.

Returning, therefore, to the original assumption of close-packing in all dithionate ions and $x'' = 0.75$ (see p. 77), it has been shown that reasonably good agreement between the relative order of calculated values of log I and that of observed intensities is obtained when $u = 0.36$, $u' = 0.712$ and when $u = 0.375$, $u' = 0.712$. In each of these cases the shortest rubidium-to-oxygen distances are as follows:

1. $\underline{u = 0.36,\ u' = 0.712}$

$Rb^+(\bar{u}00)$ to nearest oxygen of dithionate ion at corner of cell , 2.85Å.

$Rb^+(\bar{u}00)$ to nearest oxygen of dithionate ion within the cell, 2.50Å.

$Rb^+(0\bar{u}',1/2)$ to nearest oxygen of dithionate ion at corner of cell, 2.51Å.

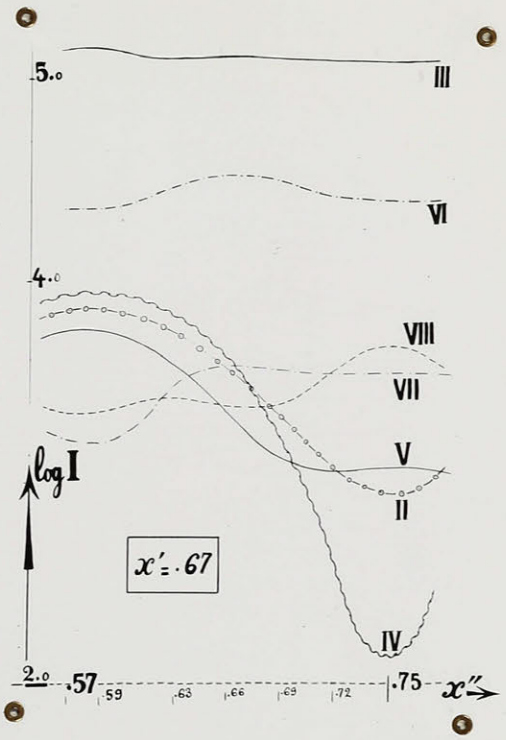

FIGURE 24

Log $I_{\{m O \bar{m} O\}}$ vs. x"

(x' = 0.67)

(u = 0.360; u' = 0.658)

2. <u>$u = 0.375$, $u' = 0.712$</u>

$Rb^+(\bar{u}00)$ to nearest oxygen of dithionate ion at corner of cell, 2.98Å.

$Rb^+(\bar{u}00)$ to nearest oxygen of dithionate ion within the cell, 2.49Å.

$Rb^+(0\bar{u}',1/2)$ to nearest oxygen of dithionate ion at corner of cell, 2.51Å.

The minimum distances (2.49Å., 2.50Å., 2.51Å.) almost certainly are too small to be admissible.

Leaving out of consideration the dithionate ion within the cell, the oxygen atoms of the dithionate ion at the corner may be turned counterclockwise about the vertical three-fold axis until the distances between the rubidium ions at $(0\bar{u}',1/2)$ and $(\bar{u}00)$, respectively, and the nearest oxygen atom of the dithionate ion at the corner of the cell are equal. For $u = 0.36$, $u' = 0.712$, the distance is 2.69Å. while for $u=0.375$, $u' = 0.712$, it is 2.77Å. Although both of these values are less than that expected (namely, approximately 2.86Å.), the second (for $u = 0.375$, $u' = 0.712$) is more acceptable than the first. It is obvious that any further rotation of the oxygen atoms either clockwise or counterclockwise will result in one of the equalized distances increasing at the expense of the other. Thus to increase the value of 2.77Å. from one rubidium ion when $u = 0.375$, $u' = 0.712$ would introduce a correspondingly <u>lower</u> value for the distance from the other rubidium ion. The values of x and y, defining the lateral positions of the oxygen atoms of the dithionate ions at the corners of the cell when the distances between the rubidium ions (uu0; u'u',1/2) and the nearest of these oxygen atoms are equal to each other and to 2.77Å., are $x = 0.160_3$, $y = 0.120_4$.

Values of log I for $\{m0\bar{m}0\}$ calculated on the basis of close-packing for the dithionate ion within the cell, $x'' = 0.75$, $u = 0.375$, $u' = 0.712$, $x = 0.160_3$, $y = 0.120_4$ are compared with observed intensities in Table XV.

TABLE XV

$(m0\bar{m}0)$ m	I (obs.)	log I (calculated)
3	v.s.	4.95
6	s.	3.97
8	m.	3.77
4	w.	3.47
7	w.	3.75
5	v.w.	2.86
2	a.	2.45

The calculated (log I) values for the seventh and second orders appear to be too high.

Moreover, it has been shown (p. 86) that for close-packing of the SO_3 groups of the dithionate ion within the cell and $x'' = 0.75$ the distance between the rubidium ion at $(\bar{u}00)$ and the nearest oxygen atom of this dithionate ion is only 2.49Å. when $u = 0.375$.

Since u and u' have been fixed at 0.375 and 0.712, respectively, and the largest value possible for a minimum rubidium-to-oxygen distance has been determined as 2.77Å. it is possible to establish permissible and prohibited ranges for x' and x'' defining the positions of the oxygen atoms of the dithionate ions within the cell. Thus, Figure 25 is similar to Figure 23 (page 83A) except that a larger area of the projection on the basal plane is shown. In Figure 25, R and R' represent the projections of the centres of the rubidium ions, the u parameters of which are $u = 0.375$ and $u' = 0.712$, respectively, at heights 0 and 0.5, respectively. The circles around S, S_1 (and equivalent points) as centres represent the projections of the loci of oxygen atom positions. The arcs drawn with R and R' as centres represent the projections of the intersections of spheres of radii 2.77Å.and centres at R and R' with planes at heights $z'_A = 0.36$ (or $z''_B = 0.64$) - shown as a line of dashes and dots - and $z''_A = 0.81$ (or $z'_B = 0.19$) - shown as a line of dashes only - respectively. Values of $x'_A(x''_B)$, $y'_A(y''_B)$, $x''_A(x'_B)$, $y''_A(y'_B)$ that are permissible for a minimum rubidium-to-oxygen distance of 2.77Å. may readily be determined from Figure 25. The limits of the ranges of values are shown in Figure 25 and in Table XVI below. Due to the three-fold axis through the point S_1 of Figure 25, three equivalent permissible ranges occur for x', y' and for x'', y'', but in establishing the parameters x', y', x'', y'' only one range of x', y' and one of x'', y'', of course, need be considered.

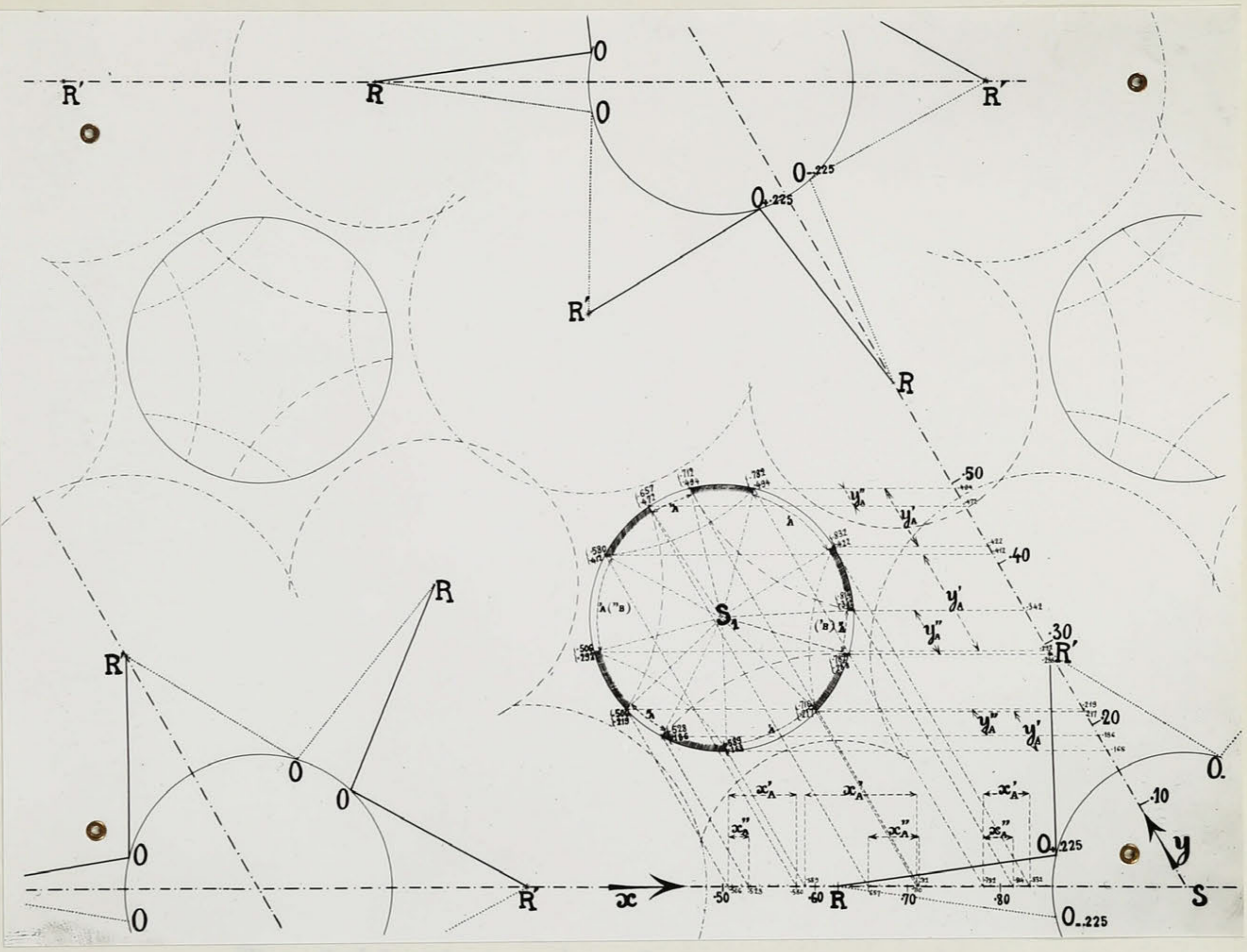

FIGURE 25

Permissible and Prohibited Ranges of x', y' and of x", y" for Rb^+-to-O^- Distance of 2.77Å.

TABLE XVI

Permissible Values of x', y', x", y"

	from	to
$x'_A(x''_B)$	0.506	0.580
$y'_A(y''_B)$	0.292	0.412
$x'_A(x''_B)$	0.782	0.832
$y'_A(y''_B)$	0.494	0.422
$x'_A(x''_B)$	0.589	0.710
$y'_A(y''_B)$	0.168	0.217
$x''_A(x'_B)$	0.657	0.712
$y''_A(y'_B)$	0.472	0.494
$x''_A(x'_B)$	0.782	0.814
$y''_A(y'_B)$	0.288	0.342
$x''_A(x'_B)$	0.506	0.528
$y''_A(y'_B)$	0.219	0.186

The following pair of ranges was selected for examination: $x'_A(x''_B) = 0.506$, $y'_A(y''_B) = 0.292$, to $x'_A(x''_B) = 0.580$, $y'_A(y''_B) = 0.412$; $x''_A(x'_B) = 0.506$, $y''_A(y'_B) = 0.219$, to $x''_A(x'_B) = 0.528$, $y''_A(y'_B) = 0.186$, (see Figure 24).

The values of log I for $\left\{ mO\bar{m}O \right\}$ calculated for different combinations of values within these ranges and for $x = 0.160_3$, $y = 0.120_4$ (see p. 87) are given in Table XVII.

TABLE XVII

$(m0\bar{m}0)$ m	I (obs.)		log I (calculated)					
		$x'_A(x''_B)$ =	0.506	0.510	0.506	0.524	0.524	0.524
		$y'_A(y''_B)$ =	0.292	0.303	0.292	0.337	0.337	0.337
		$x''_A(x'_B)$ =	0.506	0.516	0.528	0.510	0.516	0.524
		$y''_A(y'_B)$ =	0.219	0.201	0.186	0.211	0.201	0.191
3	v.s.		4.96	4.95	4.97	4.97	4.97	4.97
6	s.		4.18	4.30	4.28	4.31	4.35	4.37
8	m.		3.76	3.59	3.66	3.62	3.56	3.55
4	w.		4.06	3.78	3.64	3.62	3.43	3.17
7	w.		3.47	3.41	3.41	3.40	3.37	3.35
5	v.w.		3.60	2.84	3.08	3.02	3.11	3.24
2	a.		2.77	1.76	0.49	0.27	1.90	2.58

$(m0\bar{m}0)$ m	I (obs.)		log I (calculated)					
		$x'_A(x''_B)$ =	0.546	0.546	0.546	0.555	0.555	0.555
		$y'_A(y''_B)$ =	0.372	0.372	0.372	0.386	0.386	0.386
		$x''_A(x'_B)$ =	0.506	0.516	0.528	0.506	0.516	0.528
		$y''_A(y'_B)$ =	0.219	0.201	0.186	0.219	0.201	0.186
3	v.s.		4.96	4.97	4.97	4.96	4.96	4.96
6	s.		4.19	4.28	4.29	4.14	4.23	4.25
8	m.		3.71	3.60	3.61	3.70	3.58	3.59
4	w.		3.42	2.98	2.08	3.33	2.83	1.51
7	w.		3.55	3.51	3.50	3.63	3.60	3.59
5	v.w.		3.38	3.45	3.60	3.47	3.54	3.67
2	a.		2.26	2.80	3.16	2.55	2.96	3.28

$(m0\bar{m}0)$ m	I (obs.)		log I (calculated)					
		$x'_A(x''_B)$ =	0.570	0.570	0.570	0.580	0.580	0.580
		$y'_A(y''_B)$ =	0.404	0.404	0.404	0.412	0.412	0.412
		$x''_A(x'_B)$ =	0.506	0.516	0.528	0.506	0.516	0.528
		$y''_A(y'_B)$ =	0.219	0.201	0.186	0.219	0.201	0.186
3	v.s.		4.93	5.05	4.96	4.96	4.96	4.96
6	s.		4.08	4.13	4.19	4.07	4.17	4.18
8	m.		3.66	3.69	3.55	3.65	3.52	3.53
4	w.		3.25	2.88	0.34	3.23	2.64	$\bar{1}.62$
7	w.		3.73	3.69	3.69	3.74	3.71	3.70
5	v.w.		4.02	3.62	3.74	3.60	2.79	3.08
2	a.		2.74	$\bar{1}.96$	3.37	2.70	3.06	3.35

A careful examination of Table XVII shows that, of the combinations listed, only the following give relative orders of log I values in agreement with those of observed intensities:

$x'_A(x''_B) = 0.506$, $y'_A(y''_B) = 0.292$, $x''_A(x'_B) = 0.528$, $y''_A(y'_B) = 0.186$;
$x'_A(x''_B) = 0.524$, $y'_A(y''_B) = 0.337$, $x''_A(x'_B) = 0.516$, $y''_A(y'_B) = 0.201$;
$x'_A(x''_B) = 0.546$, $y'_A(y''_B) = 0.372$, $x''_A(x'_B) = 0.506$, $y''_A(y'_B) = 0.219$.

Of these, the first may be discarded since the value of log I for the fourth order is almost equal to that for the eighth order. In the case of the third, the log I value for the fifth order is not very much lower than that of the fourth.

It will be noted in Table XVII that, with $x'_A(x''_B) = 0.524$, $y'_A(y''_B) = 0.337$, decreasing or increasing the values of $x''_A(x'_B)$, $y''_A(y'_B)$ leads to unacceptable relative values of log I.

In the following Table XVIII are recorded the results of a series of calculations with values of $x'_A(x''_B)$ in the neighbourhood of 0.524 and 0.546 and with values of $x''_A(x'_B)$ between 0.506 and 0.516.

TABLE XVIII

$(m0\bar{m}0)$ m	I (obs.)		log I (calculated)					
		$x'_A(x''_B)$ =	0.524	0.538	0.538	0.538	0.535	0.530
		$y'_A(y''_B)$ =	0.337	0.361	0.361	0.361	0.356	0.347
		$x''_A(x'_B)$ =	0.516	0.516	0.510	0.506	0.506	0.506
		$y''_A(y'_B)$ =	0.201	0.201	0.211	0.219	0.219	0.219
3	v.s.		4.97	4.97	4.97	4.98	4.97	4.97
6	s.		4.35	4.31	4.27	4.23	4.24	4.26
8	m.		3.56	3.60	3.65	3.72	3.71	3.69
4	w.		3.43	3.13	3.39	3.51	3.56	3.64
7	w.		3.37	3.44	3.47	3.48	3.51	3.43
5	v.w.		3.11	3.35	3.29	3.27	3.84	3.79
2	a.		1.90	2.62	2.23	1.88	1.63	0.32

$(m0\bar{m}0)$ m	I (obs.)		log I (calculated)		
		$x'_A(x''_B)$ =	0.546	0.546	0.552
		$y'_A(y''_B)$ =	0.372	0.372	0.381
		$x''_A(x'_B)$ =	0.510	0.506	0.506
		$y''_A(y'_B)$ =	0.211	0.219	0.219
3	v.s.		4.97	4.96	4.96
6	s.		4.23	4.19	4.16
8	m.		3.65	3.71	3.71
4	w.		3.28	3.42	3.36
7	w.		3.54	3.55	3.60
5	v.w.		3.40	3.38	3.45
2	a.		2.48	2.26	2.46

The only other sets of values that appear to be as satisfactory as $x'_A(x''_B) = 0.524$, $y'_A(y''_B) = 0.337$, $x''_A(x'_B) = 0.516$, $y''_A(y'_B) = 0.201$ are the closely related pair, $x'_A(x''_B) = 0.538$, $y'_A(y''_B) = 0.361$, $x''_A(x'_B) = 0.506$, $y''_A(y'_B) = 0.219$ and $x'_A(x''_B) = 0.538$, $y'_A(y''_B) = 0.361$, $x''_A(x'_B) = 0.510$, $y''_A(y'_B) = 0.211$, of which the first shows better agreement between the log I values for the fourth and seventh orders and yields a lower and hence more acceptable value of log I for the second order.

From the data of Tables XVII and XVIII, therefore, it may be concluded that values of x', y', x'', y'' probably are close to one of the sets

$$\begin{array}{lcl} x'_A(x''_B) = 0.524 & & x'_A(x''_B) = 0.538 \\ y'_A(y''_B) = 0.337 & \text{or} & y'_A(y''_B) = 0.361 \\ x''_A(x'_B) = 0.516 & & x''_A(x'_B) = 0.506 \\ y''_A(y'_B) = 0.201 & & y''_A(y'_B) = 0.219 \end{array}$$

It is now of interest to see if any distinction can be made between these two sets on the basis of the relative order of log I values and of observed intensities of diffraction effects from other forms. As a matter of record, calculations also will be shown for $x'_A(x''_B) = 0.546$, $y'_A(y''_B) = 0.372$, $x''_A(x'_B) = 0.506$, $y''_A(y'_B) = 0.219$, because, although it has been noted that log I values for $\{m0\bar{m}0\}$ are not highly satisfactory for this set, it will be shown later that it denotes an orientation of oxygen atoms more nearly comparable to that of Huggins and Frank for $K_2S_2O_6$ than does either of the other sets under examination.

It will be shown later (p. 103) that for the three sets of values of x', y', x'', y'' acceptable results for log $I_{\{m0\bar{m}m\}}$ are not obtained when $z' = z'_B$ and $z'' = z''_B$. In the following Table XIX, values of log I for $\{m0\bar{m}m\}$, calculated for the combinations of x'_A, y'_A, x''_A, y''_A shown, are compared with observed intensities.

TABLE XIX

$(m0\bar{m}m)$ m	I (obs.)		log I (calculated)		
		$x_A' =$	0.524	0.538	0.546
		$y_A' =$	0.337	0.361	0.372
		$x_A'' =$	0.516	0.506	0.506
		$y_A'' =$	0.201	0.219	0.219
1	s.(-)		3.80	3.78	3.78
2	m.		3.27	3.33	3.35
5	m.		3.38	3.42	3.42
3	v.w.		3.01	3.11	3.06
4	a.		2.49	2.25	2.18

Satisfactory values for log I are obtained in each of the three cases. On the basis of the data presented in Table XIX, the highest value (0.546) of x_A' may be considered as slightly better than the other two since the difference between the second (m.) and fifth (m.) orders is less and that between the second (m.) and third (v.w.) and between the third (v.w.) and fourth (a.) is greater than for either of the other combinations.

Reflections from $\{m0\bar{m}m\}$, therefore, appear to favour values of x_A', x_A'' close to 0.546, 0.506, respectively, whereas those from $\{m0\bar{m}0\}$ indicate values in the neighbourhood of 0.538, 0.506, respectively, or 0.524, 0.516, respectively. It is of interest, therefore, to consider the relative intensity of reflections from $\{mm\bar{2m}0\}$ and from $\{mm\bar{2m}m\}$.

The general structure factor for $\{mm\bar{2m}0\}$ is given by

$$
\begin{aligned}
F = {} & Rb^{1+}(\cos m\,4\pi u + i \sin m\,4\pi u \\
& + \cos m\,4\pi u' + i \sin m\,4\pi u' + 2 \cos m\,2\pi u \\
& - 2\,i \sin m\,2\pi u + 2 \cos m\,2\pi u' - 2\,i \sin m\,2\pi u') \\
& + 6\,S^{2+} + 2\,O^{1-}\Big[\cos m\,2\pi(x+y) + i \sin m\,2\pi(x+y) \\
& + \cos m\,2\pi(y-2x) + i \sin m\,2\pi(y-2x) \\
& + \cos m\,2\pi(x-2y) + i \sin m\,2\pi(x-2y) \\
& + \cos m\,2\pi(x'+y') + i \sin m\,2\pi(x'+y') \\
& + \cos m\,2\pi(y'-2x') + i \sin m\,2\pi(y'-2x') \\
& + \cos m\,2\pi(x'-2y') + i \sin m\,2\pi(x'-2y') \\
& + \cos m\,2\pi(x''+y'') + i \sin m\,2\pi(x''+y'') \\
& + \cos m\,2\pi(y''-2x'') + i \sin m\,2\pi(y''-2x'') \\
& + \cos m\,2\pi(x''-2y'') + i \sin m\,2\pi(x''-2y'')\Big]
\end{aligned}
$$

The values of $(\sin\theta)/\lambda$, log P and the scattering factors of Rb^{1+}, S^{2+}, O^{1-} are recorded in Table XX.

TABLE XX

(mm$\overline{2m}$0) m	$(\sin\theta)/\lambda$ x 10^{-8}	log P	Rb^{1+}	S^{2+}	O^{1-}
1	0.100	0.797	32.64	12.7	8.30
2	0.200	0.452	27.44	10.4	6.45
3	0.300	0.2095	24.22	8.95	4.48
4	0.400	0.0377	22.19	8.11	3.06
5	0.500	0.0154	19.71	7.40	2.26
6	0.600	0.324	16.89	6.55	1.82

Values of log I for the first six orders of (mm$\overline{2m}$0) for the values of x', y', x", y" under discussion are compared with observed intensities in Table XXI, where W. indicates the evaluation of the relative intensities in the present investigation, H. records the observations of Hägg (5) and H. & F. those of Huggins and Frank (4).

TABLE XXI

$(mm\overline{2m}0)$	I (obs.)				log I (calculated)		
m				x'_A =	0.524	0.538	0.546
	W.	H.	H.& F.	y'_A =	0.337	0.361	0.372
				x''_A =	0.516	0.506	0.506
				y''_A =	0.201	0.219	0.219
1	m.	w.(-)	a.		3.92	3.93	3.92
2	a.	w.(-)	a.(v.w.)		3.87	4.25	3.82
3	w.	m.	m.s.(m.)		4.22	4.33	4.35
4	a.	v.w.	a.		3.29	3.58	3.63
5	w.	-	-		3.45	3.56	3.53
6	s.(-)	-	-		4.10	4.07	4.11

It will be seen that the observations of Hägg are in general agreement with those of Huggins and Frank regarding the relative intensities of the first four orders (the only ones examined by Hägg and by Huggins and Frank) whereas the present investigation raises the intensity of the first order to "medium" and reduces the third to "weak". Due to the shape of the crystal and to its positions relative to the incident beam for reflections from $\{mm\overline{2m}0\}$ each diffraction spot on the present films appears as three very small dots instead of as a single spot. In consequence, it was exceptionally difficult to estimate the relative intensities of the diffraction effects from $\{mm\overline{2m}0\}$. In this particular case, therefore, it is probable that the mutually supporting data of Hägg and of Huggins and Frank are more reliable than those of the present investigation. With this assumption, the best agreement between calculated values of log I in Table XXI and observed intensities occurs for $x'_A(x''_B) = 0.546$, $x''_A(x'_B) = 0.506$ and for $x'_A(x''_B) = 0.524$, $x''_A(x'_B) = 0.516$.

It should be mentioned that Hägg's estimation of $(33\bar{6}0)$ includes $(50\bar{5}1)$ and that of $(44\bar{8}0)$ includes $(10\bar{1}5)$ since the intensities of powder lines are involved. The effect of $(10\bar{1}5)$ on the estimation for $(44\bar{8}0)$ is of no consequence as is evident from a comparison of the observed intensities (v.w. or a.) for the diffraction effect from this plane in Table XXI. Furthermore, for $x'_A = 0.538$, $F^2_{(33\bar{6}0)} = 13{,}130$ and $F^2_{(50\bar{5}1)} = 8{,}815$; $P_{(33\bar{6}0)} = 1.620$ and $P_{(50\bar{5}1)} = 1.634$ (mean, 1.627). Hence $\log P|F|^2 = \log P + \log\left[F^2_{(50\bar{5}1)} + F^2_{(33\bar{6}0)}\right] = 0.2113 + 4.3413 = 4.55$ as compared with 4.33 for $(33\bar{6}0)$ alone. Thus, the superimposition of $(50\bar{5}1)$ on $(33\bar{6}0)$ does not raise log I for the latter to a value that invalidates the agreement between the observations of Hägg and of Huggins and Frank shown in Table XXI.

The only available observations for $\left\{\underline{mm\bar{2}mm}\right\}$ are due to Hägg and comprise only the first three orders.

The general structure factor for $\left\{\underline{mm\bar{2}mm}\right\}$ is given by

$$\begin{aligned}
F = Rb^{1+}\Big[&\cos m\,4\pi u + i\sin m\,4\pi u \\
&+ 2\cos m\,2\pi u - 2i\sin m\,2\pi u \\
&+ \cos m\pi\,(\cos m\,4\pi u' + i\sin m\,4\pi u' \\
&+ 2\cos m\,2\pi u' - 2i\sin m\,2\pi u')\Big] \\
&+ 2S^{2+}(\cos m\,2\pi u'' + \cos m\,2\pi u''' + \cos m\,2\pi u'''')
\end{aligned}$$

$$
\begin{aligned}
&+ O^{1-}\Big[\cos m\,2\pi(x+y+z) + i\sin m\,2\pi(x+y+z)\\
&+ \cos m\,2\pi(-2x+y+z) + i\sin m\,2\pi(-2x+y+z)\\
&+ \cos m\,2\pi(x-2y+z) + i\sin m\,2\pi(x-2y+z)\\
&+ \cos m\,2\pi(x+y-z) + i\sin m\,2\pi(x+y-z)\\
&+ \cos m\,2\pi(-2x+y-z) + i\sin m\,2\pi(-2x+y-z)\\
&+ \cos m\,2\pi(x-2y-z) + i\sin m\,2\pi(x-2y-z)\\
&+ \cos m\,2\pi(x'+y'+z') + i\sin m\,2\pi(x'+y'+z')\\
&+ \cos m\,2\pi(-2x'+y'+z') + i\sin m\,2\pi(-2x'+y'+z')\\
&+ \cos m\,2\pi(x'-2y'+z') + i\sin m\,2\pi(x'-2y'+z')\\
&+ \cos m\,2\pi(x'+y'-z') + i\sin m\,2\pi(x'+y'-z')\\
&+ \cos m\,2\pi(-2x'+y'-z') + i\sin m\,2\pi(-2x'+y'-z')\\
&+ \cos m\,2\pi(x'-2y'-z') + i\sin m\,2\pi(x'-2y'-z')\\
&+ \cos m\,2\pi(x''+y''+z'') + i\sin m\,2\pi(x''+y''+z'')\\
&+ \cos m\,2\pi(-2x''+y''+z'') + i\sin m\,2\pi(-2x''+y''+z'')\\
&+ \cos m\,2\pi(x''-2y''+z'') + i\sin m\,2\pi(x''-2y''+z'')\\
&+ \cos m\,2\pi(x''+y''-z'') + i\sin m\,2\pi(x''+y''-z'')\\
&+ \cos m\,2\pi(-2x''+y''-z'') + i\sin m\,2\pi(-2x''+y''-z'')\\
&+ \cos m\,2\pi(x''-2y''-z'') + i\sin m\,2\pi(x''-2y''-z'')\Big]
\end{aligned}
$$

Values of $(\sin\theta)/\lambda$, log P and the scattering factors of Rb^{1+}, S^{2+}, O^{1-} are recorded in Table XXII.

TABLE XXII

$(mm\bar{2}mm)$ m	$(\sin\theta)/\lambda$ $\times 10^{-8}$	log P	Rb^{1+}	S^{2+}	O^{1-}
1	0.1270	0.6838	30.9	12.04	7.8
2	0.2540	0.3133	25.6	9.50	5.37
3	0.3810	0.0623	22.6	8.24	3.3

Calculated values of log I for $\{mm\overline{2m}m\}$ are compared with Hägg's observed intensities in Table XXIII.

TABLE XXIII

$(mm\overline{2m}m)$ m	I (obs.) Hägg		log I (calculated)		
		$x'_A =$	0.524	0.538	0.546
		$y'_A =$	0.337	0.361	0.372
		$x''_A =$	0.516	0.506	0.506
		$y''_A =$	0.201	0.219	0.219
1	s.		4.98	4.99	5.00
2	v.w.		3.71	3.76	3.76
3	v.w.		2.73	2.57	2.45

For this series $x'_A = 0.524$, $x''_A = 0.516$ is to be preferred due to the slightly lower log I value for the second order and to the fact that for this combination the difference between the log I values for the second and third orders is less than in either of the other cases.

From the data of Tables XVII, XVIII, XIX, XXI and XXIII, however, it is impossible to make very sharp distinctions among the three sets of values for x'_A, y'_A, x''_A, y''_A. The available evidence appears to indicate $x'_A = 0.524$, $x''_A = 0.516$ or $x'_A = 0.538$, $x''_A = 0.506$ rather than $x'_A = 0.546$, $x''_A = 0.506$ but the present qualitative treatment is inadequate to enable a definite decision to be reached.

The coordinates of the point on the circle about S_1 in Figure 25 (p. 88A) equidistant from $x'_A = 0.524$, $y'_A = 0.337$ and $x'_A = 0.538$, $y'_A = 0.361$ are $x'_A = 0.532$, $y'_A = 0.349$. The coordinates of the point equidistant from $x''_A = 0.516$,

$y''_A = 0.201$ and $x''_A = 0.506$, $y''_A = 0.219$ are $x''_A = 0.509$, $y''_A = 0.209$.

For these positions log I values for $\{m0\bar{m}0\}$ are very satisfactory as shown in Table XXIV.

TABLE XXIV

$(m0\bar{m}0)$ m	I (obs.)	log I (calc.) $x'_A = 0.532$, $y'_A = 0.349$, $x''_A = 0.509$, $y''_A = 0.209$
3	v.s.	4.98
6	s.	4.30
8	m.	3.63
4	w.	3.49
7	w.	3.42
5	v.w.	3.18
2	a.	1.74

It may be concluded, therefore, that the lateral parameters of the oxygen atoms of the dithionate ions inside the cell have the approximate values $x'_A = 0.53_2$, $y'_A = 0.34_9$, $x''_A = 0.50_9$, $y''_A = 0.20_9$.

Values of log I for $\{m0\bar{m}m\}$, $\{mm\bar{2m}0\}$ and $\{mm\bar{2m}m\}$ calculated with these parameters are recorded in Table XXV. It will be observed that acceptable agreement between calculated values of log I and observed intensities is obtained in each case. The data of Table XXV may be compared directly with those of Tables XIX, XXI and XXIII.

TABLE XXV

$x'_A = 0.532$, $y'_A = 0.349$; $x''_A = 0.509$, $y''_A = 0.209$

$(m0\bar{m}m)$ m	I (obs.)	log I (calc.)	$(mm\overline{2m}0)$ m	I (obs.)	log I (calc.)	$(mm\overline{2m}m)$ m	I (obs.)	log I (calc.)
1	s.(-)	3.81	1	w.(-)	3.93	1	s.	4.99
2	m.	3.33	2	w.(-)	3.86	2	v.w.	3.73
5	m.	3.39	3	m.	4.27	3	v.w.	2.79
3	v.w.	3.00	4.	v.w.	3.43			
4	a.	2.28	5	?w.	3.52			
			6	?s.(-)	4.06			

(f) Distinction between u''''_A and u''''_B.

As previously mentioned (p.65), a consideration of reflections from $\{0001\}$ leads to an ambiguity in the determination of u'''' (and hence of x', y', z', x'', y'', z'') due to the fact that curves of log I vs. u'''' are symmetrical about a value of $u'''' = 0.335$. It has been shown (p. 69) that u'''' probably has a value close to $u''''_A = 0.25$ or $u''''_B = 0.42$.

A distinction between u''''_A and u''''_B, however, may be made on the basis of reflections from $\{m0\bar{m}m\}$.

The general structure factor for $\{m0\bar{m}m\}$ is given by

$$
\begin{aligned}
F = \mathrm{Rb}^{1+} & (1 + \cos m\pi + 2\cos m\,2\pi u \\
& + 2\cos m\pi \cos m\,2\pi u') \\
& + 2\,\mathrm{S}^{2+}\left[\cos m\,2\pi u'' + \cos m\pi \cos m\pi\left\{-(1/3) + 2u'''\right\}\right. \\
& \left. + \cos m\pi\left\{-(1/3) + 2u''''\right\}\right] \\
& + 2\,\mathrm{O}^{1-}\left[\cos m\,2\pi(x+z) + \cos m\,2\pi(z-y)\right. \\
& + \cos m\,2\pi(y+z-x) + \cos m\,2\pi(x'+z') \\
& + \cos m\,2\pi(z'-y') + \cos m\,2\pi(y'+z'-x') \\
& + \cos m\,2\pi(x''+z'') + \cos m\,2\pi(z''-y'') \\
& \left. + \cos m\,2\pi(y''+z''-x'')\right]
\end{aligned}
$$

Values of (sin θ)/λ, log P and the scattering factors of Rb^{1+}, S^{2+}, O^{1-} are recorded in Table XXVI.

TABLE XXVI

$(m0\bar{m}m)$ m	(sin θ)/λ x 10^{-8}	log P	Rb^{1+}	S^{2+}	O^{1-}
1	0.0976	0.809	33.6	12.6	8.30
2	0.1852	0.465	27.8	10.45	6.55
3	0.2928	0.225	24.5	9.10	4.70
4	0.3904	0.049	22.4	8.30	3.17
5	0.4860	0.009	20.0	7.50	2.40

It has been shown (Table XIX, p. 94 and Table XXV, p.101) that for $u_A''' = 0.25$, $z_A' = 0.36$, $z_A'' = 0.81$ (consult p. 72) reasonably satisfactory values of log I are obtained for the different orders of $\{m0\bar{m}m\}$ for certain combinations of x_A', y_A', x_A'', y_A''. In Table XXVII are presented corresponding values of log I calculated for the alternative values of $u_B'''(=0.42)$, $z_B'(=0.19)$, $z_B''(=0.64)$, x_B', y_B', x_B'', y_B''.

TABLE XXVII

$(m0\bar{m}m)$ m	I (obs.)			log I (calculated)			
		x_B''	=	0.524	0.532	0.538	0.546
		y_B''	=	0.337	0.349	0.361	0.372
		x_B'	=	0.516	0.509	0.506	0.506
		y_B'	=	0.201	0.209	0.219	0.219
1	s.(-)			3.98	3.96	3.96	3.96
2	m.			1.41	1.71	1.09	1.24
5	m.			3.36	3.33	3.33	3.36
3	v.w.			2.52	2.79	2.95	3.01
4	a.			2.82	2.64	2.67	2.78

The calculated values of log I for the second order alone are sufficient to eliminate u''''_B, z'_B, z''_B. It follows, therefore, that $u'''' = u''''_A = 0.25$, $z' = z'_A = 0.36$ and $z'' = z''_A = 0.81$ (see p. 72).

(g) <u>Summary of Rubidium Dithionate Parameters</u>.

For convenience, the preceding data on the vertical and lateral parameters of $Rb_2S_2O_6$ are summarized in Table XXVIII. To facilitate comparison with the corresponding values for $K_2S_2O_6$, the data of Huggins and Frank and of Helwig (revised) given in Table I (p. 35) are repeated in Table XXVIII.

TABLE XXVIII

Atom	Special Positions	$Rb_2S_2O_6$ (This Thesis)	$K_2S_2O_6$	
			Huggins & Frank	Helwig (revised)
S	(c)	0,0,.165	0,0,.16	0,0,.16
S	(d)	1/3,2/3,.25	1/3,2/3,.27	1/3,2/3,.27
S	(d)	1/3,2/3,.58	1/3,2/3,.59	1/3,2/3,.59
Rb(K)	(e)	.375,.375,0	.375,.375,0	.39,.39,0
Rb(K)	(f)	.712,.712,1/2	.690,.690,1/2	.69,.69,1/2
O	(g)	.160,.120,.225	.165,.11,.23	.09,.18,.22
O	(g)	$.53_2,.34_9,.36$	.615,.17,.34	.48,.24,.35
O	(g)	$.50_9,.20_9,.81$	.505,.21,.80	.58,.42,.79

In Table XXVIII it will be observed that the present data for $Rb_2S_2O_6$ are relatively close to those of Huggins and Frank for $K_2S_2O_6$ except for $x' = 0.53_2$, $y' = 0.34_9$ (this thesis), $x' = 0.615$, $y' = 0.17$ (Huggins and Frank). This discrepancy is not as large as it appears in Table XXVIII, however, because the three-fold nature of the axis through the dithionate ion places an oxygen atom in the position x' = 0.65_2, y' = 0.18_3. Thus for detailed comparison with the data of Huggins and Frank the oxygen atom coordinates 0.53_2, 0.34_9, 0.36 of this thesis in Table XXVIII may be replaced by 0.65_2, 0.18_3, 0.36. The other values of x', y' examined in detail in the present investigation, namely, 0.524, 0.337; 0.538, 0.361; 0.546, 0.372, are equivalent to 0.662, 0.188; 0.640, 0.176; 0.630, 0.175, respectively, in terms of the oxygen atom employed by Huggins and Frank from which to designate x', y' coordinates. The least satisfactory parameters (0.546, 0.372) from the point of view of the present study of the structure of $Rb_2S_2O_6$, therefore, are the most nearly comparable to the corresponding parameters of Huggins and Frank for $K_2S_2O_6$. The exact values of Huggins and Frank (0.615, 0.17) for x', y' are equivalent to 0.553, 0.383 in terms of the present data and it has been shown in Table XVIII (p. 92) that values of x' = 0.552, y' = 0.381 (x" = 0.506, y" = 0.219 - very close to 0.505, 0.21 of Huggins and Frank, see Table XXVIII) lead to unacceptable values of log I for $\{m0\bar{m}0\}$. The difference between the values of the x', y' coordinates for $Rb_2S_2O_6$ of the present investigation and those of Huggins and Frank for $K_2S_2O_6$, although not as large as it appears in Table XXVIII, nevertheless is justifiable on the basis of available experimental evidence.

On the other hand, the large differences between the (revised) parameters of Helwig for $K_2S_2O_6$ and those of

Huggins and Frank for $K_2S_2O_6$ and of the present investigation for $Rb_2S_2O_6$ are not due simply to a difference in choice of equivalent oxygen atoms to which values of x, y, x', y', x", y" are referred. They are due to appreciable differences in the relative orientation of the oxygen atoms about the vertical axes.

The projection of the structure of $Rb_2S_2O_6$ on the basal plane is shown to scale in Figure 26, where the unit cell is outlined in red. Symmetry elements are represented by the usual conventional symbols and the coordinates u, u', x, x' x", y, y', y" are indicated. Rubidium (Rb^+), sulphur (S^{++}) and oxygen (O^-) ions, respectively, have been drawn as circles of decreasing radii. The circumferences of these circles are shown as lines of different widths to indicate different heights in the cell. The values of the vertical parameters u", u"', u"", z, z', z" are given for one example of each. Since the sulphur atoms occur in pairs on the same verticals, the parameters (1-u"; 1-u"'; 1-u"") of the atoms higher in the cell are shown as solid figures while the parameters (u"; u"'; u"") of those lower in the cell are indicated by chequered figures.

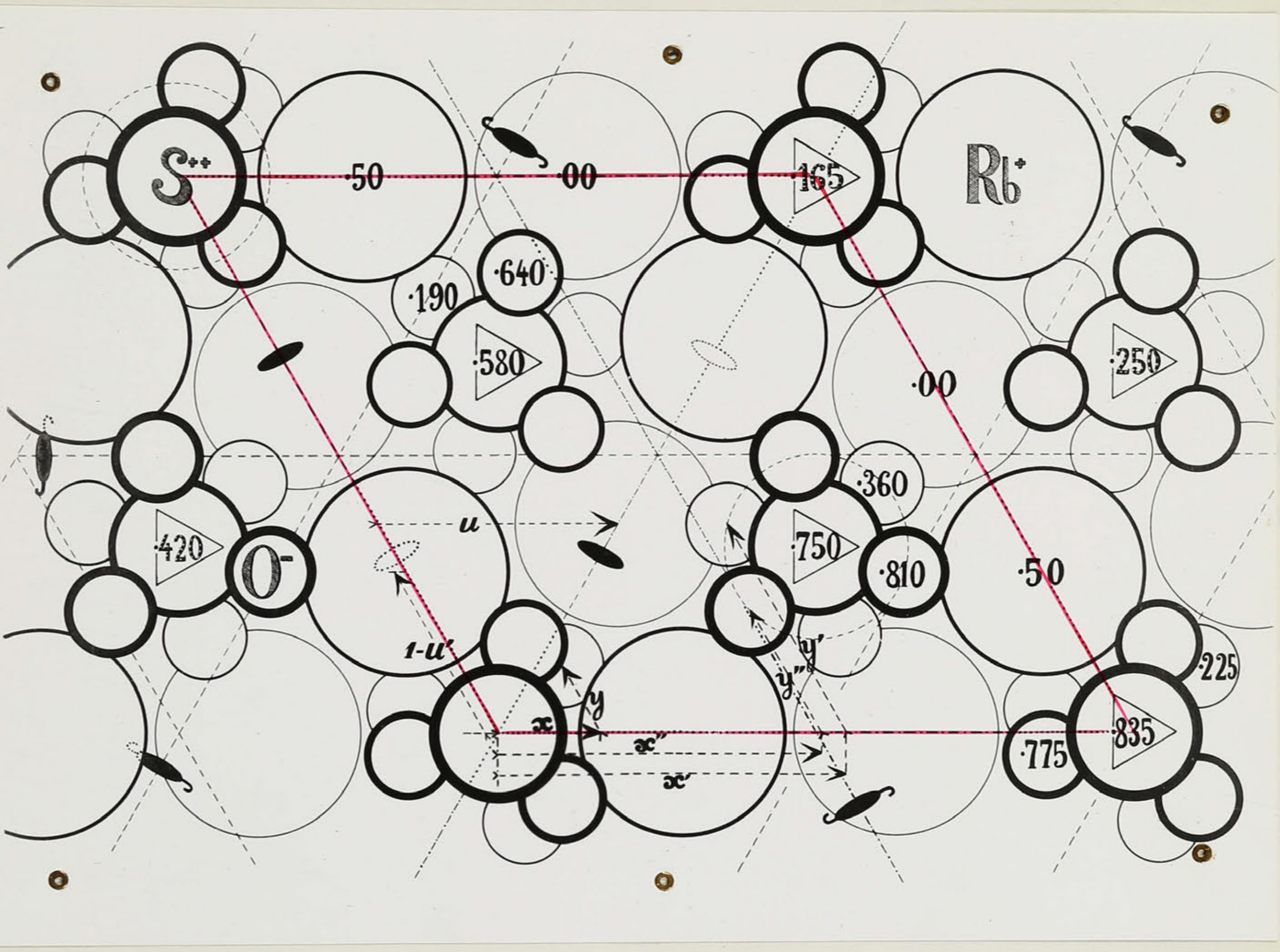

FIGURE 26

Projection of Structure of $Rb_2S_2O_6$ on Basal Plane

DISCUSSION

It is clear from Table XXVIII (p. 103) that the parameters determined for $Rb_2S_2O_6$ in the present investigation are in general much closer to the corresponding parameters of $K_2S_2O_6$ found by Huggins and Frank (4,21) than to those reported by Helwig (3). Since it is to be expected that corresponding parameters of $Rb_2S_2O_6$ and of $K_2S_2O_6$ might be identical or very nearly so, the present study of the structure of rubidium dithionate suggests that the parameters of Huggins and Frank for $K_2S_2O_6$ probably are more nearly correct than the corresponding parameters of Helwig in those cases where the two sets of values are not in agreement with each other.

That neither the complete set of parameters for $K_2S_2O_6$ given by Huggins and Frank nor that due to Helwig may be applied to $Rb_2S_2O_6$ without modification, is clear from the data of the following Tables XXIX to XXXIII, inclusive. In these Tables, the intensities of the diffraction effects from $Rb_2S_2O_6$ observed by Hagg (5) and by Huggins and Frank (4) are compared with the present observations and corresponding values of log I calculated for $\{0001\}$, $\{m0\bar{m}0\}$, $\{m0\bar{m}m\}$, $\{mm\overline{2m}0\}$, $\{mm\overline{2m}m\}$ by the direct application of the $K_2S_2O_6$ parameters of Huggins and Frank and of Helwig (as given in Table XXVIII, p. 103) to $Rb_2S_2O_6$ are shown in conjunction with the log I values calculated with the parameters derived in the present investigation (Table XXVIII, p. 103). In these Tables, data of Huggins and Frank or those based thereon are indicated by H.& F. and those of the present investigation by W. A dash (-) signifies absence of available data.

TABLE XXIX

(0001)	I(obs.)			log I (calc.)		
l	Hägg	H.& F.	W.	Helwig	H.& F.	W.(p.68)
4	w.	m.	v.s.	4.52	4.53	4.49
6	-	-	s.	4.02	4.15	4.13
5	a.	a.	m.	3.44	3.24	3.68
2	w.(+)	m.w.	w.	4.17	4.11	4.31
3	a.	a.	w.	2.92	2.77	3.50
1	-	a.	v.w.	3.48	3.36	3.29
7	-	-	a.	1.51	2.62	1.93

It will be observed that the relative intensities noted in the present investigation are consistently higher than corresponding observations of Hägg or of Huggins and Frank except in the case of the second order. It has been pointed out previously (pp. 66, 67, 68) that, under all conditions, log I values for this order relative to those for the other orders are unsatisfactory. Evaluating this order as "medium" instead of "weak", to bring it into harmony with the observations of Hägg and of Huggins and Frank, however, does not improve the results materially, since the value of log I (see last column of Table XXIX) lies between those of the fourth (v.s.) and sixth (s.) orders. Hägg's estimation of "weak" for the fourth order is not in agreement with the observations of Huggins and Frank and of the present study. Furthermore, the anomalous log I value for the second order is not improved appreciably by the application of the $K_2S_2O_6$ parameters of Huggins and Frank or of Helwig. The calculated value of log I for (0002), therefore, remains as an unsatisfactory result in the determination of the structure of rubidium dithionate.

It appears also from the data of Table XXIX that the $K_2S_2O_6$ parameters of Huggins and Frank and of Helwig lead to log I values for the first (v.w.) order that are too high compared with that of the third (w.), even if the evaluation of the fifth order as "medium" compared with "zero" ("absent") in the other two studies be considered as high. It may be noted, however, that reflections from the fifth order certainly occur on the present films and appear to be of stronger intensity than are those of the third and first orders.

Finally, the log I value (2.62) for the seventh order calculated on the basis of the $K_2S_2O_6$ parameters of Huggins and Frank is rather high.

TABLE XXX

$(m0\bar{m}0)$	I (obs.)			log I (calc.)		
m	Hagg	H.& F.	W.	Helwig	H.& F.	W.(p.100)
3	s.	s.	v.s.	4.90	5.02	4.98
6	m.	m.(m.s.)	s.	3.91	4.39	4.30
8	-	-	m.	2.90	3.08	3.63
4	v.w.(?)	a.	w.	1.83	1.32	3.49
7	w.	a.	w.	3.56	3.06	3.42
5	v.w.	w.(a.)	v.w.	3.72	3.36	3.18
2	a.	a.	a.	3.59	3.30	1.74
1	-	a.	-	2.96	2.53	2.31

From the data of Table XXX it is apparent that the application of the $K_2S_2O_6$ parameters of Helwig and of Huggins and Frank lead to log I values for the fourth order of $(m0\bar{m}0)$ that are too low and to values of log I for the seventh, fifth and second orders that are too high compared particularly with the value for the eighth order. It may be noted that, in general, the parameters of Huggins and Frank lead to somewhat less objectionable results for log I than do those of Helwig. Neither set of parameters, however, gives as satisfactory a series of log I values for $\{m0\bar{m}0\}$ as that of the last column of Table XXX. This is particularly significant since the three sets of observed relative intensities shown in Table XXX are in satisfactory mutual agreement.

TABLE XXXI

$(m0\bar{m}m)$	I (obs.)			log I (calc.)		
m	Hägg	H.& F.	W.	Helwig	H.& F.	W.(p.101)
1	-	-	s.(-)	3.31	2.77	3.81
2	v.w.	-	m.	3.10	2.12	3.33
5	-	-	m.	3.90	3.84	3.39
3	a.	-	v.w.	1.95	3.47	3.00
4.	v.w.	-	a.	3.22	2.96	2.28

In Table XXXI the values of log I calculated with the $K_2S_2O_6$ parameters of Huggins and Frank for the first and second orders of $(m0\bar{m}m)$ are too low compared with the values for the fifth, third and fourth orders. Furthermore, the value for the fourth order is somewhat high.

The $K_2S_2O_6$ parameters of Helwig yield log I values for the fifth and fourth orders that are too high compared with the values for the first and second orders and the value for the third order (1.95) is lower than one would expect even for a "very weak" reflection.

The paper of Huggins and Frank (4) contains no data on the relative intensities of reflections from $\{m0\overline{mm}\}$ for $Rb_2S_2O_6$.

TABLE XXXII

$(mm\overline{2m}0)$	I (obs.)			log I (calc.)		
m	Hägg	H.& F.	W.	Helwig	H.& F.	W.(p.101)
1	w.(-)	a.	m.	3.54	3.77	3.93
2	w.(-)	a.(v.w.)	a.	3.52	3.87	3.86
3	m.	m.s.(m.)	w.	4.66	4.58	4.27
4	v.w.	a.	a.	3.93	3.43	3.43
5	-	-	w.	3.52	3.44	3.52
6	-	-	s.(-)	3.90	3.91	4.06

Reasons already have been given (p. 96) for considering the mutually supporting observations of relative intensities for $\{mm\overline{2m}0\}$ of Hägg and of Huggins and Frank as more reliable than those of the present investigation.

Log I values for $\{mm\overline{2m}0\}$ are not wholly satisfactory with any of the sets of parameters under consideration. Those of the present investigation show the smallest discrepancy between the sixth (s.-) and third (m.) orders. On the other hand, the $K_2S_2O_6$ parameters of Helwig give the most satisfactory relative values for the fifth (w.), first (w.-) and second (w.-) orders but that for the fourth (v.w.) order is too high.

TABLE XXXIII

$(mm\overline{2m}m)$	I (obs.)			log I (calc.)		
m	Hägg	H.& F.	W.	Helwig	H.&F.	W.(p.101)
1	s.	-	-	4.98	5.05	4.99
2	v.w.	-	-	3.80	3.73	3.73
3	v.w.	-	-	3.61	3.11	2.79

The data of Table XXXIII are too meagre to warrant any detailed discussion. Relative log I values are reasonably good for each of the three sets of parameters although in each case that for the second order appears to be rather high as does also that for the third order based on Helwig's parameters and that for the same order based on the parameters of Huggins and Frank.

It is of interest to summarize and to discuss the more interesting interatomic distances in the structure of rubidium dithionate as found in the present investigation. The dimensions of the dithionate ion are as follows: sulphur-to-sulphur distance, 2.09Å. (p.63); sulphur-to-oxygen (in the same SO_3 group), 1.49₅Å.(p.62); oxygen-to-oxygen (adjacent in the same SO_3 group), 2.50₄Å. (p.73). Although the general structure (O_3-S-S-O_3) of this anion has not been determined directly either in $K_2S_2O_6$ or in $Rb_2S_2O_6$, it has lent itself readily to placement in the unit cells on the basis of existing conditions of symmetry and has led to the elucidation of structures for which calculated intensities of diffraction effects are in reasonably satisfactory agreement with qualitative observations.

In its general characteristics (two rings of oxygen atoms at the corners of equilateral triangles joined through two sulphur atoms on a line through their centres), it has been employed by Hägg (45) in an attempt to determine the structure of caesium dithionate (space group, D_{3h}^4 or D_6^6, _i.e._, not isomorphous with $K_2S_2O_6$ and $Rb_2S_2O_6$). The assumed structure is that which is to be expected on chemical grounds (44, p.549) and it has been shown (p.54) to be in harmony with the results of Raman Effect studies of sodium dithionate in aqueous solution (34). Although the lattice energy of the sulphates presumably is lower than is that of the corresponding dithionates, there appears to be no structural peculiarity in $K_2S_2O_6$ or in $Rb_2S_2O_6$ that would lead one to expect the experimental fact that dithionates in general decompose at low or moderate temperatures, depending on the cation, into sulphur dioxide and the appropriate sulphate.

In the structure of $Rb_2S_2O_6$ the distances between the centres of adjacent rubidium ions is more than adequate. Even if u were equal to u', the centres of rubidium ions would be separated by $0.5\ c_o = 3.17_5$Å. and the ionic diameter of Rb^+ is approximately 3.04Å. (10, p.192).

Minimum rubidium-to-oxygen distances already have been discussed at some length (see p. 79 _et seq._) and evidence has been presented to justify relative positions of rubidium ions and oxygen atoms leading to a minimum rubidium-to-oxygen distance of 2.77Å. As pointed out previously, this value is lower than that of 2.86Å. to be expected on the basis of known potassium-to-oxygen distances and known differences between the atomic domains of rubidium and of potassium (see pp. 79,80). With values of u and u' established as 0.375 and 0.712, respectively, rubidium-to-oxygen distances can be increased only by diminishing the value of R' (see p. 73 and Figure 19A, p.73A). This may be effected either by increasing the height of the SO_3 pyramid ($r = (R/3) = (h/4)$, see p. 63 and Figure 15, p. 62A) and retaining the original sulphur-to-oxygen distance or by decreasing the sulphur-to-oxygen distance and retaining the original height of the SO_3 pyramid. Since possible variations of the distance between a sulphur atom and the nearest plane of oxygen atoms has been examined (pp. 67, 68, 69) and it has been shown that the most acceptable value probably is close to $0.06c_0 = 0.381$Å. the second alternative alone need be considered at this point.

In either case, of course, when the distance between adjacent oxygen atoms of the same SO_3 group is diminished, the distance between the rubidium ions and the nearest oxygen atom of the dithionate ions at the corners of the cell and the shorter distance between a rubidium ion and the nearest oxygen atom of the dithionate ion within the cell are increased. If no change in the height of the SO_3 pyramid be made, the sulphur-to-oxygen distance must be diminished. The following Table XXXIV shows the magnitude of these changes when the value of R' is reduced from 1.44_6Å. (p. 73) to 1.40Å. and to 1.30Å., respectively.

TABLE XXXIV

R'	O^--to-O^-	Rb^+-to-O^- (corner)	Rb^+-to-O^- (inside)	S^{++}-to-O^-
1.44_6Å	2.50_4Å.	2.77Å.	2.86Å.	1.49_5Å.
1.40Å.	2.42_5Å.	2.81Å.	2.88Å.	1.45Å.
1.30Å.	2.25Å.	2.86Å.	2.90Å.	1.35Å.

Although R' = 1.30 leads to the best rubidium-to-oxygen distances, the distance between adjacent oxygen atoms (2.25Å.) almost certainly is too small for O^{1-} on the basis of diameters of 1.20Å. for O°, 2.70Å. for O^{2-} and 2.66Å. for $(OH)^-$ (10, p. 192).

In the following Table XXXV, values of log I for $\{m0\bar{m}0\}$, $\{m0\bar{m}m\}$, $\{mm\overline{2m}0\}$ and $\{mm\overline{2m}m\}$ calculated on the basis of R' = 1.40 are compared with previously given values for R' = 1.44_6. For the calculations involving R' = 1.40, the final values of this thesis (Table XXVIII, p. 103) for all parameters except x, y, x', y', x", y" have been employed. On changing R' from 1.44_6 to 1.40 the coordinates x and y (defining the positions of the oxygen atoms of the dithionate ions at the corners of the cell) have been altered to maintain equal distances from the rubidium ions (uu0; u', u', 1/2) to these oxygen atoms. The oxygen atoms of the dithionate ions within the cell (the positions of which are defined by x', y' and x", y") have been maintained in the same angular positions around the vertical axes as for R = 1.44_6, new values of x', y' and of x", y", therefore, arising from their movement towards the axis (S_1 of Figure 25, p. 88A or 0 of Figure 19A, p. 73A) due to the lower value of R'.

TABLE XXXV

R' = 1.44_6	R' = 1.40
x = 0.160	x = 0.155
y = 0.120	y = 0.120
x' = 0.53_2	x' = 0.53_6
y' = 0.34_9	y' = 0.34_9
x" = 0.50_9	x" = 0.51_5
y" = 0.20_9	y" = 0.21_2

$(m0\overline{m}0)$ m	I (obs.)	log I (calc.) R' = 1.44_6	1.40
3	v.s.	4.98	4.99
6	s.	4.30	4.29
8	m.	3.63	3.64
4	w.	3.49	3.49
7	w.	3.42	3.46
5	v.w.	3.18	3.24
2	a.	1.74	1.86
1	-	2.31	2.28

$(m0\overline{mm})$ m	I (obs.)	log I (calc.) R' = 1.44_6	1.40
1	s.(-)	3.81	3.89
2	m.	3.33	3.57
5	m.	3.39	3.28
3	v.w.	3.00	2.93
4	a.	2.28	2.58

$(mm\overline{2m}0)$ m	I (obs.)	log I (calc.) R' = 1.44_6	1.40
1	w.(-)	3.93	4.10
2	w.(-)	3.86	3.76
3	m.	4.27	4.24
4	v.w.	3.43	3.33
5	? w.	3.52	3.44
6	? s.(-)	4.06	4.06

$(mm\overline{2m}m)$ m	I (obs.)	log I (calc.) R' = 1.44_6	1.40
1	s.	4.99	4.99
2	v.w.	3.73	3.81
3	v.w.	2.79	2.51

A detailed examination of the data presented in Table XXXV shows that although R' = 1.40 leads to slightly better results for $\{m0\bar{m}0\}$ in that the values of log I for the fourth and seventh orders are more nearly the same, the results calculated with R' = 1.446 for $\{m0\bar{m}m\}$ are decidedly better (compare the second and fifth orders) and those for $\{mm2\bar{m}0\}$ (compare the first and sixth orders) and for $\{mm\overline{2m}m\}$ (compare the second and third orders) are slightly better than corresponding results calculated for R' = 1.40.

Hence, on the basis of the present qualitative evidence, there seems to be no valid reason for appreciably decreasing the value of R' (and thus reducing the sulphur-to-oxygen and oxygen-to-oxygen distances) in spite of the fact that such a procedure would lead to a somewhat larger minimum rubidium-to-oxygen distance than 2.77Å.

The usefulness and importance of interatomic distances as a guide in the elucidation of a structure with many undetermined parameters has been amply illustrated throughout the present study of the structure of rubidium dithionate. For example, without the restrictions regarding a minimum rubidium-to-oxygen distance utilized in the diagram showing permissible and prohibited ranges for values of x', y', and x", y" (Figure 25, p. 88A), evaluation of these parameters would have been still more uncertain than actually proved to be the case. This is evident from the data of Table XXXVI where log I values for $\{m0\bar{m}0\}$, based on a few combinations of x, y, x', y', x", y" selected from calculations incidental to the work of this thesis but discarded as leading to rubidium-to-oxygen distances less than 2.77Å., are presented. Values of parameters not shown in Table XXXVI are those of Table XXVIII (p. 103). The last column, for comparison, contains the log I values already given for the complete set of parameters finally adopted (Table XXVIII).

TABLE XXXVI

$(m0\bar{m}0)$ m	I (obs.)			log I (calculated)			
		x =	0.144	0.161	0.167	0.160	0.160
		y =	0.144	0.118	0.083	0.120	0.120
		x'=	0.823	0.823	0.832	0.553	0.532
		y'=	0.460	0.460	0.426	0.172	0.349
		x"=	0.722	0.722	0.760	0.506	0.509
		y"=	0.225	0.225	0.262	0.219	0.209
3	v.s.		4.96	4.96	4.94	4.96	4.98
6	s.		4.17	4.18	3.83	4.17	4.30
8	m.		3.82	3.75	3.67	3.68	3.63
4	w.		3.63	3.55	3.33	3.30	3.49
7	w.		3.68	3.47	3.52	3.60	3.42
5	v.w.		3.09	3.35	3.23	3.13	3.18
2	a.		1.91	1.72	2.35	2.52	1.74

Any one of the first four series, but particularly the first, would be satisfactory if no minimum limit were assumed for rubidium-to-oxygen distances. Without going into unnecessary details, however, it may be noted that calculated distances between rubidium and oxygen atoms for each of the first four sets of parameters in Table XXXVI show at least one such distance in each structure that is considerably lower than 2.77Å.

The general character of the structure of rubidium dithionate as shown in Figure 26 is that of an almost close-packed assemblage of positive rubidium ions cemented together by negatively charged dithionate ions. In the main, relative atomic positions are reasonable on the assumption of mutual compensation between electrostatic attractions and repulsions among the three kinds of ions (Rb^+, S^{++}, O^-) involved. It will be observed in Figure 26 that the oxygen atoms of the dithionate ions within the cell are very nearly close-packed whereas those of the dithionate ions at the corners of the cell are not. It has already been shown that the latter circumstance arises from the fact that the distances between rubidium ions at heights 0 (or 1) and 1/2, respectively, and the nearest oxygen atoms of this ion are equal to each other. The distances between rubidium ions and nearest oxygen atoms of the dithionate ions within the cell also are approximately equal to one another (<u>cir</u>. 2.89Å.), the different relative positions of the ions within the cell compared with those at the corners thus permitting an approximately close-packed arrangement of oxygen atoms in the former case.

In conclusion it may be stated that the final parameters for rubidium dithionate given in Table XXVIII probably represent as close an approximation to the true values as it is possible to obtain with a purely qualitative treatment of relative intensities. In view of the conflicting results of Huggins and Frank and of Helwig for potassium dithionate and the data presented in this thesis for rubidium dithionate it is obvious that any further work on the structures of these two substances should be undertaken only with adequate equipment for exact quantitative treatment of intensities. It has already been mentioned (p. 46) that such equipment was not available for the present investigation.

APPENDIX TO SECTION II

THE FECHNER LAW

"The sensation varies as the logarithm of the excitation."

The Fechner Law is the integral form of the experimental observations of Bouguer on which photometric methods are based.

Bouguer observed that if an intensity, I, is just distinguishable visually from another intensity, $I + \Delta I$, then $(\Delta I)/I \geqq 1/100$. If $(\Delta I)/I = 1/100$ be considered as a measure of what may be called the "quantum" or "grain" of sensation that is just perceptible and if only medium intensities and spots of about the same size (conditions that are fulfilled in the present instance) be involved, Bouguer's relation holds and is independent of the first intensity (46, p.1447).

Let two intensities, the nth and $(n+1)$th, in a series be just distinguishable from each other and thus differ by a "quantum" or "grain" of sensation, s. Then

$$s = (I_{n+1} - I_n)/I_n = 1/100$$

for any value of n.

By integration, since

$$I_{n+1} - I_n = \Delta I_n,$$

$$I = Ke^{cs},$$

or,

$$\log_e I = cs + \log_e K,$$

where c is a variable increasing by whole numbers (1,2,3,...) and $s = 1/100$ = a constant.

Thus the intensities must increase exponentially in order to create impressions corresponding to successive whole numbers.

Curves giving the variation of contrast sensitivity with field brightness (47, p.192) show that the former is a constant in the usual brightness range involved in the examination of photographic films by transmitted light. Thus, between 100 candles/(metre)^2 and 10,000 candles/(metre)^2, $\Delta B/B$ is a constant and the visual sensation function is a straight line when the abscissae are logarithmic, i.e., "the sensation varies directly as the logarithm of the stimulus over the useful range of field brightness."

SECTION III

TWINNING IN POTASSIUM AND RUBIDIUM DITHIONATES

SECTION III

TABLE OF CONTENTS

INTRODUCTION TO SECTION III

As mentioned in the Introduction to Section II, Hägg's paper on potassium and rubidium dithionates (5) is of particular interest because it is probable that his crystal of rubidium dithionate was twinned. In connection with the Laue diagrams which he obtained from the two dithionates, Hägg says, "Bezüglich der Symmetrie der Lauephotogramme ist es bemerkenswert, dass während die Photogramme von $K_2S_2O_6$ die Lauesymmetrie D_{3d} deutlich zeigen, die Photogramme von $Rb_2S_2O_6$ beinahe die Lauesymmetrie D_{6h} besitzen." Regarding photographs taken with the beam along the c̲ and a̲ axes, respectively, of crystals of $K_2S_2O_6$ and of $Rb_2S_2O_6$, respectively, "dort sieht man wie bei $Rb_2S_2O_6$ eine Symmetrie niedriger als D_{6h} nur im Photogramm entlang der zweizähligen Achse aber nicht mehr im Photogramm entlang der trigonalen Achse wahrgenommen werden kann." (5, p.267). As a matter of fact a close examination of Hägg's Figure 1d. (5, p. 266) shows that, insofar as relative positions of spots only are concerned, the symmetry is that of Figure 2E of this thesis (p. 10A), i.e., D_6^h. Only when the relative intensities of the diffraction spots are considered does the centre appear solely as the trace of a two-fold axis (i.e., D_3^d).

Hägg apparently was aware of the possibility of twin formation because he states that, "Die Lösungen wurden bei 85° abgedampft um die Zwillingsbildung zu vermeiden, die nach Fock unterhalb etwa 70° sehr ausgeprägt wird." (5, p.266). The reference to Fock is not very convincing because Fock's statement (23, 24) was simply that he obtained <u>one</u> trigonal crystal of $K_2S_2O_6$ by evaporation between 70°C. and 80°C. whereas at lower temperatures only hexagonal crystals were observed. It may be mentioned that Wyrouboff (23), who cites Fock's work, claims to have been unable to obtain trigonal crystals.

Hägg suggests two alternative explanations for the alleged fact that, although crystals of $K_2S_2O_6$ clearly show the Laue symmetry of D_3^d, the Laue symmetry of $Rb_2S_2O_6$ is "nearly" that of D_6^h. According to Hägg, "Entweder besitzt in beiden Salzen das Metallatomgitter die Lauesymmetrie D_{6h}, die dann zu überwiegen beginnt wenn die Metallatome schwerer werden, oder der Übergang von Kalium- zu Rubidiumatomen ist von einer Parameteränderung begleitet, die eine Annäherung an höhere Symmetrie verursacht." (5, p. 267).

Experience in this laboratory has shown that the tendency to twin formation at ordinary temperatures is very much more pronounced in rubidium dithionate than it is in the potassium salt. During the determination of the space group of $K_2S_2O_6$, Helwig (1) encountered no crystals of that salt possessing pseudo-hexagonal Laue symmetry although Hankel and Lindenberg (48) elsewhere have concluded from piezo-electrical studies that $K_2S_2O_6$ crystals usually are twins.

In preparing crystals of rubidium dithionate for the structure investigation described in Section II of the present thesis, evaporation was allowed to proceed always at room temperature. Although most of the specimens showed pseudo-hexagonal Laue symmetry, a few were obtained clearly showing the Laue symmetry of D_3^d both with respect to the relative intensities of equivalent spots on the photographs and to their geometrical arrangement around the spot due to the undiffracted beam. The proportion of such trigonal crystals as compared with those giving pseudo-hexagonal photographs, similar to Hägg's reproductions, appeared to increase with the number of recrystallizations. Attempts to prepare twinned crystals of $K_2S_2O_6$, on the other hand, led to the identification of only one specimen showing pseudo-hexagonal Laue symmetry.

This experience tends to invalidate Hägg's tacit assumption that his crystal of $Rb_2S_2O_6$ was not twinned because it was grown at a certain temperature.

Having obtained trigonal and pseudo-hexagonal crystals of both $K_2S_2O_6$ and $Rb_2S_2O_6$, the investigation of the nature of the twinning in these substances was undertaken. For future reference it may be noted that the hexagonal symmetry of the Laue diagrams of the twinned crystals is exhibited only by the geometrical position of apparently equivalent points and not by their relative intensities. In this thesis, therefore, the prefix "pseudo" is employed to indicate this fact as, for example, in the terms "pseudo-hexagonal" and "planes of pseudo-symmetry."

As will be mentioned later, the trigonal and pseudo-hexagonal crystals of $K_2S_2O_6$ and of $Rb_2S_2O_6$ available for this investigation were too imperfect from a crystallographic point of view to permit formal study of the twinning with an optical goniometer. It was of interest, therefore, to examine the adequacy of X-ray methods for this purpose.

X-RAY INVESTIGATION AND RESULTS

Laue photographs were taken of trigonal and pseudo-hexagonal crystals of $K_2S_2O_6$ using tungsten radiation and with the beam along a, b and c axes, respectively. Corresponding pictures were obtained of trigonal and pseudo-hexagonal crystals of $Rb_2S_2O_6$ with molybdenum radiation. The photographs are reproduced in Figures 27 to 38, inclusive. In the case of the potassium dithionate the plate-holder was given a vertical shift of about 2 cms. in a direction normal to the X-ray beam in order to increase the range of diffraction angles available for examination.

The photographs were analyzed by means of gnomonic projections. Outlines of these projections are shown in Figures 39 to 44, inclusive, in which only those spots of interest in the twinning question are shown.

In these Figures the black circles indicate the

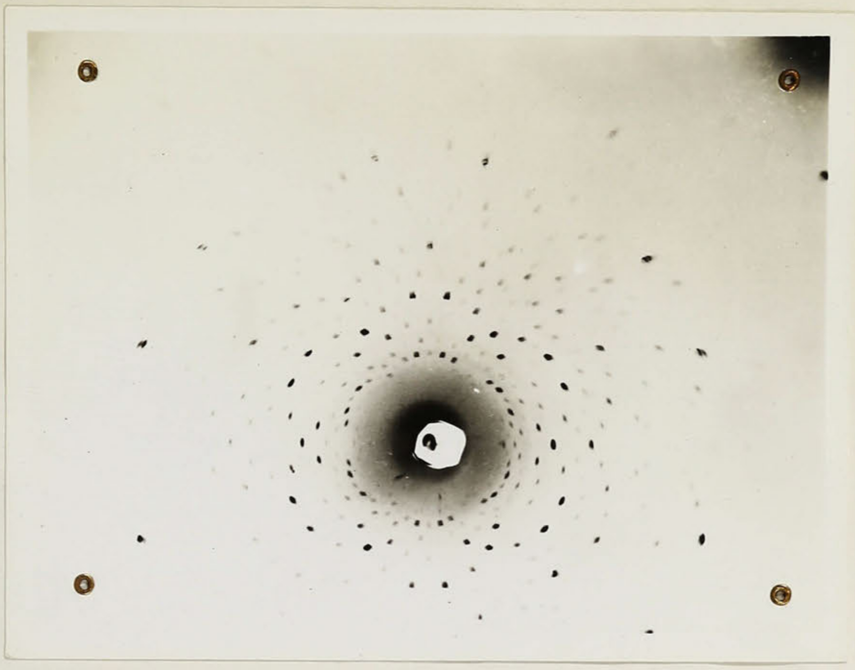

FIGURE 27

Trigonal $K_2S_2O_6$

Beam along c axis

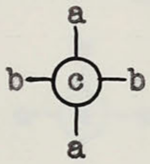

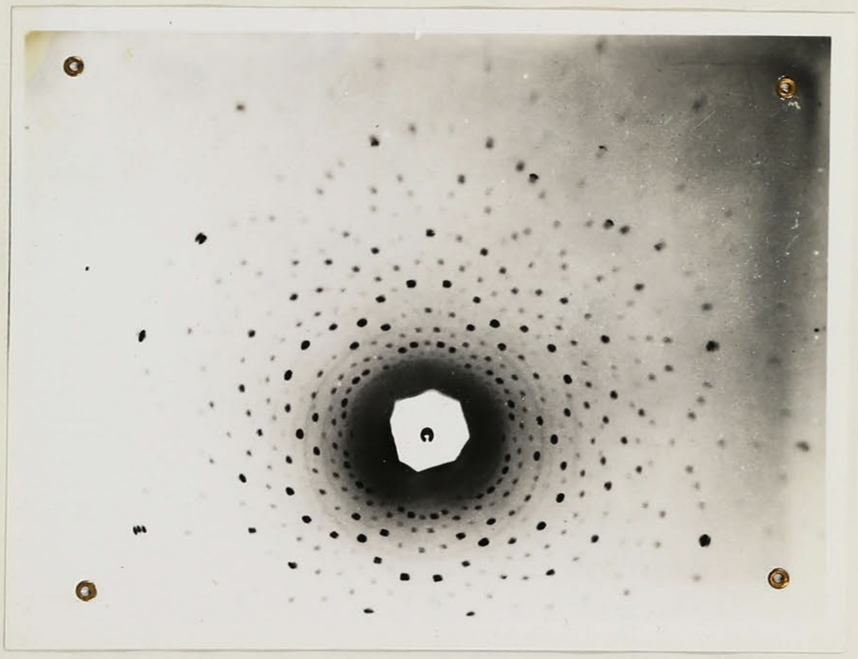

FIGURE 28

Pseudo-hexagonal $K_2S_2O_6$

Beam along c axis

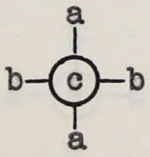

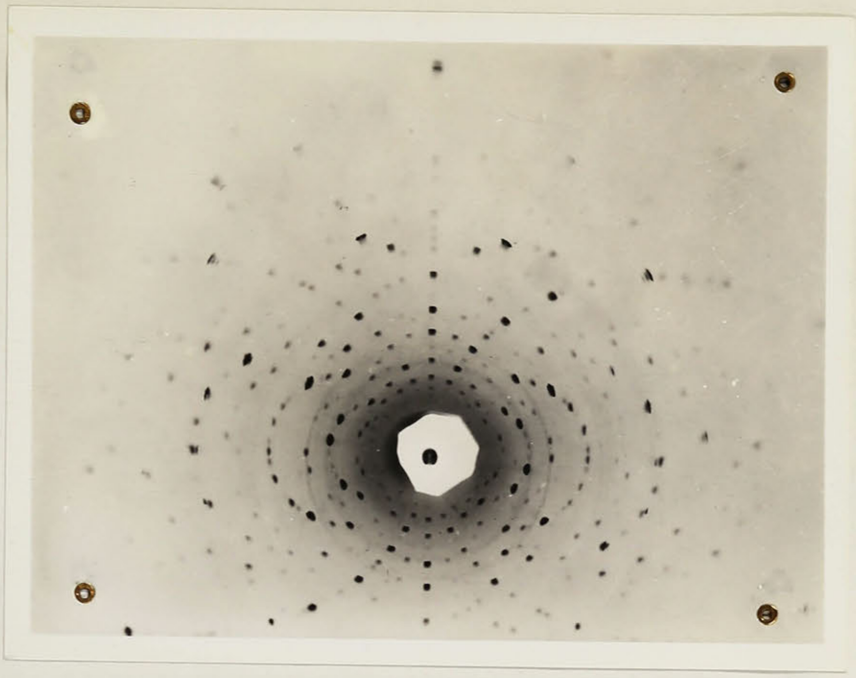

FIGURE 29

Trigonal $K_2S_2O_6$

Beam along a axis

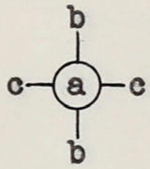

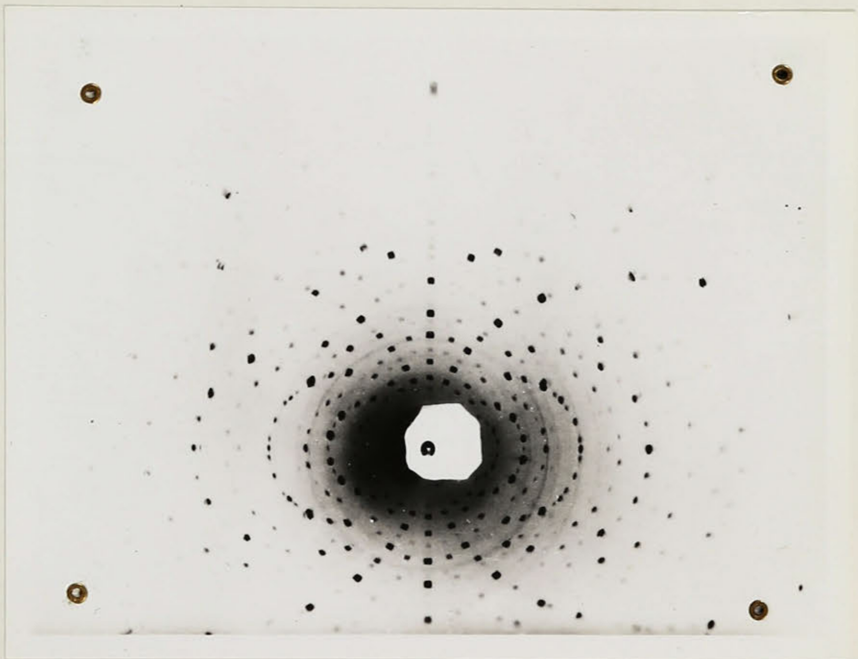

FIGURE 30

Pseudo-hexagonal $K_2S_2O_6$

Beam along a axis

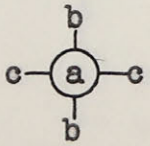

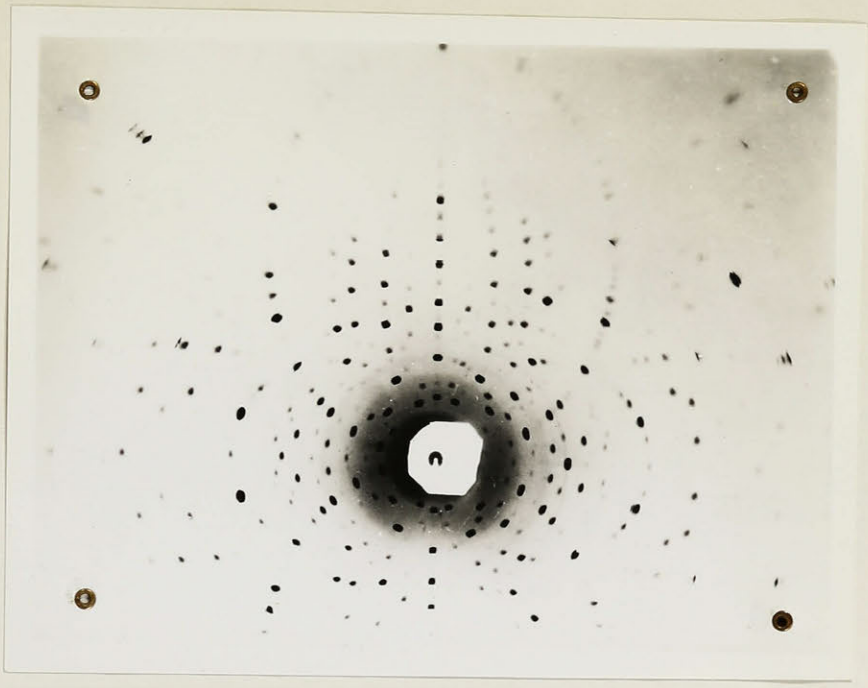

FIGURE 31

Trigonal $K_2S_2O_6$

Beam along b axis

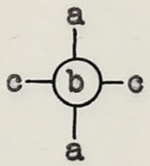

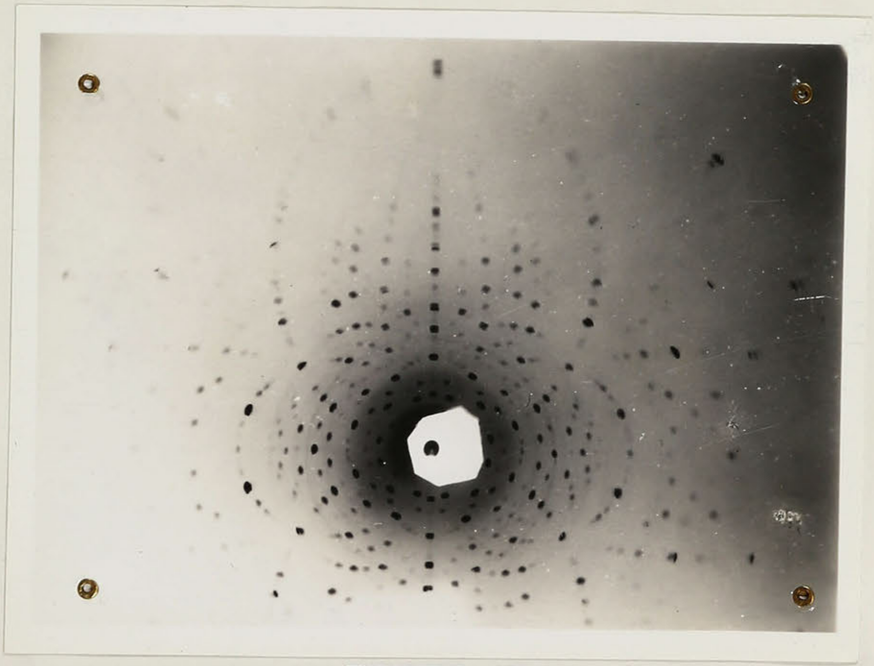

FIGURE 32

Pseudo-hexagonal $K_2S_2O_6$

Beam along b axis

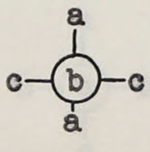

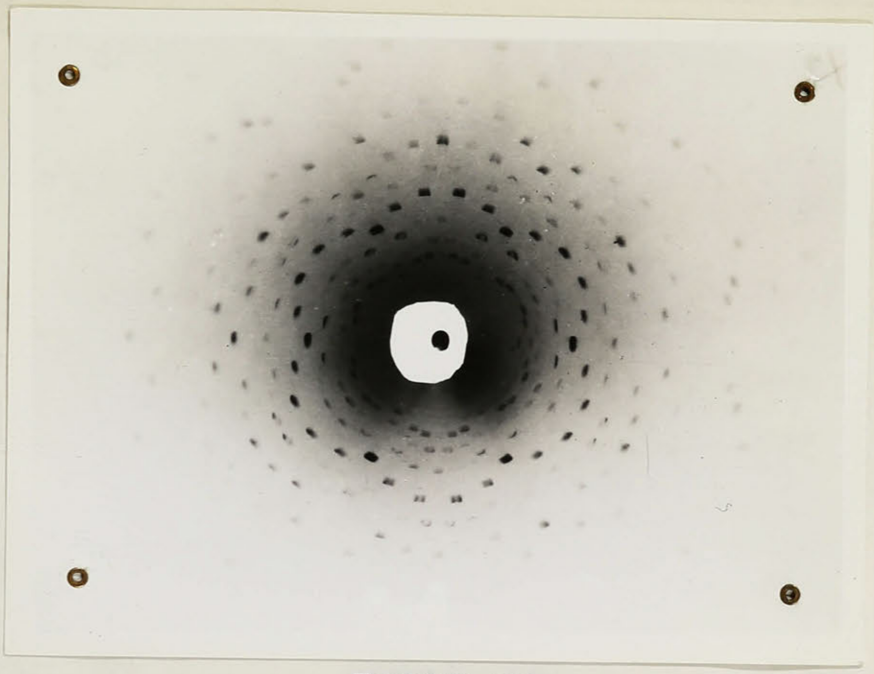

FIGURE 33

Trigonal $Rb_2S_2O_6$

Beam along c axis

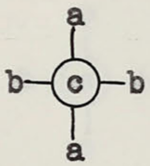

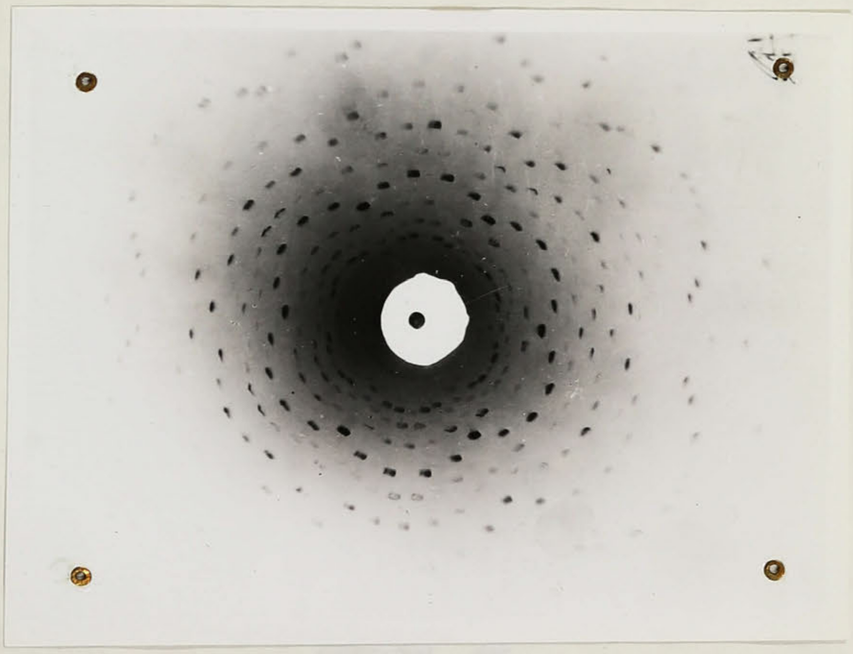

FIGURE 34

Pseudo-hexagonal $Rb_2S_2O_6$

Beam along c axis

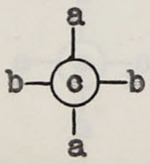

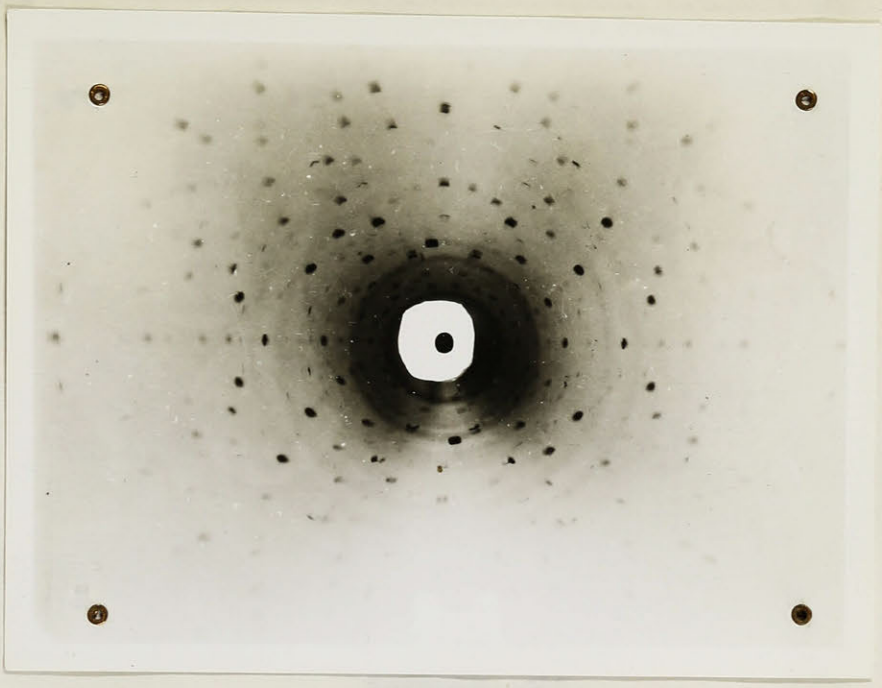

FIGURE 35

Trigonal $Rb_2S_2O_6$

Beam along a axis

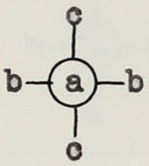

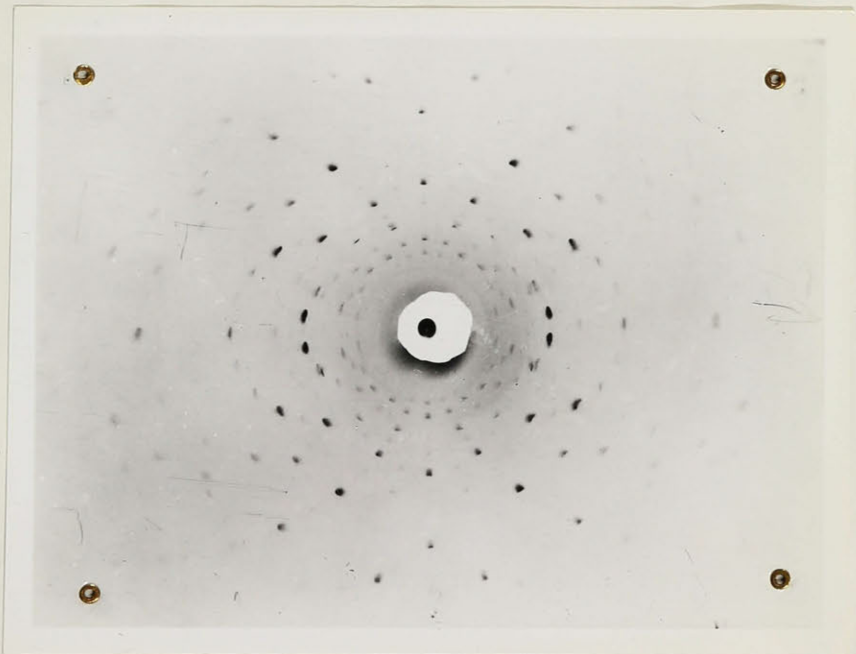

FIGURE 36

Pseudo-hexagonal $Rb_2S_2O_6$

Beam along a axis

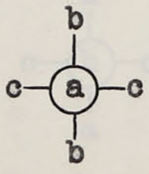

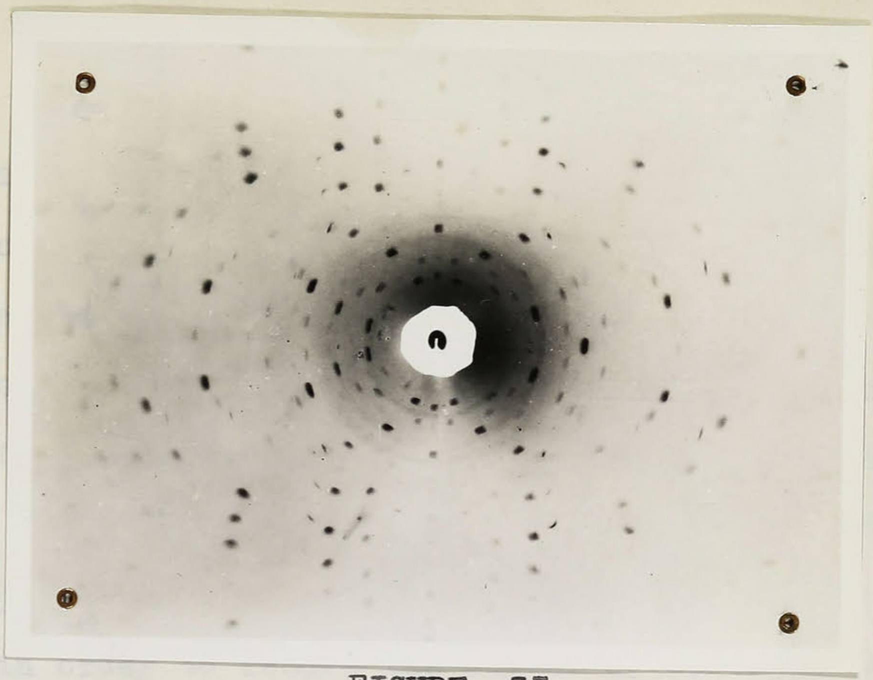

FIGURE 37

Trigonal $Rb_2S_2O_6$

Beam along b axis

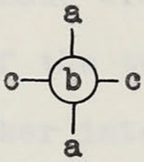

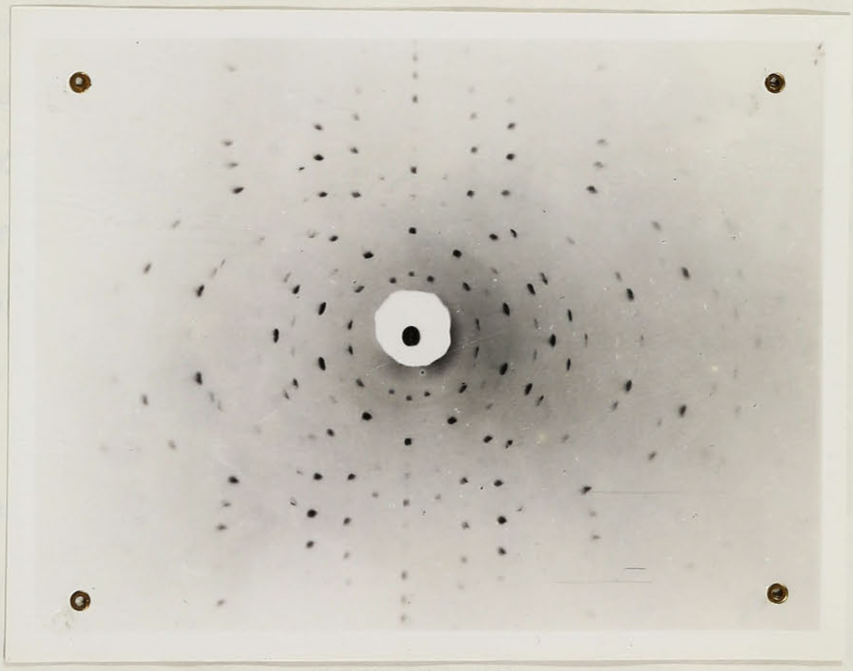

FIGURE 38

Pseudo-hexagonal $Rb_2S_2O_6$

Beam along b axis

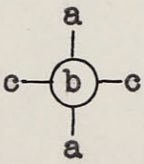

projections of planes absent in the twins but present in the single crystals, while the open circles indicate the projections of corresponding planes present in the twins and in the single crystals in order to emphasize the appearance of the plane of pseudo-symmetry that appears in Laue diagrams of the twins. These latter points have been omitted, however, from the projections of photographs taken with the beam along the c axis in order to reduce the number of spots in the Figures and thus avoid confusion. The open circles enclosing the letter S and the asterisks (✳) indicate the projections of planes represented on the Laue diagrams by spots of stronger intensity in photographs of the twins than in those of the single crystals and of weaker intensity in photographs of the twins than in those of the single crystals, respectively. In each Figure the scale of the crystal-to-plate distance in terms of that of the projection net is indicated and is identified by the letter d. The shaded areas represent the areas of the ac, bc and ab planes of the unit cells in the appropriate projections.

About 3000 points were dealt with in the case of $K_2S_2O_6$ and indexing was relatively easy due to the large number of zones intersecting in each of the points of simple indices. Fewer spots were available in the diagrams of $Rb_2S_2O_6$ for the following reasons: molybdenum instead of tungsten radiation was employed; the crystal of $Rb_2S_2O_6$ was somewhat larger than that of $K_2S_2O_6$, thus involving greater absorption of diffracted rays; no shift of the plate-holder was made in the case of $Rb_2S_2O_6$; with the beam along the a axis, the directions of the b and c axes relative to the long and short edges of the photographic plate inadvertently were interchanged for the single crystal and the twin, respectively, so that only those areas of the plates governed by the shorter dimension were available for comparison. As will be seen from an examination of Tables I to XVIII and Figures 39 to 44, however, the number of diffraction spots examined was more than adequate for the purpose desired.

The following series of Tables I to XVIII, inclusive, and Figures 38 to 44, inclusive, summarize the results obtained. In the Tables are given the indices of planes corresponding to points on the gnomonic projections that are (a) present on that of the twin but absent from that of the single crystal, (b) of stronger intensity in that of the twin than in that of the single crystal, (c) of weaker intensity in that of the twin than in that of the single crystal, for $K_2S_2O_6$ with the beam along the c (Tables I, II, III), a (Tables IV, V, VI) and b (Tables VII, VIII, IX) axes, respectively. Tables I, II, III are summarized in Figure 39, Tables IV, V, VI in Figure 40 and Tables VII, VIII, IX in Figure 41, respectively. Tables X to XVIII, inclusive, and Figures 42 to 44, inclusive, present corresponding data for $Rb_2S_2O_6$. It should be noted that only those planes about which no doubt existed are included in these Tables and Figures.

An interesting feature of these data is that very few planes of the same indices appear in corresponding Tables for $K_2S_2O_6$ and for $Rb_2S_2O_6$, respectively.

TABLE I

$K_2S_2O_6$. c axis. Present in Twin. Absent in Single Crystal.

$(70\bar{7}1)$
$(0\bar{7}71)$
$(\bar{7}701)$

$(8\bar{1}\bar{7}1)$
$(\bar{8}711)$
$(71\bar{8}1)$
$(1\bar{8}71)$
$(\bar{1}\bar{7}81)$
$(\bar{7}8\bar{1}1)$

$(65,\overline{11},2)$
$(5,\overline{11},62)$
$(\overline{11},6,52)$
$(11,\bar{5}\bar{6}2)$
$(\bar{5}\bar{6},11,2)$
$(\bar{6},11,\bar{5}2)$

$(70\bar{7}2)$
$(0\bar{7}72)$
$(\bar{7}702)$

$(6\bar{7}13)$
$(\bar{1}7\bar{6}3)$
$(\bar{7}163)$
$(7\bar{6}\bar{1}3)$
$(\bar{6}\bar{1}73)$
$(16\bar{7}3)$

$(70\bar{7}3)$
$(\bar{7}703)$
$(0\bar{7}73)$

$(73,\overline{10},3)$
$(10,\bar{3}\bar{7}3)$
$(3,\overline{10},73)$
$(\bar{3}\bar{7},10,3)$
$(\overline{10},733)$
$(\bar{7},10,\bar{3}3)$

$(0,\overline{10},10,3)$
$(10,0,\overline{10},3)$
$(\overline{10},10,03)$

$(76,\overline{13},3)$
$(\bar{7},13,\bar{6}3)$
$(13,\bar{6},\bar{7}3)$
$(6,\overline{13},7,3)$
$(\bar{6},\bar{7},13,3)$
$(\overline{13},763)$

$(49,\overline{13},3)$
$(\bar{4},13,\bar{9}3)$
$(13,\bar{9}\bar{4}3)$
$(9,\overline{13},43)$
$(\bar{9}\bar{4},13,3)$
$(\overline{13},493)$

$(68,\overline{14},3)$
$(14,\bar{8}\bar{6}3)$
$(8,\overline{14},63)$
$(\bar{8}\bar{6},14,3)$
$(\overline{14},683)$
$(\bar{6},14,\bar{8}3)$

$(95,\overline{14},3)$
$(5,\overline{14},93)$
$(14,\bar{5}\bar{9}3)$
$(\overline{14},953)$
$(\bar{5}\bar{9},14,3)$
$(\bar{9},14,\bar{5}3)$

$(1,\overline{10},94)$
$(\bar{1}\bar{9},10,4)$
$(\bar{9},10,\bar{1}4)$
$(\overline{10},914)$
$(10,\bar{1}\bar{9}4)$
$(91,\overline{10},4)$

TABLE II

$K_2S_2O_6$. c axis. Stronger in Twin than in Single Crystal.

$(04\bar{4}1)$
$(\bar{4}041)$
$(4\bar{4}01)$

$(\bar{6}601)$
$(60\bar{6}1)$
$(0\bar{6}61)$

$(\bar{2}6\bar{4}1)$
$(4\bar{6}21)$
$(\bar{4}\bar{2}61)$
$(\bar{6}241)$
$(6\bar{4}\bar{2}1)$
$(24\bar{6}1)$

$(8\bar{8}01)$
$(08\bar{8}1)$

$(5,\overline{12},71)$

$(18\bar{7}2)$

$(\bar{2}\bar{5}72)$

$(\bar{8}352)$
$(\bar{3}8\bar{5}2)$
$(5\bar{8}32)$
$(8\bar{5}\bar{3}2)$
$(\bar{5}\bar{3}82)$

$(18\bar{9}2)$
$(9\bar{8}\bar{1}2)$
$(8\bar{9}12)$
$(\bar{1}9\bar{8}2)$

$(\bar{7},12,\bar{5}2)$
$(75,\overline{12},2)$
$(\overline{12},752)$

$(\bar{7}\bar{2}93)$
$(\bar{9}273)$
$(9\bar{7}\bar{2}3)$
$(7\bar{9}23)$

$(9\bar{4}\bar{5}3)$
$(4\bar{9}53)$
$(\bar{9}543)$
$(\bar{4}\bar{5}93)$
$(59\bar{4}3)$

$(4,\overline{12},83)$
$(\bar{4}\bar{8},12,3)$
$(\overline{12},843)$
$(\bar{8},12,\bar{4}3)$
$(12,\bar{4}\bar{8}3)$

$(\bar{9}813)$
$(\bar{1}\bar{8}93)$

$(\bar{1},\overline{11},12,3)$
$(1,\overline{12},11,3)$
$(11,1,\overline{12},3)$

$(11,\bar{2}\bar{9}3)$
$(\bar{9},11\bar{2}3)$

$(\overline{11},923)$
$(2,\overline{11},93)$
$(\bar{2}\bar{9},11,3)$

$(\overline{10},193)$
$(\bar{9}\bar{1},10,3)$
$(\bar{1},10,93)$
$(9,\overline{10},13)$
$(10,\bar{9}\bar{1}3)$

$(10,\bar{6}\bar{4}3)$
$(6,\overline{10},43)$
$(\bar{4},10,\bar{6}3)$
$(\overline{10},463)$
$(\bar{6}\bar{4},10,3)$

$(\overline{12},2,10,3)$
$(\overline{10},\bar{2},12,3)$
$(10,\overline{12},23)$
$(12,\overline{10},\bar{2}3)$

TABLE III

$K_2S_2O_6$. c axis. Weaker in Twin than in Single Crystal.

$(\bar{2}\bar{1}31)$
$(\bar{3}121)$
$(\bar{3}211)$

$(\bar{2}\bar{4}61)$

$(\bar{4}401)$

$(7\bar{7}03)$
$(\bar{7}073)$

$(\bar{7}\bar{6},13,3)$

$(\bar{4}\bar{6},10,3)$

$(\bar{7}253)$

$(\bar{9}453)$
$(\bar{5}\bar{4}93)$

$(\bar{1}\bar{6}73)$
$(1\bar{7}63)$

$(\bar{9}723)$
$(\bar{7}9\bar{2}3)$
$(2\bar{9}73)$
$(\bar{2}\bar{7}93)$

$(1,\overline{10},93)$
$(\bar{1}\bar{9},10,3)$
$(7,\overline{10},33)$

$(9,\overline{10},14)$
$(10,\bar{9}14)$

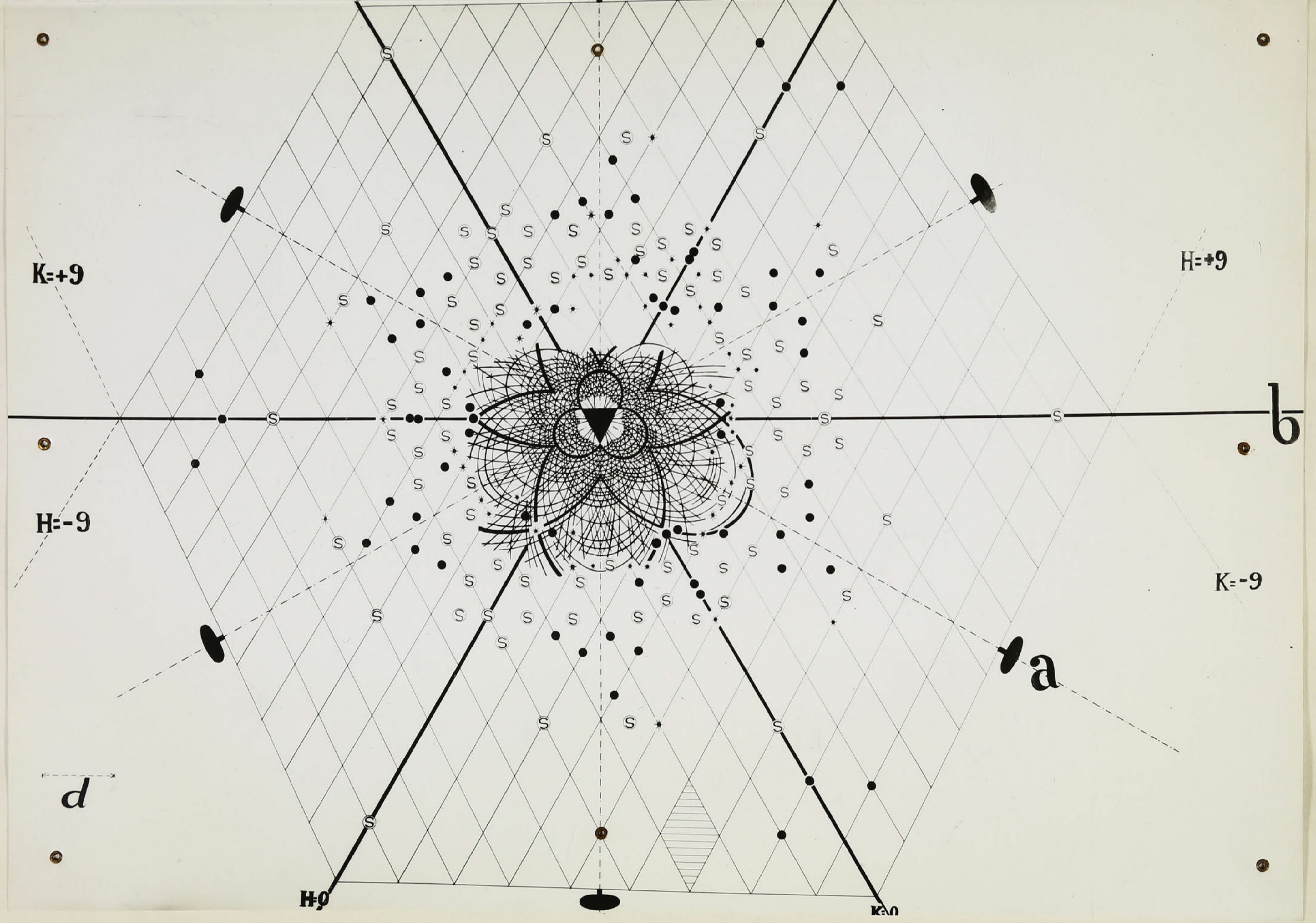

FIGURE 39 Gnomonic Projection $K_2S_2O_6$ Beam along c axis

TABLE IV

$K_2S_2O_6$. a axis.
Present in Twin.
Absent in Single Crystal.

$(1\bar{1}0\bar{4})$
$(10\bar{1}4)$

$(35\bar{8}4)$
$(3\bar{8}54)$

$(3\bar{1}\bar{2}\bar{5})$
$(3\bar{2}\bar{1}5)$

$(35\bar{8}\bar{5})$
$(3\bar{8}55)$

$(43\bar{7}5)$
$(4\bar{7}3\bar{5})$

$(12,\bar{7}\bar{5},17)$
$(12,\bar{5}\bar{7},\overline{17})$

TABLE VI

$K_2S_2O_6$. a axis.
Weaker in Twin
than in Single Crystal.

$(1\bar{2}11)$

$(44\bar{8}1)$

$(3\bar{9}62)$

$(2\bar{1}\bar{1}\bar{3})$

$(3\bar{2}\bar{1}4)$

$(4\bar{4}05)$

$(12,\bar{7}\bar{5},14)$

TABLE V

$K_2S_2O_6$. a axis. Stronger in Twin than in Single Crystal.

$(3\bar{9}61)$

$(4,\overline{14},10,\bar{1})$

$(57,\overline{12},\bar{1})$

$(33\bar{6}\bar{2})$
$(33\bar{6}2)$

$(45\bar{9}\bar{2})$

$(2\bar{9}7\bar{2})$

$(2\bar{5}3\bar{2})$

$(34\bar{7}\bar{3})$
$(34\bar{7}3)$
$(43\bar{7}\bar{3})$

$(13\bar{4}\bar{3})$
$(1\bar{4}3\bar{3})$

$(10\bar{1}\bar{3})$
$(1\bar{1}03)$

$(24\bar{6}3)$

$(21\bar{3}3)$

$(45\bar{9}3)$

$(3\bar{2}\bar{1}\bar{4})$
$(3\bar{1}\bar{2}4)$
$(1\bar{3}24)$

$(4\bar{4}0\bar{5})$

$(21\bar{3}\bar{5})$

$(31\bar{4}\bar{6})$
$(4\bar{1}\bar{3}\bar{6})$
$(1\bar{4}3\bar{6})$
$(3\bar{4}1\bar{6})$
$(4\bar{3}\bar{1}6)$

$(54\bar{9}6)$

$(3\bar{5}2\bar{6})$
$(5\bar{3}\bar{2}\bar{6})$
$(5\bar{2}\bar{3}6)$

$(53\bar{8}6)$

$(5\bar{5}06)$
$(50\bar{5}6)$

$(41\bar{5}\bar{6})$

$(73,\overline{10},6)$

$(53\bar{8},10)$

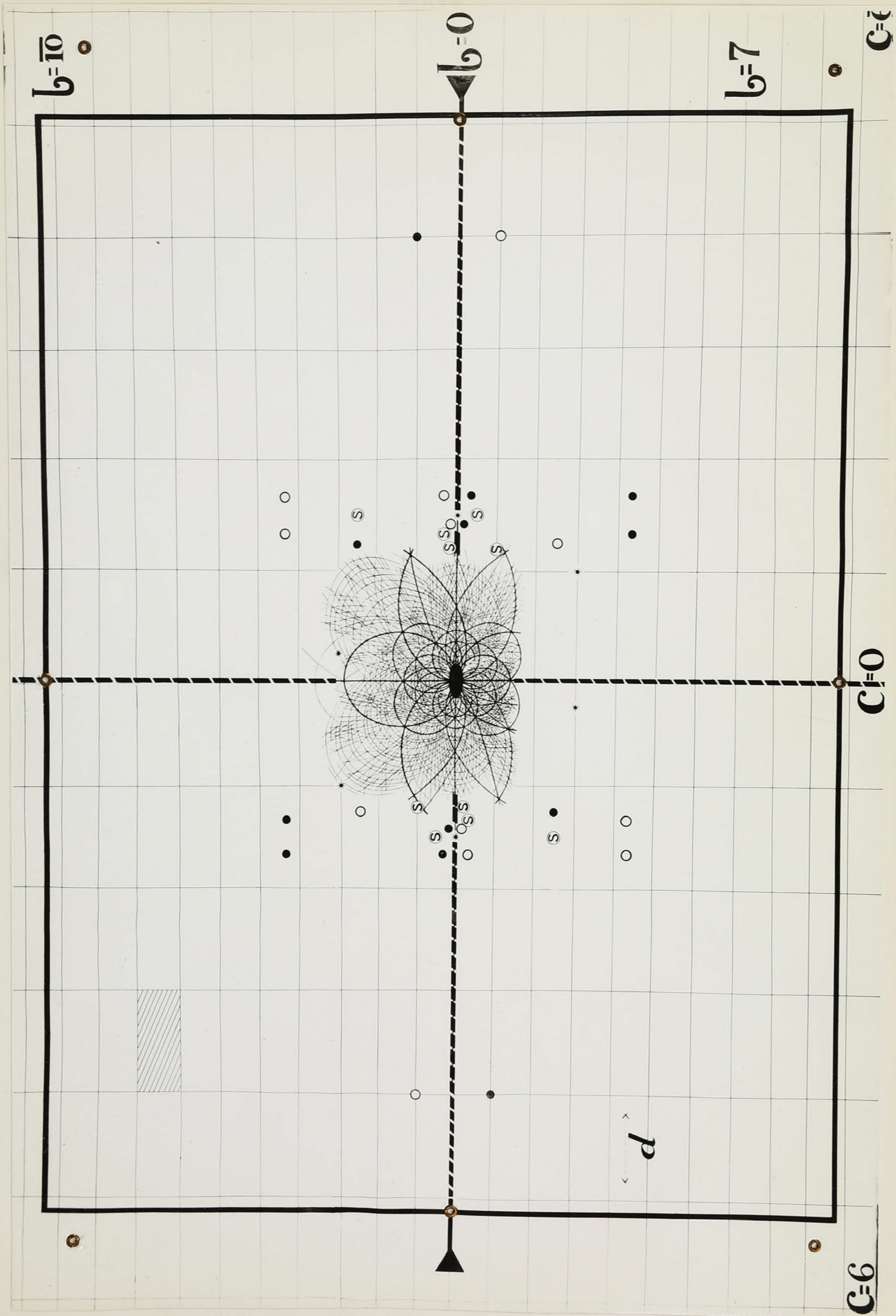

FIGURE 40 Gnomonic Projection $K_2S_2O_6$ Beam along a axis

TABLE VII

$K_2S_2O_6$. b axis.
Present in Twin.
Absent in Single Crystal.

$(6\bar{2}\bar{4}1)$
$(\bar{6}42\bar{1})$

$(12,\bar{4}\bar{8}\bar{1})$
$(\overline{12},84\bar{1})$

$(6\bar{2}\bar{4}\bar{3})$
$(\bar{6}42\bar{3})$

$(9\bar{2}\bar{7}3)$
$(\bar{9}723)$

$(10,\bar{3}\bar{7}3)$
$(\overline{10},733)$

$(01\bar{1}4)$

$(02\bar{2}5)$

$(21\bar{3}5)$
$(\bar{2}3\bar{1}5)$

TABLE VIII

$K_2S_2O_6$. b axis.
Stronger in Twin
than in Single Crystal.

$(6\bar{2}\bar{4}1)$
$(\bar{6}421)$

$(6\bar{1}\bar{5}2)$

$(\overline{10},732)$

$(01\bar{1}3)$

$(7\bar{1}\bar{6}\bar{3})$

$(6\bar{1}\bar{5}3)$
$(\bar{5}6\bar{1}3)$

$(6\bar{2}\bar{4}3)$

$(\bar{6}514)$

$(\bar{2}3\bar{1}\bar{4})$
$(21\bar{3}\bar{4})$

$(\bar{2}4\bar{2}5)$

$(20\bar{2}\bar{5})$
$(\bar{2}20\bar{5})$

$(\bar{3}4\bar{1}5)$
$(31\bar{4}5)$

$(\bar{5}506)$
$(50\bar{5}6)$

$(23\bar{5}6)$
$(\bar{2}5\bar{3}6)$
$(\bar{3}5\bar{2}6)$
$(32\bar{5}6)$

$(\bar{1}4\bar{3}\bar{6})$
$(13\bar{4}\bar{6})$

$(\bar{5}6\bar{1}\bar{6})$
$(51\bar{6}\bar{6})$

$(\bar{1}4\bar{3}\bar{6})$
$(13\bar{4}\bar{6})$

$(03\bar{3}8)$

TABLE IX

$K_2S_2O_6$. b axis. Weaker in Twin than in Single Crystal.

$(8\bar{2}\bar{6}1)$

$(5\bar{1}\bar{4}\bar{1})$

$(11\bar{2}2)$

$(\bar{5}322)$

$(5\bar{1}\bar{4}2)$

$(\bar{4}312)$
$(4\bar{1}\bar{3}2)$

$(20\bar{2}3)$
$(02\bar{2}\bar{3})$
$(\bar{2}203)$

$(\bar{2}3\bar{1}\bar{3})$
$(21\bar{3}\bar{3})$

$(\bar{3}4\bar{1}\bar{3})$

$(415\bar{3})$

$(50\bar{5}\bar{3})$
$(\bar{5}50\bar{3})$

$(6\bar{2}\bar{4}3)$

$(\overline{10},91\bar{3})$

$(\bar{7}70\bar{3})$

$(\bar{5}6\bar{1}\bar{3})$

$(7\bar{1}\bar{6}3)$
$(\bar{7}613)$

$(03\bar{3}\bar{4})$

$(21\bar{3}4)$
$(\bar{2}3\bar{1}4)$
$(\bar{1}3\bar{2}\bar{4})$
$(12\bar{3}\bar{4})$

$(31\bar{4}\bar{4})$
$(\bar{3}4\bar{1}\bar{4})$

$(\bar{3}5\bar{2}4)$

$(32\bar{5}\bar{5})$
$(\bar{3}5\bar{2}\bar{5})$

$(\bar{1}3\bar{2}5)$
$(12\bar{3}5)$

$(\bar{6}8\bar{2}\bar{5})$

$(\bar{3}4\bar{1}\bar{5})$

$(\bar{4}5\bar{1}\bar{5})$

$(02\bar{2}\bar{5})$

$(\bar{5}7\bar{2}\bar{5})$

$(\bar{2}5\bar{3}\bar{6})$
$(23\bar{5}\bar{6})$
$(32\bar{5}6)$
$(\bar{3}5\bar{2}6)$

$(13\bar{4}6)$
$(\bar{1}4\bar{3}6)$

$(\bar{8},13,\bar{5},\overline{10})$

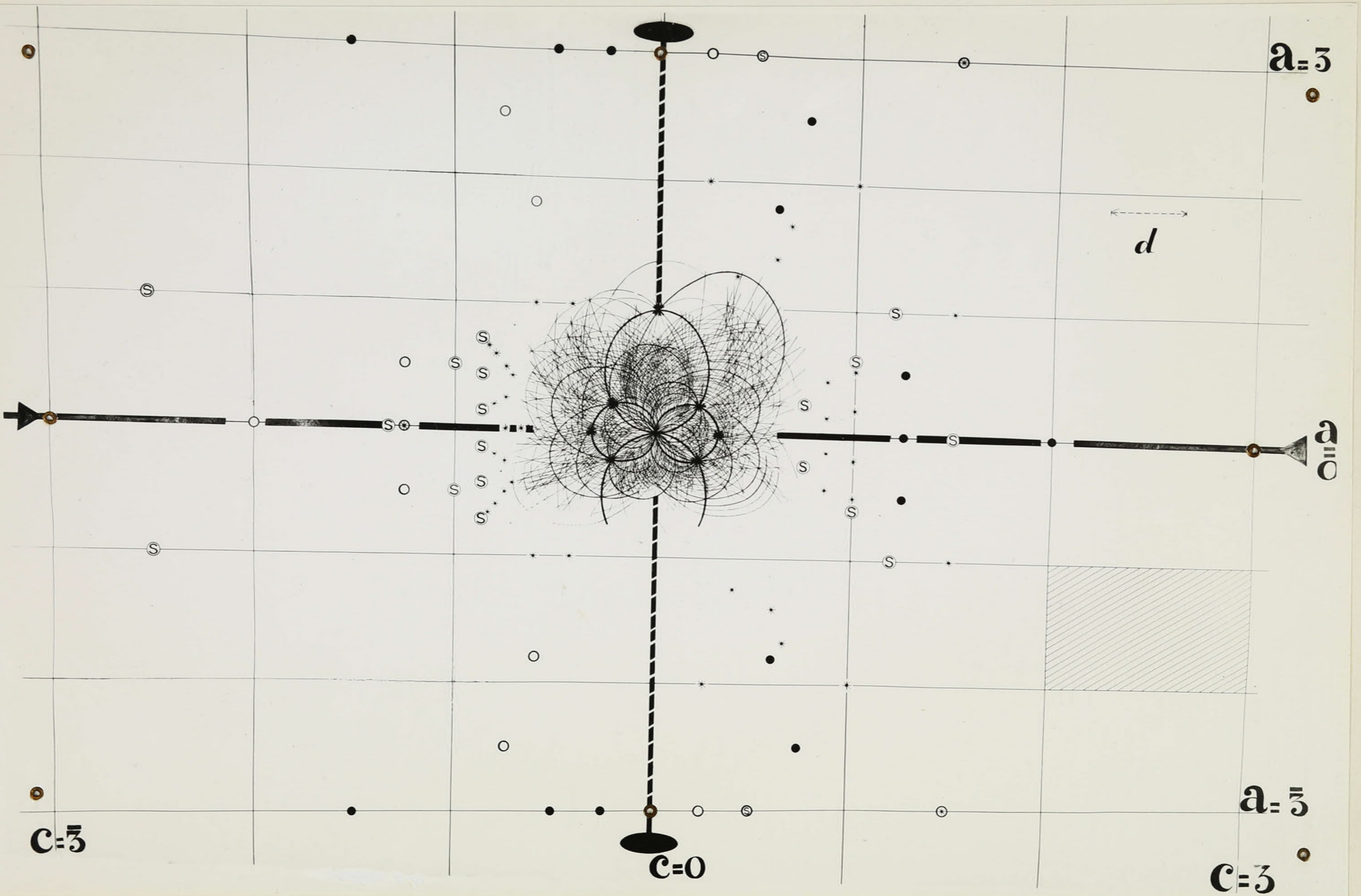

FIGURE 41 Gnomonic Projection $K_2S_2O_6$ Beam along b axis

TABLE X

$Rb_2S_2O_6$. c axis.
Present in Twin.
Absent in Single Crystal

$(8\bar{8}03)$
$(08\bar{8}3)$
$(\bar{8}083)$

$(\bar{7}9\bar{2}3)$
$(\bar{9}723)$
$(2\bar{9}73)$
$(\bar{2}\bar{7}93)$
$(9\bar{2}\bar{7}3)$
$(72\bar{9}3)$

$(7,\overline{10},33)$
$(10,\bar{7}33)$

TABLE XI

$Rb_2S_2O_6$. c axis.
Stronger in Twin
than in Single Crystal

$(6\bar{5}\bar{1}1)$
$(5\bar{6}11)$
$(51\bar{6}1)$
$(6\bar{1}\bar{5}1)$
$(\bar{1}6\bar{5}1)$
$(15\bar{6}1)$
$(\bar{5}6\bar{1}1)$
$(\bar{6}5\bar{1}1)$
$(\bar{6}151)$
$(\bar{5}\bar{1}61)$
$(\bar{1}\bar{5}61)$
$(1\bar{6}51)$

$(7\bar{7}02)$
$(07\bar{7}2)$
$(\bar{7}072)$

$(54\bar{9}2)$
$(45\bar{9}2)$
$(\bar{4}9\bar{5}2)$
$(\bar{5}9\bar{4}2)$
$(\bar{9}452)$
$(\bar{9}542)$
$(\bar{5}\bar{4}92)$
$(\bar{4}\bar{5}92)$
$(4\bar{9}52)$
$(5\bar{9}42)$
$(9\bar{4}\bar{5}2)$
$(9\bar{5}\bar{4}2)$

$(\bar{7}612)$
$(\bar{6}7\bar{1}2)$
$(1\bar{7}62)$
$(\bar{1}\bar{6}72)$
$(7\bar{1}\bar{6}2)$
$(61\bar{7}2)$

TABLE XII

$Rb_2S_2O_6$. c axis.
Weaker in Twin
than in Single Crystal.

$(4\bar{4}01)$
$(04\bar{4}1)$
$(\bar{4}041)$

$(7\bar{7}01)$
$(07\bar{7}1)$
$(\bar{7}071)$

$(1\bar{4}31)$
$(\bar{1}\bar{3}41)$
$(\bar{4}311)$
$(\bar{3}4\bar{1}1)$
$(31\bar{4}1)$
$(4\bar{1}\bar{3}1)$

$(70\bar{7}2)$
$(\bar{7}702)$
$(0\bar{7}72)$

$(5\bar{5}02)$
$(\bar{5}052)$
$(05\bar{5}2)$

$(5\bar{6}12)$
$(6\bar{5}\bar{1}2)$
$(\bar{1}6\bar{5}2)$
$(15\bar{6}2)$
$(\bar{6}152)$
$(\bar{5}\bar{1}62)$

$(1\bar{6}52)$
$(\bar{1}\bar{5}62)$
$(\bar{6}512)$
$(\bar{5}6\bar{1}2)$
$(51\bar{6}2)$
$(6\bar{1}\bar{5}2)$

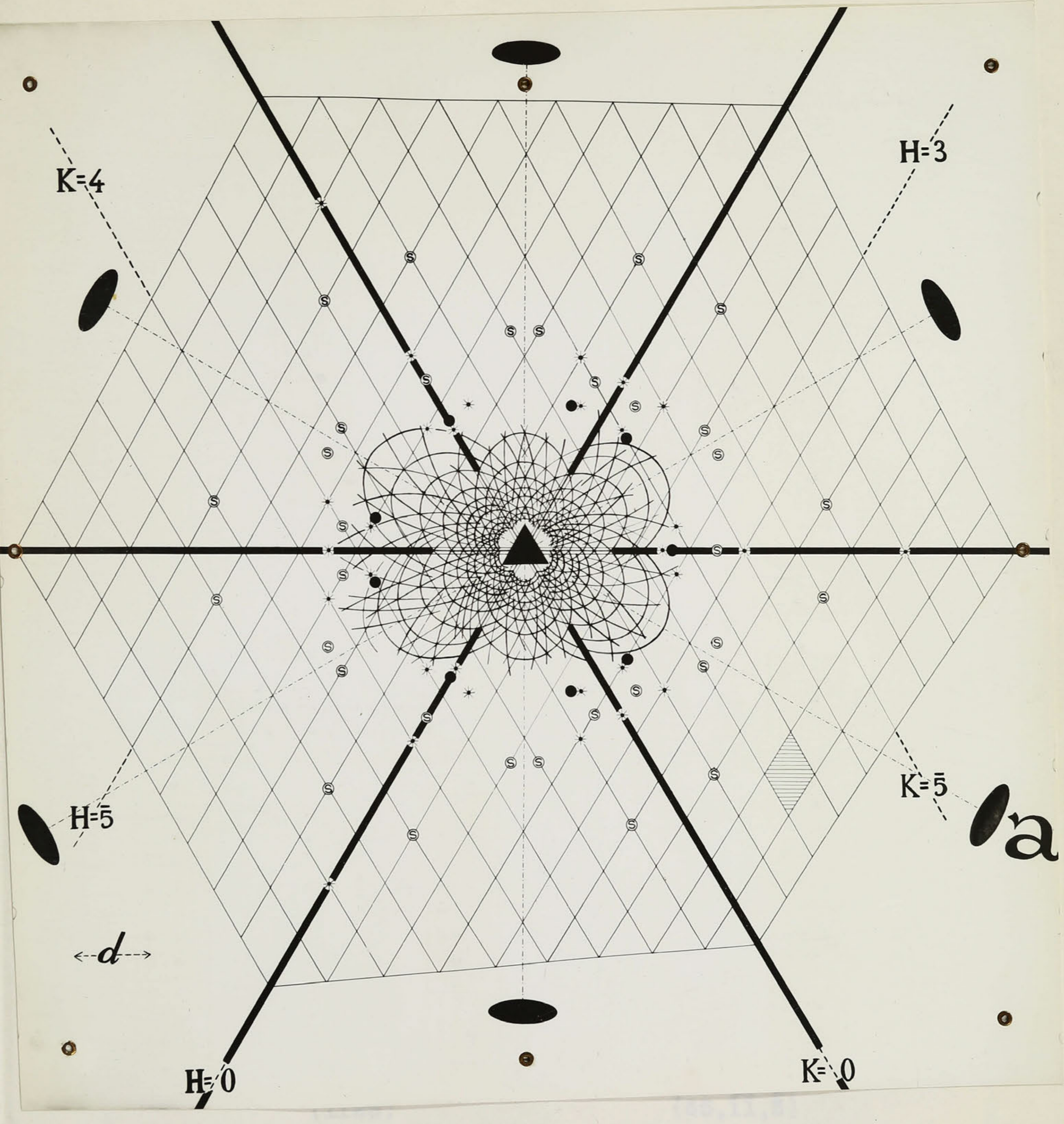

FIGURE 42

Gnomonic Projection

$Rb_2S_2O_6$

Beam along c axis

TABLE XIII

$Rb_2S_2O_6$. a axis.
Present in Twin.
Absent in Single Crystal.

$(12\bar{3}\bar{1})$
$(1\bar{3}21)$

$(10\bar{1}3)$
$(1\bar{1}0\bar{3})$

$(2\bar{6}4\bar{3})$
$(24\bar{6}3)$

$(20\bar{2}\bar{5})$
$(2\bar{2}05)$

TABLE XIV

$Rb_2S_2O_6$. a axis.
Stronger in Twin
than in Single Crystal.

$(13\bar{4}\bar{1})$
$(1\bar{4}31)$

$(12\bar{3}\bar{2})$
$(1\bar{3}22)$

$(34\bar{7}\bar{3})$
$(3\bar{7}43)$

TABLE XV

$Rb_2S_2O_6$. a axis. Weaker in Twin than in Single Crystal.

$(35\bar{8}0)$
$(3\bar{8}50)$

$(23\bar{5}1)$
$(2\bar{5}3\bar{1})$
$(23\bar{5}\bar{1})$
$(2\bar{5}31)$

$(4\bar{9}5\bar{2})$
$(45\bar{9}2)$

$(1\bar{2}1\bar{3})$
$(11\bar{2}3)$

$(23\bar{5}\bar{3})$
$(2\bar{5}33)$

$(3\bar{7}4\bar{3})$
$(34\bar{7}3)$

$(21\bar{3}\bar{4})$
$(2\bar{3}14)$

$(6,\overline{11},5\bar{5})$
$(65,\overline{11},5)$
$(6,\overline{11},55)$
$(65,\overline{11},\bar{5})$

FIGURE 43 Gnomonic Projection $Rb_2S_2O_6$ Beam along a axis

TABLE XVI

$Rb_2S_2O_6$. b axis.
Present in Twin.
Absent in Single Crystal.

$(9\bar{2}\bar{7}1)$
$(\bar{9}721)$

$(10,\bar{2}\bar{8}1)$
$(\overline{10},821)$

$(9\bar{2}\bar{7}2)$
$(\bar{9}722)$

$(10\bar{1}3)$
$(\bar{1}103)$

$(4\bar{1}\bar{3}\bar{3})$
$(\bar{4}31\bar{3})$

$(6\bar{1}\bar{5}4)$
$(\bar{6}514)$

$(5\bar{1}\bar{4}4)$
$(\bar{5}414)$

$(7\bar{1}\bar{6}4)$
$(\bar{7}614)$

$(38,\bar{7},31,4)$
$(\overline{38},31,74)$

$(02\bar{2}5)$

$(81\bar{9}5)$
$(\bar{8}9\bar{1}5)$

$(14\bar{5}7)$
$(\bar{1}5\bar{4}7)$

TABLE XVIII

$Rb_2S_2O_6$. b axis.
Weaker in Twin
than in Single Crystal.

$(8\bar{3}\bar{5}0)$
$(\bar{8}530)$

$(8\bar{3}\bar{5}1)$
$(8\bar{3}\bar{5}\bar{1})$
$(\bar{8}531)$
$(\bar{8}53\bar{1})$

$(01\bar{1}\bar{2})$

$(4\bar{1}\bar{3}\bar{4})$
$(\bar{4}31\bar{4})$

$(31\bar{4}\bar{5})$
$(\bar{3}4\bar{1}\bar{5})$

$(62\bar{8}5)$
$(\bar{6}8\bar{2}5)$

$(32\bar{5}6)$
$(\bar{3}5\bar{2}6)$

$(12\bar{3},\overline{10})$
$(\bar{1}3\bar{2},\overline{10})$

TABLE XVII

$Rb_2S_2O_6$. b axis. Stronger in Twin than in Single Crystal.

$(7\bar{1}\bar{6}0)$
$(\bar{7}610)$

$(6\bar{1}\bar{5}0)$
$(\bar{6}510)$

$(8\bar{1}\bar{7}0)$
$(\bar{8}710)$

$(4\bar{1}\bar{3}1)$
$(\bar{4}311)$

$(5\bar{1}\bar{4}1)$
$(\bar{5}411)$

$(6\bar{1}\bar{5}1)$
$(\bar{6}511)$

$(7\bar{1}\bar{6}1)$
$(\bar{7}611)$

$(7\bar{2}\bar{5}\bar{1})$
$(\bar{7}52\bar{1})$

$(3\bar{1}\bar{2}\bar{2})$
$(\bar{3}21\bar{2})$

$(01\bar{1}\bar{3})$

$(50\bar{5}3)$
$(\bar{5}503)$

$(20\bar{2}3)$
$(\bar{2}203)$

$(11\bar{2}4)$
$(\bar{1}2\bar{1}4)$

$(30\bar{3}4)$
$(\bar{3}304)$

$(21\bar{3}\bar{4})$
$(\bar{2}3\bar{1}\bar{4})$

$(30\bar{3}\bar{4})$
$(\bar{3}30\bar{4})$

$(12\bar{3}5)$
$(\bar{1}3\bar{2}5)$

$(23\bar{5}6)$
$(\bar{2}5\bar{3}6)$

$(43\bar{7}\bar{7})$
$(\bar{4}7\bar{3}\bar{7})$

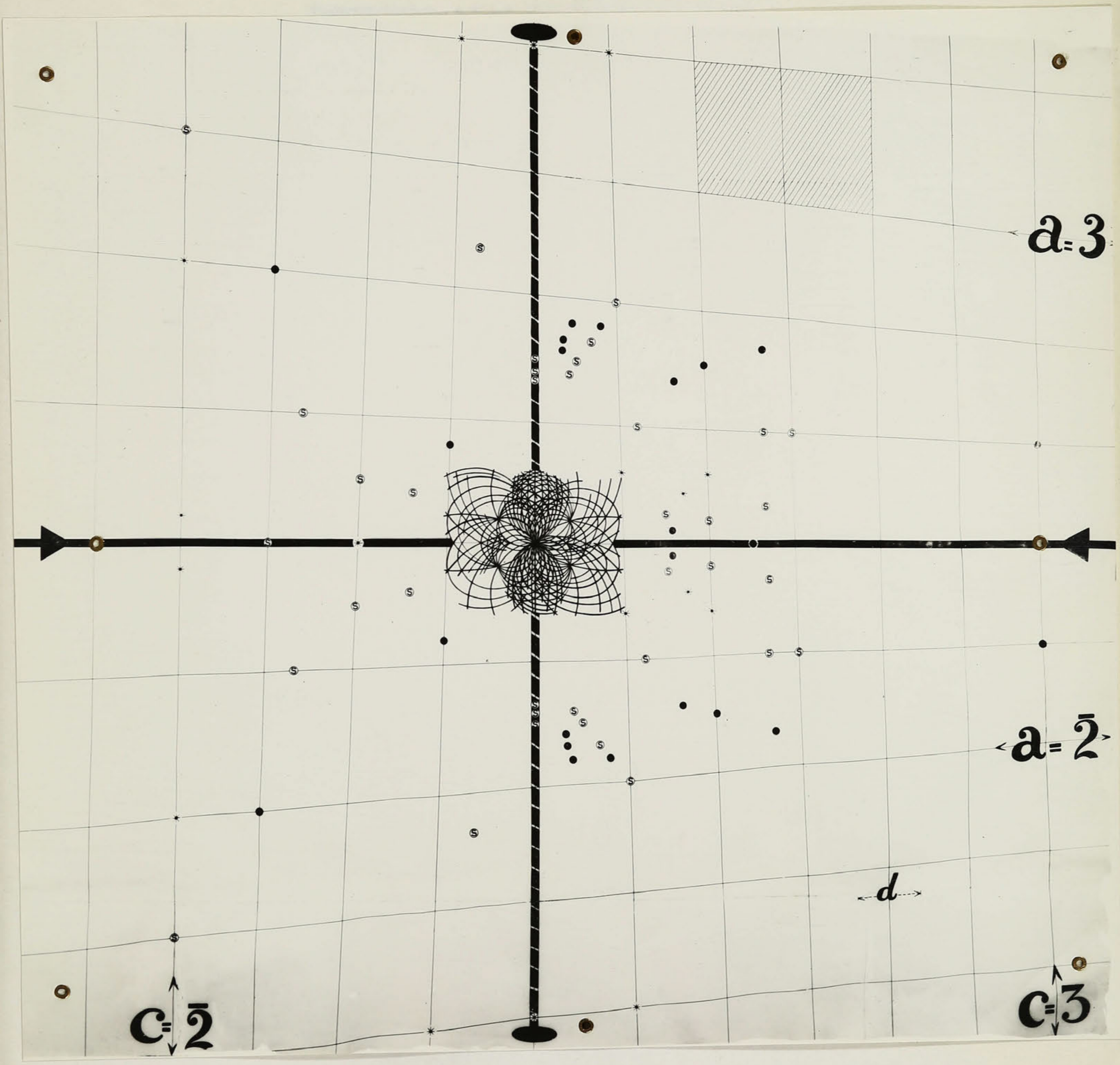

FIGURE 44

Gnomonic Projection

$Rb_2S_2O_6$

Beam along b axis

INTERPRETATION OF LAUE DIAGRAMS

An examination of Tables I to XVIII and Figures 39 to 44 suggests that the twinned crystals are derived from the single crystal by a rotation of 60° (or 180°) about the *c* axis in $K_2S_2O_6$ and in $Rb_2S_2O_6$, respectively. The pseudo-hexagonal (twinned) specimens, therefore, appear to be due to the interpenetration of two single trigonal crystals having their *c* axes in common but otherwise bisecting each other. Since the gnomonic projections of the *c* axis Laue diagrams do not distinguish planes of the form $\{\bar{H}\bar{K}.L\}$ from those of the form $\{\bar{H}\bar{K}.\bar{L}\}$ no distinction can be made on the basis of these projections alone between an ordinary rotation of 60° (or 180°) and a two-fold axis of rotary-reflection.

Turning now to the *a* axis Laue diagrams (Tables IV and XIII, Figures 40 and 43) it will be seen that all the points added by twinning appear in pairs across the centre as the trace of a two-fold axis perpendicular to the diagram. These points may be considered as due to planes introduced by the reflection of corresponding planes in the single crystal across the *ac* or *ab* planes acting as planes of pseudo-symmetry.

From the *b* axis Laue diagrams it appears that, of the points added by twinning, some are in the trace of the *bc* plane (which is a plane of symmetry in the single crystal) and others appear in pairs, one on each side of the trace of the *bc* plane, so that they may be considered as due to a reflection of corresponding planes in the single crystal across the *ab* planes acting as planes of pseudo-symmetry.

Thus, in the Laue diagrams of the twins, the *ac* and *ab* planes appear as planes of pseudo-symmetry in addition to the normal plane of symmetry *bc*.

This result is sufficient to show that in twinning the *c* axis appears to act as an axis of simple rotation and not as one of rotary-reflection, as will be clear from the following argument.

Consider first the effect of a simple rotation of 60° about the *c* axis on the trigonal space group D_3^2, the Laue symmetry elements of which are those of D_3^d (see Figure 45A). A 60° rotation about the *c* axis of the points on the stereographic projection of D_3^d and superposition on the original diagram is identical with D_6^h since the basal (*ab*) plane and the *ac* planes thereby appear as planes of symmetry as in Figure 45C. It may be noted that the same result is obtained by a rotation of the points of Figure 45A about one of the *b* axes (at 30° to the *a* axes) and superposition on the original diagram. From the point of view of Laue photographs, Figures 45A and 45C may be simplified as in Figures 45B and 45D, respectively, since X-ray methods are unable to distinguish the planes (HK.L) and ($\bar{H}\bar{K}.\bar{L}$) one from the other. Thus the points *+u* and *-u* in Figures 45A and 45C appear as a single spot (corresponding to

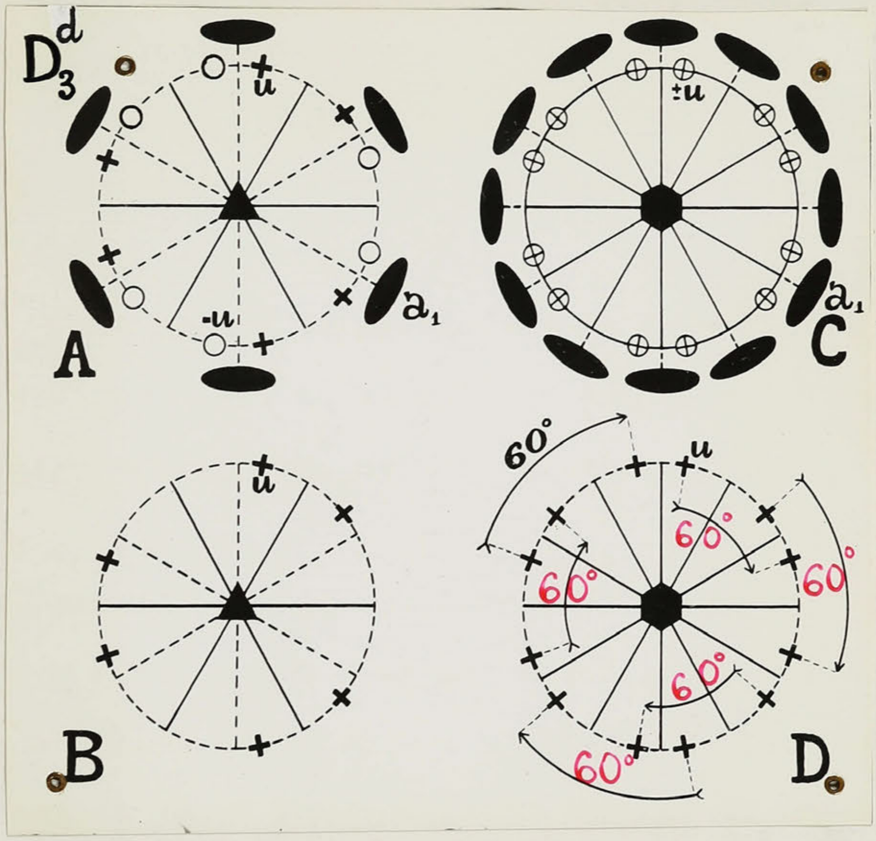

FIGURE 45

Diagram illustrating the Effect of a Simple Rotation of 60° about the c Axis on the Stereographic Projection and Laue Symmetry of D_3^d

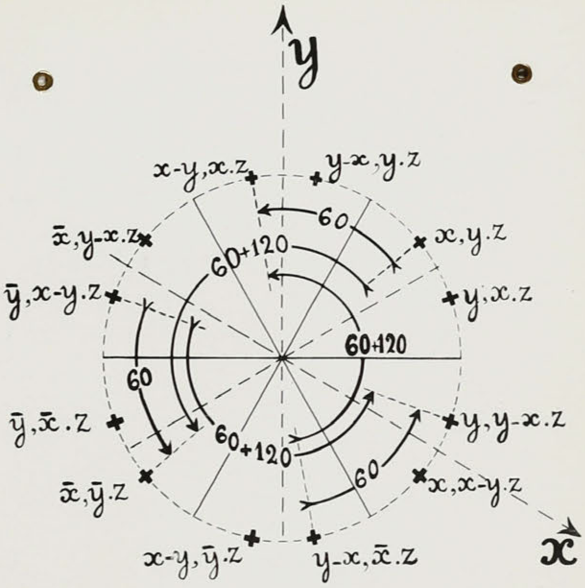

FIGURE 46

Diagram showing Equivalence of 60° and 180° Rotations about the Triad c Axis *u*) in a Laue photograph. Furthermore, it is clear from Figure 46 that a rotation of 60° about the *c* axis is equivalent to one of 180° (*i.e.*, 60° + 120°) when this axis is one of three-fold symmetry.

In order to visualize more easily the effects of a simple rotation of 180° and of a rotary-reflection, respectively, on the Laue symmetry of D_3^d, a triangular pyramid of the 18th. (D_3) class (13, v.1, p.351) may be employed. Such a model was constructed of cardboard and a long pin was used to fix it about the *c* axis while other pins indicated normals to the faces. The indices of the faces of such a *right* pyramid (see Figure 47) are

1. $(21\bar{3}1)$, *i.e.*, (241) in trirectangular coordinates,
2. $(\bar{1}\bar{2}31)$, *i.e.*, $(\bar{1}\bar{5}1)$ in trirectangular coordinates,
3. $(\bar{1}101)$, *i.e.*, $(\bar{1}11)$ in trirectangular coordinates.

Twinning due to a simple rotation of 180° (see Figure 47) would add the planes

1'. $(12\bar{3}1)$, *i.e.*, (151) in trirectangular coordinates,
2'. $(\bar{2}\bar{1}31)$, *i.e.*, $(\bar{2}\bar{4}1)$ in trirectangular coordinates,
3'. $(1\bar{1}01)$, *i.e.*, $(1\bar{1}1)$ in trirectangular coordinates.

Similarly, the faces of the corresponding *left* pyramid have the indices $(3\bar{1}\bar{2}1)$, $(\bar{3}211)$, $(0\bar{1}11)$, to which twinning due to a rotation of 180° would add $(\bar{3}121)$, $(3\bar{2}\bar{1}1)$ and $(01\bar{1}1)$.

But, since X-ray methods cannot distinguish directly

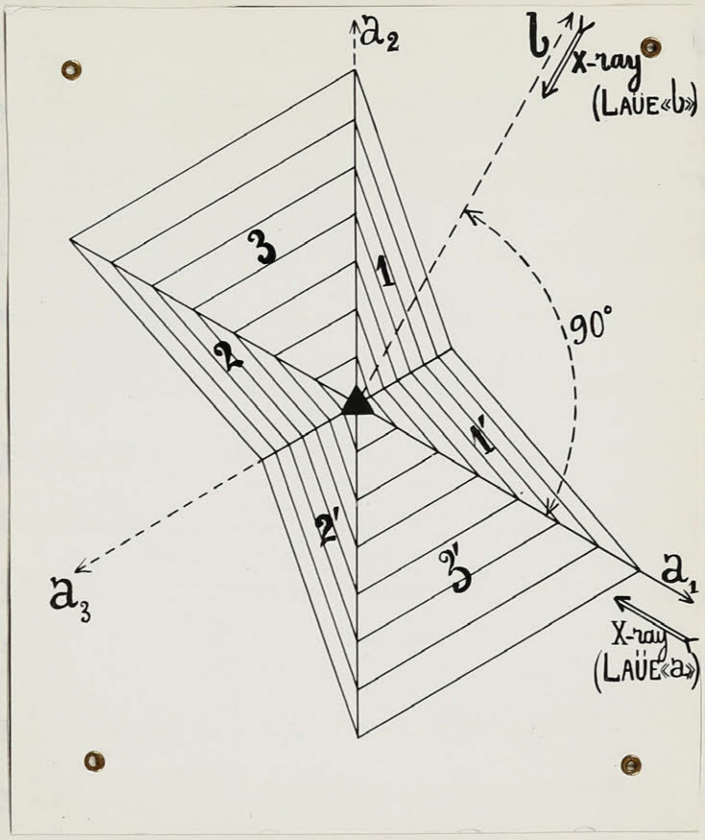

FIGURE 47

Diagram illustrating the Effect of Twinning by Rotation of 180° about c axis on Right Triangular Pyramid of 18th. Class between left- and right-handed crystals, only the <u>right</u> pyramid need be considered.

Diffraction spots due to planes of the <u>right</u> pyramid are represented in Figure 48 by points on schematic <u>a</u> and <u>b</u> axis gnomonic projections in the quadrants specified below, where l = lower, u = upper, L = left, R = right. The indices of the planes are recorded also in terms of trirectangular coordinates which may be determined directly from Figure 48.

No.	Plane	a axis	b axis
1	$(21\bar{3}1)$	lL, $(12,1/2)=(241)$	lR, $(1/2,1,1/4)=(241)$
2	$(\bar{1}\bar{2}31)$	uL, $(\bar{1}\bar{5}1)$	uR, $(1/5,1,\overline{1/5})=(15\bar{1})$
3	$(\bar{1}101)$	uR, $(1\bar{1}\bar{1})$	lL, $(\bar{1}11)$

The planes added by twinning due to a simple rotation of 60° (or 180°) about the <u>c</u> axis, their positions in Figure 48 and their orthohexagonal indices are as follows.

No.	Plane	a axis	b axis
1'	$(12\bar{3}1)$	lL, (151)	lR, $(1/5,1,1/5)=(151)$
2'	$(\bar{2}\bar{1}31)$	uL, $(\bar{1}\bar{2},1/2)=(\bar{2}\bar{4}\bar{1})$	uR, $(1/2,1,\overline{1/4})=(24\bar{1})$
3'	$(1\bar{1}01)$	lR, $(\bar{1}1\bar{1})$	uL, $(\bar{1}1\bar{1})$

Thus, in Laue diagrams of D_3^2 (in which the <u>a</u> axes are two-fold axes and the <u>bc</u> planes appear as planes of symmetry (D_3^d)) twinning due to a 60° (or 180°) rotation about the <u>c</u> axis introduces points that make the <u>ac</u> and <u>ab</u> planes appear as planes of pseudo-symmetry (D_6^h) at least insofar as relative positions of apparently equivalent points are concerned. This

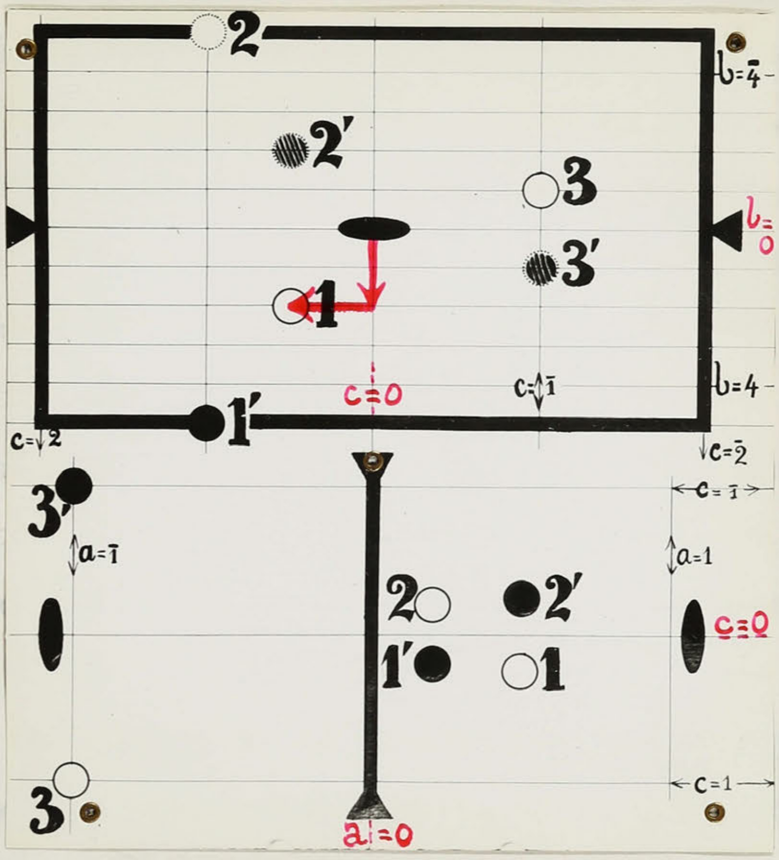

FIGURE 48

Schematic Laue Diagrams

Twinning of Right Triangular Pyramid of

18th.Class by 180° Rotation about c axis is clear from Figure 49 where the points corresponding to 1, 2, 3, 1', 2', 3' and due to the operation of the two-fold (a) axis and the apparent (bc) plane of symmetry are shown.

Figures 48 and 49 may be compared directly with Figures 40, 41, 43, 44 if the schematic diagrams with the beam along the b axis in Figures 48 and 49 first be turned counterclockwise through 90°. It will be observed that the same type of symmetry is exhibited by the schematic diagrams and the corresponding gnomonic projections. Thus the Laue diagrams of the pseudo-hexagonal $K_2S_2O_6$ and $Rb_2S_2O_6$ possess the pseudo-symmetry to be expected on the assumption of a simple rotation of 60° (or 180°) about the c axis.

The same method of analysis may be employed to show that the assumption of a rotary-reflection is not consistent with the observed facts.

The effect on the same model of a right pyramid of a rotation through 180° about the c axis, followed by a reflection, is represented in Figure 50. Twinning of this kind would add the following planes to those previously listed as 1, 2, 3.

1". $(12\bar{3}\bar{1})$, i.e., $(15\bar{1})$ in trirectangular coordinates,
2". $(1\bar{1}0\bar{1})$, i.e., $(1\bar{1}\bar{1})$ in trirectangular coordinates,
3". $(\bar{2}\bar{1}3\bar{1})$, i.e., $(\bar{2}\bar{4}\bar{1})$ in trirectangular coordinates.

With the same conventions as before, these planes would be represented on the gnomonic projections of a and b

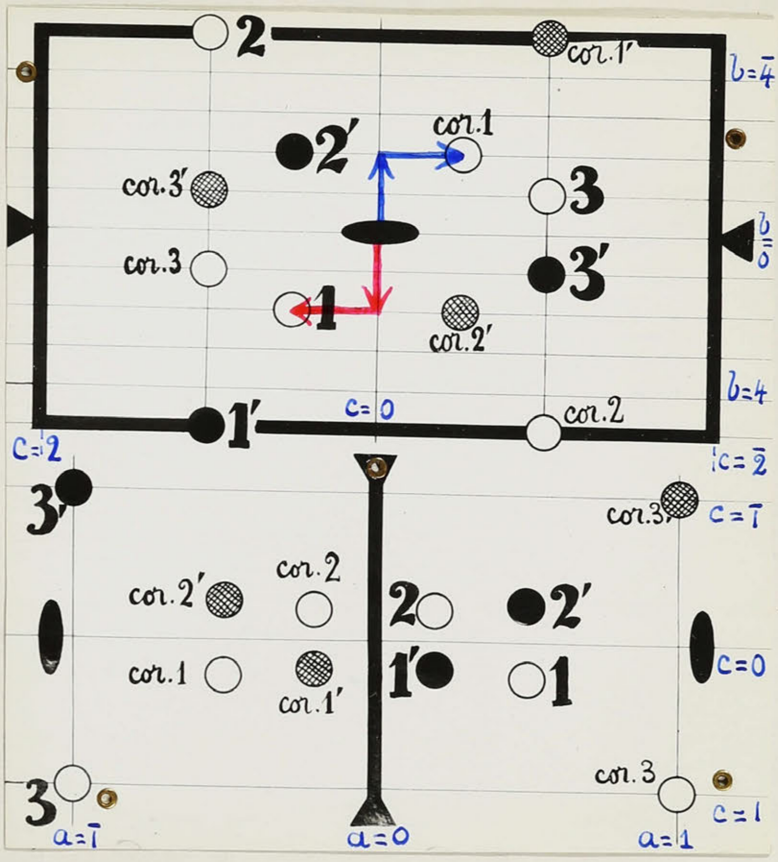

FIGURE 49

Schematic Laue Diagrams

Same as Figure 48 but showing Introduction of Pseudo-symmetry Planes due to Twinning

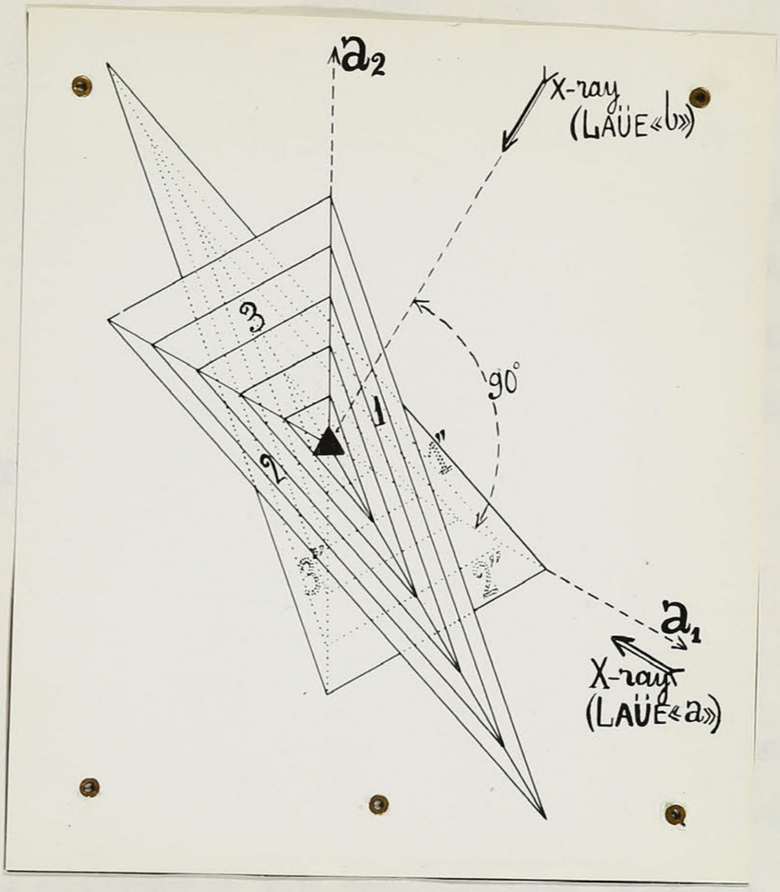

FIGURE 50

Diagram illustrating the Effect of Twinning by Rotary-reflection on a Right Triangular Pyramid of 18th.Class axis diagrams by the points designated below.

No.	a axis	b axis
1	1L,(12,1/2)=(241)	1R,(1/2,1,1/4)=(241)
2	uL,$(\bar{1}\bar{5}1)$	uR,$(1/5,1,\overline{1/5})=(15\bar{1})$
3	uR,$(1\bar{1}\bar{1})$	1L,$(\bar{1}11)$
1"	uL,$(\bar{1}\bar{5}1)$	uR,$(1/5,1,\overline{1/5})=(15\bar{1})$
2"	uR,$(1\bar{1}\bar{1})$	1L,$(\bar{1}11)$
3"	1L,(12,1/2)=(241)	1R,(1/2,1,1/4)=(241)

Thus, in both cases,

$1 \equiv 3''$

$2 \equiv 1''$

$3 \equiv 2''$

so that spots are <u>not</u> introduced in previously unoccupied positions by a twinning due to a two-fold axis of rotary-reflection and this is contrary to the observations recorded in Figures 40, 41, 43, and 44.

It is clear, therefore, that, from the gnomonic projections of Laue photographs taken with the X-ray beam along <u>a</u> and <u>b</u> axes, respectively, of trigonal trapezohedral crystals, it is possible to distinguish a twinning that appears to be derived from a 60° (or 180°) rotation about the <u>c</u> axis from one that is due to the operation of the <u>c</u> axis as a two-fold axis of rotary-reflection. In fact the Laue method would not show the existence of twinning in the latter case since a plane (HK.L) becomes the plane $(\bar{H}\bar{K}.L)$ by a simple rotation of 180°

and finally $(\bar{H}\bar{K}.\bar{L})$ by a subsequent reflection and $(\bar{H}\bar{K}.\bar{L})$ is indistinguishable from (HK.L) by X-ray methods of analysis.

Beyond differentiation between twinning due to an apparent rotation about the c axis and that due to a rotary-reflection the Laue method alone is powerless as will be evident from the following discussion of its limitations.

LIMITATIONS OF THE LAUE METHOD

The most common types of twinning found in crystals of the trigonal trapezohedral class are represented in Figure 51, where the stereographic projections of right- and left-handed crystals are designated R and L, respectively. RR and LL represent corresponding projections for complete penetration twins of two right- and two left-handed crystals, respectively, and RL that for one right- and one left-handed crystal. Finally, RRLL represents the stereographic projection of complete holohedral twinning and may be considered as due to a combination of two right- and two left-handed individuals, of RR and LL, or of two RL, twins, respectively. It is obvious that the projections of RR and LL have the symmetry of D_6, that of RL has the symmetry of D_3^h while that of RRLL has the symmetry of D_6^h.

But, since the X-ray method automatically introduces a centre of symmetry, it is clear that, insofar as Laue symmetry is concerned, $R \equiv L \equiv D_3^d$ and $RR \equiv LL \equiv RL \equiv RRLL \equiv D_6^h$, the

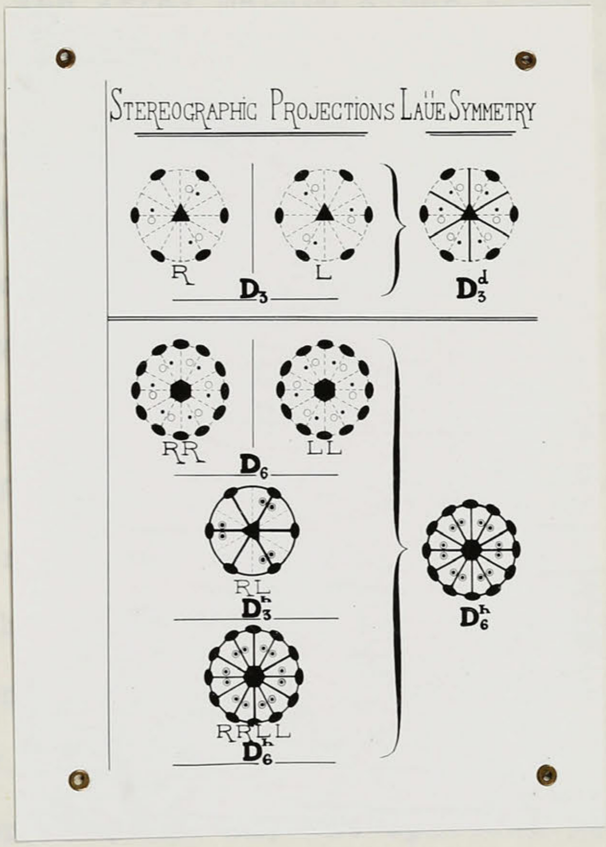

FIGURE 51

Stereographic Projections

of Possible Twins in D_3

diagram of the latter class being derived from that of the former by a rotation of 60° (or 180°) and superposition on the original. The X-ray method alone, therefore, is unable to distinguish the four types of twinning represented in Figure 51 one from another. It may be mentioned that a simple reflection of R or L across a plane normal to the c axis and superposition on the original diagram is identical with RL, although W.L. Bragg (49, p. 179) refers to it as another type of twinning. An examination of Figure 51, however, shows that the addition of a plane of symmetry normal to the c axis immediately converts either R or L into RL.

Of the four possible types of twinning, it is evident that measurements of optical activity may be employed to supplement the X-ray data and limit the possible types in any specific case. Thus for RR (and LL) the specific rotation will be the same as in R (and L), whereas for RL and RRLL the specific rotation will be less, and may be zero, depending on the relative proportions of the R and L constituents.

OPTICAL EXAMINATION

Twinned crystals of $K_2S_2O_6$ and of $Rb_2S_2O_6$ were examined optically with the following results. In each case the existence of twinning was established by Laue photographs.

$K_2S_2O_6$.

Only one crystal of $K_2S_2O_6$ possessing pseudo-hexagonal symmetry was obtained. Consequently this specimen was employed throughout the Laue investigation already described. It had thus been subjected to prolonged exposure to X-radiation before the necessity for optical measurements was realized. It was found that crystals of $K_2S_2O_6$ and of $Rb_2S_2O_6$ turn pink and then purple after extended exposure to the X-ray beam. In the case of the specimen of $K_2S_2O_6$ under discussion a pronounced purple tint was observed. Marked dichroism was manifested, the ordinary ray (ω) appearing colourless while the extraordinary ray (ε) was violet.

Furthermore, the basal plane face was absent from one end of the crystal and the specimen was too small to permit cutting one. Finally, tabular fluid inclusions parallel to the basal plane were present.

Under these circumstances, therefore, a study of the optical activity of this crystal could not be made.

$Rb_2S_2O_6$.

Unlike $K_2S_2O_6$, several pseudo-hexagonal crystals of $Rb_2S_2O_6$ were obtained. A comparatively large specimen was selected and the fact of twinning was verified by means of a Laue photograph. This specimen was not subjected to prolonged exposure to X-radiation and hence dichroism, although of the same character as that encountered in $K_2S_2O_6$, was slight. The purple tint of the crystal in ordinary light was limited to the region that had been exposed to X-rays.

No evidence of optical activity could be detected in this crystal of $Rb_2S_2O_6$ although the probable error in the measurement of specific rotatory power was estimated at less than (1/4)°/mm. under the existing conditions.

Since the specific rotation of a trigonal (untwinned) crystal of $Rb_2S_2O_6$ has been established in Section II of this thesis (see p. 42) as between 1.8° and 2.2° per mm., it follows that twinning in rubidium dithionate must be of the RL or RRLL type (see Figure 51). This conclusion receives some indirect confirmation from the fact that Topsøe and Christiansen (26) observed no optical activity in crystals of rubidium dithionate whereas Wyrouboff (23) reports very slight activity. It may be inferred, therefore, that these investigators examined twinned crystals composed of different relative proportions of R and L constituents.

DISCUSSION

It is clear from the arguments presented in this Section of the thesis that the Laue method enables a distinction to be made between a twinning in the trigonal trapezohedral class (D_3) due to an apparent rotation about the <u>c</u> axis and one due to a rotary-reflection. This is another instance of the interest attached to Laue photographs obtained with the beam along lateral axes as emphasized in Section I of the present thesis. Limitations of the Laue method, however, prohibit any distinction among the types of twinning designated RR, LL, RL and RRLL. Nevertheless, there are occasions when a crystal suitable for Laue photographs but unsuitable for complete crystallographic examination will permit measurements of optical activity to be made.

In such a case, as in the twinned $Rb_2S_2O_6$ crystal discussed in this Section, a distinction can be made between RR (and LL) on the one hand and RL and RRLL on the other. Thus the X-ray method coupled with studies of optical activity enables some progress to be made in the determination of the nature of twinning in certain cases where the more exact methods of formal crystallography cannot be applied in full.

Specifically, the work of the present Section has identified a twin of $Rb_2S_2O_6$ as of the RL or RRLL type. Due to the reasons already given it was impossible to do more with a twinned crystal of $K_2S_2O_6$ than to determine that the twinning was not due to a rotary-reflection. From crystallographic studies, however, Fock (24) has stated that twins of $K_2S_2O_6$ are of the RR (or LL) type. If this is correct, twinning in the isomorphous $K_2S_2O_6$ and $Rb_2S_2O_6$ is of different types.

It is of interest to note that Schubnikow and Zinserling (50) have employed Laue diagrams (only, however, with the beam along the <u>c</u> axis) together with optical studies to demonstrate that mechanical twinning in quartz due to pressure is of the Dauphiné (RR and LL) type.

There is no doubt that the rubidium dithionate crystal of Hägg, to which reference already has been made, was a twin. His reproduction (5, p.266) of the Laue photograph with the beam along the c axis apparently possesses the symmetry of D_6^h both with respect to the geometrical positions of diffraction spots and to their relative intensities. The photograph obtained with the beam along an a axis, however, shows the symmetry of D_6^h only when the relative positions of the diffraction spots are considered. If the relative intensities of apparently equivalent spots are examined it will be seen that the symmetry actually is that of D_3^d. Considered in conjunction with Laue photographs of crystals of potassium dithionate that admittedly and clearly show the symmetry of D_3^d, this fact should have been sufficient to suggest the presence of twinning in the crystal (or crystals) of rubidium dithionate examined. Instead, Hägg suggested the hypotheses cited in the Introduction (p. 124) to this Section to account for the fact that a crystal, which was expected to show the symmetry of D_3^d, in reality appeared to possess pseudo-D_6^h symmetry.

As noted previously (p. 125), Hägg suggests (a) that the lattice of the metal ions may possess the Laue symmetry of D_6^h and that this lattice may have a dominating influence on the Laue symmetry exhibited by the crystal as a whole when the relatively heavier rubidium ions are involved or (b) that in passing from $K_2S_2O_6$ to $Rb_2S_2O_6$ a change in parameters may occur of such a nature as to result in an approach to the higher symmetry.

It is of interest, therefore, to examine all the space groups of those crystal classes (D_3^h, C_6^v, D_6, D_6^h) that possess the Laue symmetry of D_6^h to determine if the special positions ($uu0$; $0\bar{u}0$; $\bar{u}00$; $u'u',1/2$; $0\bar{u}',1/2$; $\bar{u}'0,1/2$) occupied by potassium and rubidium ions in $K_2S_2O_6$ and $Rb_2S_2O_6$, respectively, are possible therein.

The space groups in which this combination $\left[\text{(e) + (f) of } D_3^2\right]$ does not occur (20, pp. 158-169) are D_{3h}^1, D_{3h}^2, C_{6v}^1, C_{6v}^2, C_{6v}^3, C_{6v}^4, D_6^2, D_6^3, D_6^4, D_6^5. If $u = u'$, the combination would be identical with (g) of D_{3h}^4. If $u = u' = (1/2)$, identity would be established with (f)+(g) of D_6^1, (f)+(g) of D_{6h}^1, (f) of D_{6h}^2, (g) of D_{6h}^4. If $\bar{u} = u'$, it would be identical with (g) of D_6^6 and (g) of D_{6h}^3, respectively.

There is, however, one set of special positions possible in a space group having the Laue symmetry of D_6^h that is identical with (e)+(f) of D_3^2 (where u and u' may have any values independently of each other). It is (f)+(g) of D_{3h}^3.

It appears, therefore, (a) that the metal ions in $K_2S_2O_6$ and in $Rb_2S_2O_6$ are on a lattice having the Laue symmetry of D_6^h and (b) that the possibility of an approach to the higher (D_6^h) symmetry due to changes in the parameters (u and u') in passing from $K_2S_2O_6$ to $Rb_2S_2O_6$ may be discarded since u and u' may have any values independently of each other without affecting the holohedral Laue symmetry of their lattice.

Qualitatively, Laue diagrams of trigonal (single) crystals of $K_2S_2O_6$ and of $Rb_2S_2O_6$ (see Figures 27, 29, 31, 33, 35, 37) are not good examples of the type of diagram to be expected from a typical trigonal crystal as, for example, α-quartz (see Figures 5, 6, 7, pp. 20A, 20B) or, particularly, tourmaline (see Figures 8, 9, 10, pp. 29A, 29B). Furthermore, the Laue diagrams of $Rb_2S_2O_6$ are less obviously trigonal than are those of $K_2S_2O_6$. It is probable, therefore, that Hägg's suggestion regarding the influence of the potassium and, notably, the rubidium ions on the Laue symmetry of the crystals as a whole is justified despite the fact that it was proposed to account for observations regarding the Laue symmetry of crystals of $Rb_2S_2O_6$ that were assumed to be single crystals but, in view of the results of the present investigation, appear to have been twins.

GENERAL BIBLIOGRAPHY

1. Helwig, G.V. Ph.D. Thesis, (Physics Dept.) McGill University, Sept. 1931.

2. Barnes, W.H. and Helwig, G.V. Can. J. Research, 4, 565-9 (June 1931).

3. Helwig, G.V. Z. Krist., 83, 485-492 (Nov. 1932).

4. Huggins, M.L. and Frank, G.O. Am. Mineralogist, 16, 580-591 (Dec. 1931).

5. Hägg, G. Z.Krist., 83, 265-273 (Aug. 1932).

6. Barnes, W.H. and Wendling, A.V. Trans. Roy. Soc. (Canada), 27, III, 133-140 (1933).

7. Barnes, W.H. and Wendling, A.V. Trans. Roy. Soc. (Canada), 27, III, 169-175 (1933).

8. Barnes, W.H. and Wendling, A.V. Am. Mineralogist, 20, 253-9 (1935).

9. Astbury, W.T. and Yardley, K. Trans. Roy. Soc. (London), A224, 221-257 (1924).

10. Wyckoff, R.W.G. The Structure of Crystals, 2nd. Ed., (Chem. Cat. Co.), New York, 1931.

11. Kulaszewski, C. Abh. math.-phys. Klasse sächs. Akad. Wiss. Leipzig, 38, 81-117 (1921).

12. Machatschki, F. Z. Krist., 70, 211-233 (1929).

13. Tutton, A.E.H. Crystallography and Practical Crystal Measurement, 2 vols., (Macmillan) London, 1922.

14. Groth, P. Chemische Krystallographie, 5 vols., (Engelmann), Leipzig, 1906-1919.

15. Schiebold, E. Abh. math.-phys. Klasse sächs. Akad. Wiss. Leipzig, 36, 119 (1919).

16. Wyckoff, R.W.G. Am. J. Sci., 50, 329 (1920).

17. Bernal, J.D. J. Sci. Instruments, 4, 273-284 (1927); 5, 241-250 (1928); 6, 314-318, 343-353 (1929).

18. Bernal, J.D. Proc. Roy. Soc. (London), *A113*, 117-160 (1927).

19. Hintze, C. *Handbuch der Mineralogie*, Leipzig, *1897*, vol. 2, pp. 312-314.

20. Wyckoff, R.W.G. *The Analytical Expression of the Results of the Theory of Space Groups*, 2nd. Ed., (Carnegie Institution), Washington, *1930*.

21. Huggins, M.L. Am. Mineralogist, *18*, 455-457 (Oct. 1933).

22. Wyckoff, R.W.G. *The Structure of Crystals. Supplement for 1930-1934 to the Second Edition*, (Reinhold), New York, *1935*.

23. Wyrouboff, M.G. Ann. Chim. Phys., (6), *8*, 340-417 (1886).

24. Fock, A. Z. Krist., *6*, 161 (1881).

25. Piccard, J. J. f. prakt. Chem., *86*,(2), 456 (1862).

26. Topsøe, H. and Christiansen, C. Vidensk. Selsk. Skr. Kopenhagen, *9*, 661 (1873); Ann. Chim. Phys., (5), *1*, 5-99 (1874); Pogg. Ann., *Ergänzb.6*, 499-585 (1874).

27. Pape, C. Pogg. Ann., *139*, 224-239 (1870).

28. Miers, H.A. *Mineralogy*, 2nd. Ed., revised by H.L. Bowman, (Macmillan), London, *1929*.

29. Rose, H. Neus Jahrb. Min. Geol. (Beil. Bd.), *29*, 53-105 (1910).

30. Bragg, W.H. and Bragg, W.L. *X-rays and Crystal Structure*, (Bell), London, *1924*.

31. Pauling, L. and Sherman, J. Z. Krist., *81*, 1 (1932).

32. Glocker, R. *Materialprüfung mit Röntgenstrahlen*, (Springer), Berlin, *1936*.

33. *Internationale Tabellen zur Bestimmung von Kristallstrukturen*, 2 vols., (Gebrüder Borntraeger), Berlin, *1935*.

34. Pringsheim, P. and Yost, M. Z. f. Physik, *58*, 4 (1929).

35. Lewis, G.N. *Valence and the Structure of Atoms and Molecules*, (Chem. Cat. Co.), New York, *1923*.

36. Thomas, L.H. Proc. Cambridge Phil. Soc., 23, 5, 542 (1927).

37. Bragg, W.L. and West, J. Z. Krist., 69, 118 (1928).

38. Davey, W. P. A Study of Crystal Structure and Its Applications, (McGraw-Hill), New York, 1934.

39. West, J. Z. Krist., 74, 306 (1930).

40. Vegard, L. and Maurstad, A. Z. Krist., 69, 519 (1929).

41. Zachariasen, W.H. Z. Krist., 71, 501 (1929).

42. Ogg, A. Phil. Mag., 5, 354 (1928).

43. Ogg, A. Phil. Mag., 9, 665 (1930).

44. Mellor, J.W. Modern Inorganic Chemistry, (Longmans, Green), London, 1925.

45. Hägg, G. Z. physik. Chem., 18B, 327-342 (1932).

46. Roger, G.H. and Binet, L. Traité de Physiologie normale et pathologique, part X, vol. II, (Masson), Paris, 1935.

47. Hardy, A.C. and Perrin, F.H. The Principles of Optics, (McGraw-Hill), New York, 1932.

48. Hankel, W.G. and Lindenberg, H. Abh. math.-phys. Klasse sächs. Akad. Wiss. Leipzig, 18, 361 (1892); 21, 11 (1894); Z Krist., 27, 515 (1897).

49. Bragg, W.L. and Bragg, W.H. The Crystalline State, vol.1, A General Survey by W.L. Bragg. (Bell), London, 1933.

50. Schubnikow, A. and Zinserling, K. Z. Krist., 83, 243-273 (1932).

GENERAL LIST OF ILLUSTRATIONS

GENERAL SUMMARY

1. The symmetry elements of Laue photographs of orthogonal crystals obtained with the X-ray beam along lateral axes and the importance thereof have been pointed out.

2. A new X-ray method for distinguishing between the members of certain pairs of space groups in the hexagonal system has been developed and has been tested by application to α-quartz and to potassium dithionate.

3. By means of this new procedure the space group of tourmaline has been established as C_{3v}^{1}.

4. The optical activity of rubidium dithionate has been measured as 1.8° to 2.2° per mm.

5. The crystal class of rubidium dithionate has been confirmed as trigonal trapezohedral.

6. The density of rubidium dithionate has been measured as 2.85_5 g. per cc. at 20°C.

7. The dimensions of the unit cell of rubidium dithionate have been determined as $a_o = 10.02$Å., $b_o = 17.39$Å., $c_o = 6.35$Å., $(c/a) = 0.6337$, $(\sin\alpha)/2 = 0.813_3$.

8. The number of formula units of $Rb_2S_2O_6$ per cell has been shown to be 3.

9. The Bravais lattice and the space group of rubidium dithionate have been established unequivocally as Γ_h and D_3^2, respectively.

10. The most probable special positions of the scattering centres in the unit cell of rubidium dithionate have been shown to be as follows.

    <u>6 Rb in</u>

    (e) $uu0$; $0\bar{u}0$; $\bar{u}00$.

    (f) $u'u',1/2$; $0\bar{u}',1/2$; $\bar{u}'0,1/2$.

    <u>6 S in</u>

    (c) $00u''$; $00\bar{u}''$.

    (d) $1/3,2/3,u'''$; $2/3,1/3,\bar{u}'''$.

    (d) $1/3,2/3,u''''$; $2/3,1/3,\bar{u}''''$.

    <u>18 O in</u>

    (g) xyz; $y-x,\bar{x}z$; $\bar{y},x-y,z$;
    $yx\bar{z}$; $\bar{x},y-x,\bar{z}$; $x-y,\bar{y}\bar{z}$.

    (g) $x'y'z'$; $y'-x',\bar{x}'z'$;$\bar{y}',x'-y',z'$;
    $y'x'\bar{z}'$; $\bar{x}',y'-x',\bar{z}'$; $x'-y',\bar{y}'\bar{z}'$.

    (g) $x''y''z''$; $y''-x'',\bar{x}''z''$; $\bar{y}'',x''-y'',z''$;
    $y''x''\bar{z}''$; $\bar{x}'',y''-x'',\bar{z}''$; $x''-y'',\bar{y}''\bar{z}''$.

11. The nature of the interatomic bonds in rubidium dithionate and the appropriate atomic F curves have been considered. It has been shown that atomic scattering factors based on data of Pauling and Sherman are more satisfactory for application to rubidium dithionate than are those of the

"Internationale Tabellen" or those determined by the Fermi-Thomas method.

12. The most probable values of the vertical parameters have been determined on the basis of diffraction data from $\{0001\}$.

13. Reasonably satisfactory values for the lateral parameters have been determined on the basis of available interatomic distances and of diffraction data from $\{m0\bar{m}0\}$, $\{m0\bar{m}m\}$, $\{mm\overline{2m}0\}$, $\{mm\overline{2m}m\}$.

14. The values of the parameters are as follows.

Rb^+ : 0.375, 0.375, 0
Rb^+ : 0.712, 0.712, 1/2
S^{++} : 0, 0, 0.165
S^{++} : 1/3, 2/3, 0.25
S^{++} : 1/3, 2/3, 0.58
O^- : 0.160, 0.120, 0.225
O^- : 0.53_2, 0.34_9, 0.36
O^- : 0.50_9, 0.20_9, 0.81

15. The structure of rubidium dithionate as found in the present investigation has been compared with the structures proposed by Helwig and by Huggins and Frank for the isomorphous potassium dithionate.

16. Data have been presented to show that neither the para-

meters of Helwig nor of Huggins and Frank for potassium dithionate can be applied without modification to rubidium dithionate.

17. On the basis of expected similarity between corresponding parameters of potassium and rubidium dithionates it has been shown that the present data for the latter salt indicate that the structure of Huggins and Frank for potassium dithionate probably is more nearly correct than is that of Helwig.

18. The use of the logarithms of values of calculated intensities instead of the more cumbersome direct figures for comparison with visually estimated intensities has been justified on the basis of the Fechner Law.

19. Trigonal and pseudo-hexagonal crystals of potassium and rubidium dithionate have been subjected to examination by the Laue method in an attempt to determine the nature of twinning in these crystals.

20. The limitations of the Laue method for this purpose have been examined.

21. It has been shown that the Laue method in conjunction with studies of optical activity is capable of allowing some progress to be made in the determination of the nature

of twinning in crystals of the trigonal trapezohedral class in certain cases where the exact methods of formal crystallography cannot be applied in full.

22. Twinning in a pseudo-hexagonal crystal of potassium dithionate of very unsatisfactory physical state has been determined as not due to a rotary-reflection.

23. A pseudo-hexagonal crystal of rubidium dithionate has been identified as of the Brazilian or of the complete hexagonal holohedry type.

24. It has been shown that a crystal of rubidium dithionate subjected to an inconclusive X-ray examination by Hägg probably was a twin.

STATEMENT OF CLAIM OF ORIGINAL WORK

The principal features of the original work contained in this thesis are as follows.

(a) The detailed geometrical deduction of the symmetry to be expected in Laue diagrams obtained from orthogonal crystals with the X-ray beam along lateral axes.

(b) The development of a new X-ray method, applicable to crystal fragments having no recognizable faces, for distinguishing between the members of certain pairs of space groups in the hexagonal system.

The application of this method to tourmaline, the space group of which had previously been determined as C_{3v}^{1} or C_{3v}^{2}, thus resulting in the unequivocal establishment of the space group as C_{3v}^{1}.

(c) The measurement of the optical activity of an untwinned crystal of rubidium dithionate.

(d) The confirmation of the space group of rubidium dithionate by more varied methods than have hitherto been applied to this crystal.

(e) The determination of the complete structure of rubidium dithionate for the first time in detail.

(f) The justification and use of the more convenient logarithms of calculated intensities instead of the more cumbersome direct values for comparison with visually estimated intensities of X-ray diffraction spots.

(g) The examination of possible applications of the Laue method, particularly with the X-ray beam along lateral axes, in conjunction with optical studies for use in the study of the nature of twinning in crystals of the trigonal trapezohedral class in cases where crystal specimens are not suitable for complete formal crystallographic study.

(h) The elimination of a possible rotary-reflection as the kind of twinning observed in a pseudo-hexagonal crystal of potassium dithionate.

(i) The determination of the twinning in a pseudo-hexagonal crystal of rubidium dithionate as either of the Brazilian or of the complete hexagonal holohedry type.